Pricing Contingent Convertible Capital - A Theoretical and Empirical Analysis of Selected Pricing Models

DISSERTATION
of the University of St. Gallen,
School of Management,
Economics, Law, Social Sciences
and International Affairs
to obtain the title of
Doctor of Philosophy in Management

submitted by

Marc Erismann

from

Beinwil am See (Aargau)

Approved on the application of

Prof. Dr. Karl Frauendorfer

and

Prof. Dr. Markus Schmid

St. Gallen, October 22, 2014

The President:

Prof. Dr. Thomas Bieger

Acknowledgments

Contents

List of Figures

List of Tables

Summary

This thesis contributes to the pricing of market and accounting triggered contingent convertible capital. By evaluating four selected pricing models in a theoretical and empirical context the foundation for a generally accepted pricing approach is broadened for practitioners and academics alike.

The thesis introduces the theory of a structural approach based on Pennacchi (2010), a credit and equity derivative approach shown by De Spiegeleer and Schoutens (2011, 2012) and a credit default swap model devised by the investment bank J.P. Morgan (Henriques and Doctor, 2011). The risky dynamics of each model are enhanced to allow for discontinuous returns. In an extensive empirical analysis on two Credit Suisse and two Lloyds Banking Group CoCos the parametrization, implementation and pricing capabilities are compared.

The model complexity is lowest for the credit derivative model and highest for the equity derivative model with discontinuous returns, whereas the data gathering and parametrization is most challenging within the structural approach. Universally it is found that the considered CoCos generate a high loss with a low probability, as the model implied trigger levels are low. The qualitative and quantitative assessment reveals that all models tend to overestimate the risk compared to the empirical observations, where the structural model shows the smallest pricing errors and is generally to be favored.

Zusammenfassung

Die vorliegende Arbeit trägt zu der Preisfindung von Markt und Bilanz aus-
gelöstem Contingent Convertible Capital bei. Durch die Evaluation vier
ausgewählter Preismodelle in einem theoretischen und empirischen Kontext
werden die Grundlagen zu einem allgemein akzeptierten Preisfindungsansatz
in der Praxis und Akademia erweitert.

Die Dissertation veranschaulicht die Preisfindung in einem strukturellen,
einem Kredit- und Eigenkapitalderivat sowie einen Credit Default Swap Modell.
Ersteres basiert auf den Grundlagen von Pennacchi (2010), das zweite und
dritte Modell wurde von De Spiegeleer and Schoutens (2011, 2012) vorgestellt
und das Letztere wurde von der Investment Bank J.P. Morgan (Henriques
and Doctor, 2011) vorgeschlagen. Des Weiteren wird die Risikodynamik der
Modelle erweitert, um unstetige Renditen abbilden zu können. Die Para-
metrisierung, Implementierung und allgemeine Güte der Modelle wird in einer
extensiven empirischen Analyse an zwei Credit Suisse und zwei Lloyds Banking
Group CoCos veranschaulicht.

Die Modellkomplexität ist am geringsten im Kreditderivat Modell und
am höchsten im Eigenkapitalderivat Modell mit unstetigen Renditen. Die
Parametrisierung ist am komplexesten im strukturellen Ansatz. Generell
kann gesagt werden, dass die untersuchten CoCos einen hohen Verlust mit
kleiner Eintrittswahrscheinlichkeit generieren, da die modellimpliziten Wand-
lungsniveaus tief sind. Die qualitative und quantitative Analyse zeigt weiter,
dass alle Preisansätze das Risiko im Vergleich zu den Marktpreisen überschät-
zen, wobei das strukturelle Modell die geringste Preisabweichung zeigt und
generell zu bevorzugen ist.

Chapter 1

Introduction and Motivation

1.1 Introduction

Over the years before the worldwide economic and financial crisis in 2007-2009 the banking sector was increasingly driven by moral hazard, lower market discipline and higher returns. The importance, interconnectedness and complexity of financial institutions increased a great deal while at the same time their capital and liquidity ratios decreased, effectively reducing their loss absorption potential (Basel Committee on Banking Supervision, 2011a; Maes and Schoutens, 2010). This inherent weakness manifested itself during the aggressive correction of the mortgage market in the U.S. when financial institutions worldwide were exposed to significant write-downs and ultimately losses which could not be borne by themselves. At the same time this sparked the global discussion on the issue of too-big-to-fail as governments and regulators realized that certain financial institutions are indeed systemically important and that the possible cost to the economy as a whole - should such an institution fail - outweighs the costs to bail them out. This resulted in a call for further regulation with a focus on strengthening the quality, quantity and transparency of loss absorbing capital with the primary aim to stabilize financial institutions in turbulent times while at the same time not hindering profitable business conduct during good times (Berg and Kaserer, 2011; Koziol and Lawrenz, 2012; Squam Lake Working Group on Financial Regulation, 2009).

Contingent convertible capital (CoCo) was introduced as a first line of defense to address aforementioned criteria. It is a long-term hybrid debt instrument with principal and scheduled coupon payments that serves the purpose of pre-arranging a re-capitalization given an event that is not controlled by the company that issues them. Recent studies by e.g. Barucci and Del Viva (2012), Hilscher and Raviv (2014), Sundaresan and Wang (2011), von Furstenberg (2011) or Albul et al. (2010) show that bankruptcy costs and cost of capital could be reduced with the right design of CoCos. A further feature the studies advocate is that the monitoring of financial institutions by investors is facilitated and moral hazard induced risk taking activities can effectively be reduced.

Regulators such as the European Banking Authority (2011), the European Commission (2011), the Financial Services Authority (2011), the Independent Commission on Banking (2011) or the Swiss Commission of Experts (2010) approve the issuance of CoCos to increase the financial buffer. Burne's (2011) estimate in early 2011 that the total CoCo market could reach up to USD 950 billion was sharply corrected downward when the Basel Committee (2011b, p. 20) concluded that "G-SIB's [Global-Systemically Important Banks] be required to meet their additional loss absorbency requirement with Common Equity Tier 1 only". However, the Basel III framework also supports the use of CoCos to meet higher national capital requirements than the global standard requirement - which for example is important for Switzerland within the Swiss SIFI (Systemically Important Financial Institutions) Policy released by the Swiss Financial Market Supervisory Authority FINMA (2011).

A handful of financial institutions have successfully raised capital with CoCo notes to be able to meet the higher buffer requirements. Until February 2012, only six CoCo issuances had taken place, whereas in the beginning of 2014, the newly established Bank of America Merrill Lynch Contingent Capital Index already comprised 48 bonds with a combined face value of approximately 58 billion US dollars. The index only comprises bonds which have a capital-dependent conversion feature, where the majority of the bonds

qualify as additional tier 1 securities. At the end of 2014, approximately 40% of the bonds had a rating of BBB, whereas the remaining 60% have a rating of BB. Furthermore, roughly 40% of the bonds feature a maturity of two to five years and another 50% a maturity of five to ten years with the remaining 10% above ten years (Bürgi, 2013; Reuters, 2014). Table 1.1 shows the details of some of the earliest CoCo issuances of the larger financial institutions, with a special focus on Switzerland.

Credit Suisse was the first bank to issue a traditional CoCo bond in February 2011, which converts into equity if their CET1 ratio undercuts a value of 7%. They subsequently offered two more equity conversion CoCos, raising a total of approximately USD 4.5 billion (Credit Suisse, 2011, 2012a, b). Similarly, the second largest Swiss bank UBS issued its first contingent capital issue in February 2012. In contrast to Credit Suisse, the UBS issuance offers a low-level trigger of a CET1 ratio of 5% and provides a write-down if the trigger is reached (UBS, 2012a, c). Recently the Swiss National Bank (2013) also designated the cantonal bank Zürcher Kantonalbank (ZKB) to be of systemical importance. ZKB as public-law institution had already issued a tier 1 subordinated bond in anticipation of this, which features a write-down mechanism if their CET1 ratio falls below a threshold of 7% (Zürcher Kantonalbank, 2013). Interestingly, also SwissRe (Swiss Re-Insurance company) issued a contingent convertible bond, which is linked to their solvency ratio as reported within the Swiss Solvency Test (SST). It provides a write-down mechanism up to 100% if the SST ratio falls below 125%, where any residual amount of the bond can be continued (Swiss Re, 2013). Lloyds Banking Group was the first large international bank that offered 29 enhanced capital notes series to its investors in exchange for existing preferred shares. The series amounts to a total of approximately GBP 7 billion and are denominated in GBP and EUR (Lloyds Banking Group, 2009a). The case of Rabobank is a second example of a non-listed company that benefits from issuing CoCos, where the face value in case of a contingency event is not converted into equity but simply written down (Rabobank, 2010, 2011). It is noted that the appetite is still high in the

market, as the recent and more than five-fold oversubscribed notes issuance in the amount of USD 3 billion of Barclay proves (Bloomberg, 2012a, b).

	Credit Suisse			UBS
Issue Name	Tier 2 Buffer Capital Notes (BCN)	Tier 2 Buffer Capital Notes (BCN)	Tier 1 Buffer Capital Notes (BCN)	Tier 2 Subordinated Notes
Issue Date	February 24th 2011	March 22nd 2012	July 31st 2012	February 22nd 2012
Maturity	30 years	20 years	perpetual	10 years
ISIN	XS0595225318	CH0181115681	XS0810846617	CH074723136
Rating	BBB+	BBB-	BB+	BBB-
Nominal Amount	USD 2 billion	CHF 750 million	USD 1.75 billion	USD 2 billion
Callability	Callable from August 24th 2016	Callable from March 22nd 2017	Callable from October 23rd 2018	Callable once on February 22nd 2017
Denomination	USD 100'000	CHF 5'000	USD 200'000	USD 250'000
Coupon	7.875%, resettable every 5yrs. starting from August 24th 2016 to mid-market USD 5y-LIBOR swap rate+5.22%	7.125% until one time reset on March 22nd 2017 to CHF mid-market 5y swap rate+6.685%	9.5% until October 23rd 2018, thereafter 6-month USD LIBOR+6.64%	7.25% until one time reset on February 22nd 2017 to USD mid-market 5y swap rate+6.06%
Trigger Level	Tier-1 ratio, 7%	Tier-1 ratio, 7%	Tier-1 ratio, 7%	Tier-1 ratio, 5%
Conversion Fraction	100%	100%	100%	
Conversion Price	maximum of 30 day average share price or USD 20	maximum of 30 day average share price or CHF 20	maximum of 30 day average share price or USD 16.57	write-down only

Table 1.1: *Issued CoCos as of June 2013 (continued)*

	ZKB	SwissRe	Lloyds	Barclays Bank
Issue Name	Tier 1 Subordinated Bonds	Contingent Write-off Loan Notes	Enhanced Capital Note (ECN)	Contingent Capital Notes (BCN)
Issue Date	January 31st 2012	March 12th 2013	December 1st 2009	November 21st 2012
Maturity	perpetual	10.5 years	9 to 22.5 years	10 years
ISIN	CH0143808332	XS0901578681	29 series (cf. A.1)	US06740L8C27
Rating	n/a	n/a	BB to BB-	BBB-
Nominal Amount	CHF 590 million	USD 750 million	GBP 4.288 billion / EUR 2.355 billion	USD 3 billion
Callability	Callable from June 30th 2017	At "Par Redemption Event"	Not callable	Not callable
Denomination	CHF 5'000	USD 200'000	GBP/EUR 1'000-100'000	USD 200'000
Coupon	3.5% resettable every 5yrs. starting from June 30th 2018 to CHF mid-market 5y swap rate+2.98%; fully deferrable	6.375% resettable every year starting from September 1st 2019 to USD 5y swap rate+5.21%	6.385% to 16.125%	7.625%
Trigger Level	Tier-1 ratio, 7%	SST < 125%	Tier-1 ratio, 5%	Tier-1 ratio, 7%
Conversion Fraction	75% - residual amount redeemed	up to 100%; residual amount continued		
Conversion Price	write-down only	100% write-down	GBP 0.59	100% write-down

Table 1.1: *Issued CoCos as of June 2013 (continued)*

	Rabobank	
Issue Name	Senior Contingent Notes	Hybrid Contingent Notes (HCN)
Issue Date	March 19th 2010	January 26th 2011
Maturity	10 years	perpetual
ISIN	XS0496281618	XS0583302996
Rating	n/a	A
Nominal Amount	EUR 1.25 billion	USD 2 billion
Callability	Not callable	Callable from July 26th 2016
Denomination	EUR 50'000	USD 100'000
Coupon	6.875%	8.375% resettable every 5yrs. starting from July 26th 2016 to 5y. US-Treasury benchmark+6.425%
Trigger Level	Equity capital ratio, 7%	Equity capital ratio, 7%
Conversion Fraction	75% - residual amount redeemed	up to 100% - residual amount continued
Conversion Price	write-down only	write-down only

Table 1.1: *Issued CoCos as of June 2013. (based on: Bürgi (2013), data sources from Credit Suisse (2011, 2012a, b), UBS (2012a, c), Lloyds Banking Group (2009a), Rabobank (2010, 2011), Barclays Bank PLC (2012), Swiss Re (2013), Zürcher Kantonalbank (2013).)*

1.2   Literature Overview

It is evident that the topic of CoCos is enjoying a lively debate among academics, regulators and financial institutions and literature is continuing to emerge and is quickly becoming vast. Up to now, most academic research focuses on the qualitative aspect of how contingent convertible capital is best designed in order for it to fulfill its primary goal to stabilize a financial institution in distress. This is also the common idea shared by all literature; but the implementation design can take many different forms.

Among the first papers to be published was by The Squam Lake Working Group (2009), who provide an economic rationale and recommend regulatory support for this new hybrid security. They see CoCos as a last resort and propose that it should not be triggered unless absolutely necessary. Therefore, they advocate a trigger mechanism that is both dependent on the decision of the respective regulatory agency and a violation of a capital adequacy ratio based on accounting values. Similarly, also McDonald (2010) proposes a multivariate trigger in his work, where the first trigger is an equity threshold based on market values and the second one is tied to a systemic index. In this case, individual banks are allowed to go bankrupt in normal times but would be saved in times of systemic distress. Also Pazarbasioglu et al. (2011) come to the conclusion that contingent capital instruments can act as a crisis prevention and management tool and should be considered within a comprehensive capital framework.

Already in 2002 Flannery put forward the idea to use Reverse Convertible Debentures with the main goal to optimize a firm's capital structure and provide an automatic un-levering mechanism should the firms equity capital deteriorate. Similarly, Albul et al. (2010) show that adding CoCos to newly created / existing capital structures can increase the firm's value. In his updated work, Flannery (2009) provides a hands-on description and evaluation of CoCos with an equity-based trigger, where upon breach the firm is un-levered to restore its minimum capital requirements. Of course also many

regulating bodies have picked up on the discussion of CoCos and their ideal implementation structure as mentioned in the previous section.

Existing Pricing Approaches

Generally speaking the pricing approaches proposed in the literature so far can be distinguished into structural, credit and equity derivative models (cf. table 1.2).

Structural Models

The structural model was pioneered by Merton in 1974 and provides a natural pricing framework for capital ratio triggered CoCo bonds. These models impose a stochastic process for the value of the assets and evaluate equity capital and debt as a function of the assets. Pennacchi (2010) applies such a structural risk model and values CoCos as claims contingent on the assets (cf. section 3.4). The model incorporates discontinuous asset returns, mean-reverting capital ratios and stochastic interest rates. This allows Pennacchi (2010) to calculate fair new issue yields depending on the debt-to-equity ratio at the time of issuance. One of the key findings of his work is that CoCos would in fact yield a riskless return if there were no jumps in the asset process. This structural model is able to include a sum of risk factors that have an impact on the value of the CoCo. However, the determination of the optimal parameter estimates is difficult in practice and has not been addressed by Pennacchi (2010). Similarly, Albul et al. (2010) apply a structural model but do not primarily focus on the pricing but they use the default model by Leland (1994) to obtain closed-form expressions that allow them to study the effects of a CoCo issue on the capital structure decision of a firm. Furthermore, they investigate the risk of stock price manipulation depending on different implementation designs. Glasserman and Nouri (2012) adapt a structural model to analyze contingent capital with a capital ratio trigger and on-going partial conversion, such that just enough debt is converted into equity to meet the minimum

requirement. They arrive at closed form solutions for the market value of such securities in a setting where the assets are modeled as a Geometric Brownian Motion. Madan and Schoutens (2011) incorporate the fact that assets and liabilities are both risky and employ conic finance techniques to introduce bid-ask-prices into their model. They argue that under the presence of risky liabilities the trigger should not be based on a core tier ratio but rather a trigger based on capital shortfall. Sundaresan and Wang (2011) argue within a structural model that an implementation using equity based market triggers can lead to multiple equilibria and price manipulations. As a consequence they propose that the coupon payment of a CoCo must be floating and equal to the risk free rate, which on the one hand ensures that the bond trades at par during its lifetime and on the other hand eliminates a value transfer between share holders and CoCo holders. Hilscher and Raviv (2014) propose a tractable form of contingent capital and provide a closed form solution for its price in a structural model. They show that an appropriate CoCo design can mitigate the stockholders' incentives to risk-shift thus concluding that CoCos may cancel out negative effects of equity-based compensation schemes. Bürgi (2013) presents a structural framework that combines multiple aspects from theoretical and practical literature, allowing him to model tier 1 triggered CoCos by imposing that there is a linear relationship between straight and tier 1 equity ratios. The model reveals large pricing differences in a time series analysis on a Credit Suisse CoCo, concluding with the fact that the parametrization in any model is attached with a lot of uncertainty and that future CoCo issuances should be designed in the form of pure write-down bonds.

Equity Derivative Models
Due to the hybrid nature of a CoCo bond another pricing approach takes the view of an equity investor and applies equity derivative techniques to replicate and value the implicit share position a CoCo investor is exposed to. De Spiegeleer and Schoutens (2011; 2012) suggest to separate the payoff of the CoCo into a zero corporate bond, a knock-in forward and a sum of binary

down-and-in options. The forward contract simulates the conversion of the bond into shares at a predetermined strike price while the binary options account for the foregone coupon payments if a conversion occurs (cf. section 3.2). One of the main conclusions is that Black-Scholes dynamics do not sufficiently cover the fat-tail dynamics that CoCos have. The model is therefore later extended by Corcuera et al. (2013) and Teneberg (2012) to incorporate higher fat-tail risk. Henriques and Doctor (2011) consider a CoCo to be a bond issued by a financial institution where the issuer has a long position in an option from the bondholder which is exercised at the occurrence of a trigger event such that the face value of the bond is converted into equity at a predetermined strike. Hence, they replicate a CoCo with an amount that gets written down to zero in the event of a trigger and an amount that gets converted into equity. These components are priced individually (cf. section 3.3). They believe that such a model accurately reflects the risk and structure of CoCo bonds and advise that conflicting interests could be mitigated by establishing a direct link between the solvency variable and the underlying equity value.

Credit Models
Since the conversion of a CoCo bond is closely connected to a firms default respectively survival probability also intensity based credit modeling lends itself as a pricing methodology. De Spiegeleer and Schoutens (2011; 2012) apply a credit derivative approach which results in a credit spread that is calculated as a function of the exogenously defined triggering probability and the corresponding expected loss in case of a conversion. They find that this method is quick to implement and is vastly applied in fixed income valuation (cf. section 3.1).

To the best knowledge of the author, Wilkens and Bethke (2014) are the first to perform an empirical assessment of a credit- and equity-derivative as well as a structural model. They parametrize and calibrate the models on two Lloyds Banking Group CoCos and one Credit Suisse CoCo and find that all

models are largely able to fit observed market prices, where the maximum observation period ranges from December 2009 to December 2011 for the Lloyds CoCos and from February 2011 to December 2011 for the Credit Suisse CoCo. Furthermore, they derive hedge ratios and compare the hedging performance of the models. They find that while the equity derivative model fares worst in their fitting analysis, it performs best in their hedge assessment and seems to be the most promising in light of its straight forward parametrization.[1]

Table 1.2 provides an overview of the aforementioned pricing approaches, showing the angle from which the models approach the problem.

Structural Models:	**Credit Models:**
Pennacchi (2010)	De Spiegeleer and Schoutens (2011)
Glasserman and Nouri (2012)	
Madan and Schoutens (2011)	
Albul et al. (2010)	
Sundaresan and Wang (2011)	
Hilscher and Raviv (2014)	
Bürgi (2013)	
	Equity Derivative Models:
	De Spiegeleer and Schoutens (2012)
	Henriques and Doctor (2011)

Table 1.2: *This table shows an overview of existing pricing approaches for contingent convertible capital. (based on: De Spiegeleer and Schoutens (2011))*

---

[1]The results of their empirical analysis are contrasted in more detail in chapter 5.

1.3   Motivation

As shown, a quickly growing market presents itself and is expected to grow even stronger in light of the stricter capital requirements set out by Basel III. Therefore, the need for capable pricing tools to enable regulators, investors and market makers to evaluate and manage this new hybrid instrument is clear.

As shown in the literature review, there co-exist several possible approaches regarding the pricing of contingent convertible capital. There is, however, no consensus among academics and practitioners alike as to which model is suited best to the task. Investors, market makers and regulators must therefore cope with significant uncertainties regarding the fair valuation, forecasting and risk management of the capital instrument (De Spiegeleer et al., 2011). De Spiegeleer and Schoutens (2011, p. 66) emphasize that "one model will likely prevail and will be accepted by most of the trading and structuring desks around the world". The question remains which one.

The motivation is to compare the performance of a number of chosen pricing models by means of theoretical and empirical analysis, practicability and computational effort. This includes the theoretical introduction of the models, discussing the data requirements and parametrization and comparing the pricing capabilities in a theoretical and extensive empirical analysis. Ultimately the challenge is to find the pricing model which is able to produce rapid and accurate prices (De Spiegeleer et al., 2011).

To cover a broad arrangement of pricing models, the thesis will introduce the theoretical foundation of a structural approach as outlined by Pennacchi (2010), a credit and equity derivative approach as suggested by De Spiegeleer and Schoutens (2011; 2012) and the J.P. Morgan pricing approach devised by Henriques and Doctor (2011). To respect the fact that a CoCo is an instrument which is driven by fat-tail events, a further motivation presents itself to incorporate the possibility of discontinuous returns as in Merton (1975) into aforementioned models.

1.4   Research Design

Having outlined the economic importance of contingent convertible capital and the resulting motivation, the subsequent chapter 2 provides a comprehensive overview of contingent convertible capital and its characteristic design features in order to introduce the qualitative framework needed to understand the behaviour, the mechanisms and most importantly the risk drivers of a CoCo.

Using this framework, the four mentioned pricing approaches are introduced in the following chapter 3 both in a setting where the risky returns are assumed to be normally distributed and on the other hand in a setting where returns are allowed to be discontinuous. Chapter 3 furthermore outlines the data requirements and parametrization techniques of the models and provides first pricing examples. An intermediary conclusion provides an overview and summary of the insights so far.

Chapter 4 includes a dynamics and sensitivity analysis to assess the model behaviour with respect to the different pricing and design parameters.

An extensive empirical analysis follows in chapter 5, where the models are parametrized on two Credit Suisse and two Lloyds Banking Group CoCos and the resulting price dynamics are qualitatively and quantitatively compared to reach a conclusion and outlook in the final chapter 6.

Chapter 2

Anatomy of CoCos

This chapter outlines the essential design characteristics of CoCos in order to get a grasp of the risk characteristics and possible value drivers that can have an impact on valuation.

2.1 CoCo Description

Contingent convertible capital is a long-term debt instrument with a maturity T that pays periodic interest c_i and serves the purpose of pre-arranging an automatic re-capitalization by either converting a fraction $0 < \alpha \leq 1$ of the face value N of the bond into common equity or suffering a write-down $0 \leq \alpha \leq 1$ when a predefined trigger event occurs.[1] This description gives raise to two flavors of contingent convertible capital: On the one hand the 'traditional' CoCo that converts into shares and on the other hand a CoCo that suffers a write-down. The latter option is the most prominent among the issuances so far and is for example interesting for privately held institutions that have no publicly traded equity. Contingent capital therefore enables raising funds in times of distress and unfavorable market conditions where it would otherwise be difficult to re-capitalize (e.g. due to a lack of investor trust or a prolonged liquidity/credit crunch). This automated capital buffer strengthens the loss

---

[1] Note that the actual maturity is unknown, as the expected lifetime of a CoCo can be shorter because of a possible early conversion or write-down.

absorbency potential and therefore acts to secure the going-concern of the individual entity and ultimately helps decrease the systemic contagion among financial institutions as could be observed during the recent financial turmoil. However, as shown by Albul et al. (2010), not only financial institutions ought to be interested in issuing contingent capital but any capital structure decision might benefit from this capital instrument, as its interest payments are tax deductible and therefore provide a tax shield effect which increases firm value.[2] Many non-financial companies could have benefited from an automatic re-capitalization to overcome negative or highly volatile cash-flow periods.

2.2 Payoff and Risk Profile

The above description suggests that a CoCo - much like a normal convertible bond - can be broken down into a bond and an equity part. The CoCo behaves like a normal corporate bond if a trigger event is unlikely, since the investor receives periodic coupon payments c_i and the bond would eventually redeem at maturity T. However, due to the risk of an early write-down or conversion into shares, the face value might not be repaid at all or suffer a haircut. Moreover, any future interest payments will be lost. It is at this point where an implicit equity position, for a CoCo that converts into shares, is no longer zero (Bürgi, 2013). In this sense, Glasserman and Nouri (2012) identify the following four preliminary value drivers of a contingent convertible bond:

1. Coupon payments on unconverted debt:
   During the lifetime of the CoCo it pays periodic interest payments c_i which add to the present value of the instrument.

---

[2]However, under U.S. tax law a fixed or ascertainable maturity date as well as the unconditional promise to pay upon maturity is generally considered to be necessary for a classification as debt (Allen & Overy LLP, 2012). Hence contingent capital instruments will most likely be treated as equity and a potential tax shield effect will not be given under U.S. jurisdiction. This is the main reason why no U.S. based institutions have issued contingent capital so far.

2. Principal payment on the unconverted debt:
   If no conversion has happened during its lifetime, the bond is redeemed at par and the principle amount repaid to the investor.

3. Dividends earned on equity after conversion:
   Once a trigger event has materialized and the bond has been converted into equity, the fixed-income investor now has a long position in shares of the company. As a result, the investor is now entitled to receive dividend payments.

4. Final value of earned equity at maturity:
   After a trigger event the investor can hold on to the shares and participate in the further share development.

To illustrate this value shift, consider the following simplified characterization of the payoff structure of a CoCo that pays coupon payments c_i and is tied to a share price trigger S^* (cf. figure 2.1):

1. At the discrete time points $t_{1,2,...,n}$, the level of the underlying S is compared to the trigger level S^* and checked whether $S > S^*$. If this is true, the CoCo is not converted and the investor receives the usual coupon payments $c_{1,2,...,T}$.

2. The alternative scenario is activated if during the lifetime of the CoCo the predefined barrier level S^* is hit by the reference underlying $\min_{0 \leq t \leq T}(S_T) \leq S^*$. In this case the CoCo gets converted into ordinary shares at a conversion ratio of C_r (cf. section 2.4) and the investor participates in the further development of the share until T. The terminal value in this case is $C_r(S_T - S^*)$ plus any dividend that might be distributed.

3. If the second scenario does not materialize, the CoCo investor receives the face value N at maturity T.
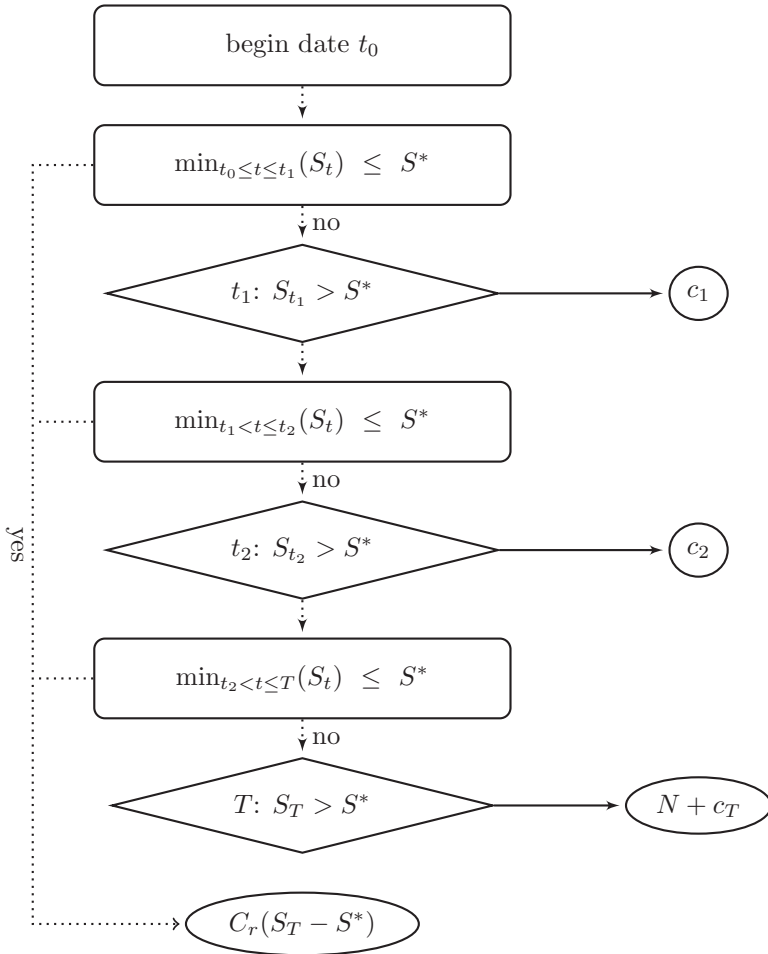
Figure 2.1: *This flowchart shows the payoff structure of a contingent convertible bond that is converted into ordinary shares with a conversion ratio C_r and a trigger price of S^*.*
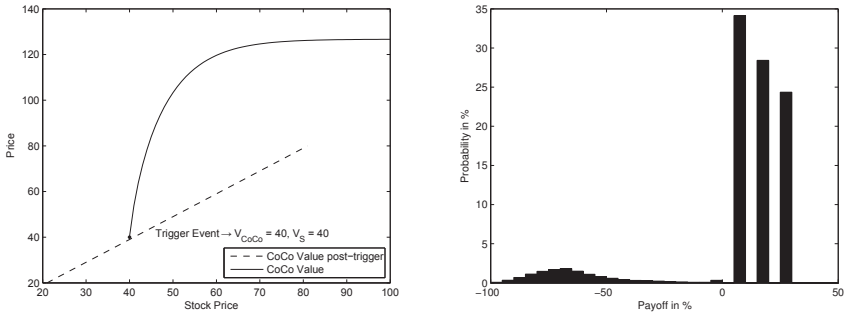
Figure 2.2: *The left-hand side graph shows the value of a generic CoCo bond that is converted into shares. The right-hand side graph shows the payoff profile of a generic CoCo. (based on: De Spiegeleer and Schoutens (2011))*

This generic payoff structure is plotted in the left-hand side graph of figure 2.2. This particular CoCo has a face value N of 100 and the trigger lies at a share price of 40, where the CoCo converts into 1 share. The initial share price is 100 and the CoCo pays an annual coupon of 10%. The behaviour clearly shows a negative convexity, as the investor is increasingly exposed to share price movements as the trigger is approached and ultimately has a one-to-one relationship to the share post-trigger. In contrast, the CoCo converges to non-convertible corporate debt if the trigger probability decreases as the share price moves further away from the trigger. This clearly illustrates the interconnectedness of the value shift between the bond and equity position driven by the trigger probability (De Spiegeleer and Schoutens, 2011). Once the CoCo holder is long in the shares, the further development of the share price will determine the ultimate payoff at maturity T, which can be seen in the right-hand graph of figure 2.2. In this example, there is a high probability that the CoCo does not get converted and the coupon payments are received, generating a return up to 30% for this three year CoCo. However, once it is triggered, the generated loss can be quite substantial.

Due to the argumentation above a CoCo clearly carries a high negative impact risk that occurs with a relatively small probability versus limited

upside potential with a high likelihood (De Spiegeleer and Schoutens, 2011; Glasserman and Nouri, 2012). It is clear that the probability of conversion is one of the main determinants that governs the payoff and the riskiness of the CoCo.

Having identified the main value drivers and the inherent risk-profile allows to subsequently treat the different price determinants that have an impact on the expected value of the bond and/or the equity part.

2.3   Conversion Trigger

The conversion trigger is the main difference of CoCos to existing hybrid debt instruments. This section discusses market-, accounting-, regulatory- and multivariate-trigger implementations with respect to the general guideline proposed by De Spiegeleer and Schoutens (2011, 2012) according to which a trigger should be designed:

- Clarity: The trigger must be universally applicable regardless of the jurisdiction of the issuer. This means that e.g. capital ratios have the same meaning and are not subject to discrepancies in accounting standards.

- Objective: There should be no subjectivity involved in the trigger. The trigger event should be well known and documented ex-ante.

- Transparent: A trigger should be observable to the investor. Ideally, this is a market driven measure that is readily available to all investors.

- Fixed: The chosen trigger should not change over the lifetime of the CoCo.

- Public: Issuing institutions should ideally make information concerning the trigger publicly available at the same time in order to avoid speculative contagion.

- Frequency: Accounting information is at most provided on a quarterly basis, which leaves a lot of room for speculation for investors about the financial condition of a company. Ideally the information should be available real-time.

Complementary to the stipulated inclusion criteria as regulatory capital, the Basel III framework furthermore defines minimum criteria for capital instruments that are allowed to be included in "Additional Tier 1 capital" (i.e. going-concern capital). Specifically, a capital instrument "classified as liabilities for accounting purposes must have principal loss absorption through either (i) conversion to common shares at an objective pre-specified trigger point or (ii) a write-down mechanism which allocates losses to the instrument at a pre-specified trigger point" (Basel Committee on Banking Supervision, 2011a, p. 17). Hence choosing the right trigger design is important and in this context different possible designs are discussed subsequently.

2.3.1 Market Trigger

A market trigger is the most simple and straightforward approach to determine the contingent event and could for example be based on the firm's stock price or its credit-spreads. Those measures are (ideally) governed by the law of supply and demand and under the assumption of liquid and efficient markets, these indicators have forward looking characteristics and should therefore reflect the financial condition of a bank most accurately and timely. There is a clear favoring towards market based triggers in current academic research as for example McDonald (2010), Haldane (2011) or Calomiris and Herring (2013) contend using a share price trigger as well as Flannery (2002; 2009) suggests using a capital ratio comprised of the book value of the debt and the market value of equity.[3] Clearly, a market trigger would limit the management's ability to deliberately manipulate such a ratio and eliminate the subjectivity inherent in e.g. a regulatory trigger. However, practitioners fear that also

---

[3]McDonald (2010) combines it with a systemic index to create a dual-trigger design.

market prices could be subject to manipulation if a CoCo is close to conversion (Flannery, 2009; McDonald, 2010; Squam Lake Working Group on Financial Regulation, 2009). If CoCo investors believe that shares will continue to decline post-trigger they put additional pressure on the stock by short selling it in order to hedge their investment and profit from share price corrections. This "self-fulfilling-prophecy" can be mitigated by specifying the conversion price in such a way that bondholders bear some loss in case of conversion (McDonald, 2010). During the "flash-crash" on May 6, 2010 almost all individual stock prices of more than 8000 firms suffered a sharp price correction and a quick reversal (Borland and Hassid, 2010). Similarly, the share price of Swiss private bank Julius Bär plummeted more than 40% on February 6th 2009 after rumors that their financial statement had been 'cooked' (Neue Zürcher Zeitung, 2009). Such a sudden spike in volatility could have forced an unjust triggering of the convertible and demonstrates a potential weakness of a market trigger.[4] A remedy to this problem would for example provide the utilization of an average share price as proposed by e.g. Duffie (2010) or Flannery (2009).

2.3.2   Accounting Trigger

Typically the solvency of a financial institution is measured using an accounting based value such as the core equity tier 1 (CET1) ratio as defined in Basel III or a solvency based measure like the Swiss Solvency Test (SST, as is the case in the SwissRe issue). These measures are clearly defined and tightly regulated and transparent in their assumptions. Thus such accounting levels lend themselves as an indication that additional capital is needed to secure the going-concern and act as a trigger point. However, there is still potential leeway in calculating the risk weighted assets on the basis of which the CET1 ratio is calculated, which in turn results in intransparency and possible distortion of the ratio. As a matter of fact Kuritzkes and Hal (2009) or Haldane (2011) argue that many of the large U.S. financial institutions that were on the brink of

---

[4]Flannery (2011) argues that some conversion errors of this kind would even be justified in light of too low capital buffers.

collapsing were reporting capital ratios in excess of the minimum requirements. A further caveat to be considered is the periodicity as accounting statements are usually published on a quarterly basis or even semi-annually, as in the case of e.g. Lloyds Banking Group (Risk Magazine, 2010). Insurance companies are even only required to submit Swiss Solvency Test reports to the FINMA on an annual basis (Swiss Financial Market Supervisory Authority, 2012). This might lead to a lagged information source and unnecessary speculation by debt and equity investors. Despite its downsides this option clearly has become the only broadly accepted implementation as all currently issued CoCos feature some sort of an accounting trigger, first and foremost to be in line with the Basel III requirements.

2.3.3   Regulatory Trigger

As regulators are interested in limiting the economic impact a governmental authority could request the conversion if they believe that the going-concern of a systemically important financial institution is at risk. Such a trigger would eliminate the risk of market manipulation and ensure the timeliness of the conversion. However the highly discretionary nature of such a trigger is almost impossible to judge by the markets, let alone being incorporated into a valuation model (De Spiegeleer and Schoutens, 2011). Interestingly, the CoCos issued by e.g. Credit Suisse and UBS can both be triggered at the discretion of the Swiss regulator FINMA (Credit Suisse, 2011, 2012a, b; UBS, 2012c).

2.3.4   Multivariate Trigger

Flannery (2009) or the Squam Lake Working Group on Financial Regulation (2009) also propose to link a conversion to multiple triggers. This could for example be a macro variable, indicating the status of the economy as a whole, linked with a micro variable that reflects the status of the issuing company. E.g. a financial index could serve as a proxy for the health of the financial sector as a whole and the share price of the individual company as the idiosyn-

Criterion	Market	Accounting	Regulatory	Multi-Variate
Clarity	high	medium	low	medium
Objectiveness	high	medium	low	medium
Transparency	high	medium	low	medium
Fixedness	high	high	low	high
Publicity	high	high	high	high
Frequency	high	medium	low	high

Table 2.1: *This table provides an overview of the different trigger designs. High, medium and low indicate a qualitative interpretation of the design criteria.*

cratic measure. This immediately raises the question whether it should be an (and / or) relationship. A systemic index might be at low levels due to single banks that are in trouble but other banks might still be doing fine. If this would force a system wide conversion without respecting the individual health of the banks, it would certainly avert a systemic crisis but it would leave banks that are in good health overcapitalized and eventually hinder a cost-effective financial intermediation. On the other hand if the idiosyncratic measure would trigger a conversion but the financial sector as a whole is doing fine, then an individual bank might not get recapitalized at all (Flannery, 2009).

To summarize, table 2.1 provides an overview of the trigger designs with a qualitative interpretation of the objective criteria according to which a trigger should ideally be implemented. E.g. a market trigger has a high level of objectiveness as opposed to a regulatory trigger, which due to its discretionary basis is not very objective.

2.4   Conversion Details

Equally as important as specifying the trigger conditions are the conversion details. As previously mentioned there exist CoCos that convert to equity

and CoCos that suffer a write-down. Write-down bonds are of course easier to design, whereas equity conversion bonds are a more delicate manner, as the number of shares needed to service the equity conversion can either be a predefined amount or determined at the time of conversion using the contemporaneous stock price. In any case the conversion fraction indicates the amount of the CoCo that gets converted or written off.

2.4.1 Conversion Fraction

The conversion fraction α determines the amount of the face value N of the CoCo that is converted into equity or written off: $N \times \alpha$. Any remaining amount $(1 - \alpha)$ might be redeemed by the issuer or is to be written off in case of a partial equity conversion (De Spiegeleer and Schoutens, 2011). Most CoCos issued so far specify a full conversion / write-off, i.e. $\alpha = 1$, however there are examples with varying α's.

2.4.2 Conversion Price and Ratio

After having determined the conversion amount αN the question remains how many shares the investor will receive in case of a conversion respectively what the conversion price for one share will be. If the conversion rate C_r is determined beforehand, i.e. at the issuance date, then the implied conversion price C_p is

$$C_p = \frac{\alpha N}{C_r} \tag{2.1}$$

On the other hand if the conversion price C_p is known then the conversion rate C_r equals

$$C_r = \frac{\alpha N}{C_p} \tag{2.2}$$

In both cases it comes down to the (implied) conversion price C_p, as the recovery rate R_{CoCo} is given by the stock price at the trigger event S_T^* divided

by the conversion price C_p

$$R_{CoCo} = \frac{S_T^*}{C_p} \tag{2.3}$$

and hence the direct loss attributable to CoCo holders is (De Spiegeleer and Schoutens, 2011)

$$L_{CoCo} = N - (1 - R_{CoCo}) = N\left(1 - \frac{S_T^*}{C_p}\right) \tag{2.4}$$

or equivalently the final payoff P_T to the CoCo holder is

$$P_T = \begin{cases} (1-\alpha)N + C_r S_T^* & \text{if converted} \\ N & \text{if not converted} \end{cases} \tag{2.5}$$

This is assuming that the CoCo investor sells the shares directly after conversion at S_T^*; another option would be to hold on to the shares, which would generate a different payoff depending on the stock price evolution.

Generally there exist three predominant ways in which the conversion price C_p can be set (De Spiegeleer and Schoutens, 2011):

1. **C_p determined at issuance, $C_p = S$**

   Setting the conversion price C_p to a pre-determined share price S at the date of issuance would immediately allow to calculate the conversion rate C_r and therefore the amount of shares that would be issued in case of conversion. This way the dilution of the existing shareholders would be known ex-ante and less severe than if the conversion price is set at the trigger date (due to the lower conversion ratio C_r). On the other hand, as the actual market price S_T^* when conversion happens is uncertain and is very likely to be in a depressed state it will be very likely that the investor will have to bear a loss upon conversion.

2. **C_p determined at conversion, $C_p = S_T^*$**

   A CoCo investor would in theory be held loss-less if the conversion price

would equal the market price at the time of conversion $N = C_r S_T^*$. In this case just enough shares would be issued to service the full conversion amount of the CoCo. In this example the conversion ratio C_r would be higher and therefore existing shareholders would suffer a higher dilution. To limit this effect a floor conversion price S_{floor} could be incorporated $C_p = \max(S_T^*, S_{floor})$. This option is most prone to market manipulation as CoCo investors might try to force a conversion at a low price to maximize their ex-post stake in the company. However, this could be mitigated by calculating the conversion price as the average share price during a pre-defined time period. In fact the Credit Suisse issuances have a floor conversion price and an averaging feature incorporated (Credit Suisse, 2011, 2012a, b).

3. **Conversion in fixed amount of shares**
   The conversion could also be specified as a fixed amount of shares. If the conversion price is not set beforehand, i.e. a conversion price equal to the market price S_T^* on the trigger date, the expected conversion amount α is uncertain.

It is clear that the choice of the conversion price is important. Currently issued bonds that convert into equity either have a predefined conversion price, as explained under point one, or a price determined at conversion but with a floor, as explained under point two above. Table 2.2 provides a summary of the conversion price designs, showing the interplay between the conversion ratio and the conversion price and a qualitative assessment of the main consequences on the attached loss, dilution and manipulation effects. E.g. a conversion price fixed at issuance (case 1) implies a low conversion ratio and conversely a high conversion price, therefore inducing a high loss to the investors but leading to a low dilution and manipulation effect.

Case	C_r	C_p	Loss	Dilution	Manipulation
1.	low	high	high	low	low
2.	high	low	low	high	high
3.	medium	medium	high	medium	high

Table 2.2: *This table provides an overview of the conversion price designs and the effects on the conversion ratio and the conversion price. Furthermore loss, dilution and manipulation effects are shown. Case 1 corresponds to a conversion price fixed at issuance, case 2 to a conversion price fixed at conversion and case 3 to a conversion into a fixed amount of shares.*

Having introduced the main framework to understand the mechanics and behaviour of CoCo bonds the next chapter moves on to introduce the theory and methodology of four different pricing models.

Chapter 3

Theory of Pricing CoCos

In its essence a CoCo shares a lot of its characteristics even with the most basic form of a convertible bond. A convertible bond is a security that has both debt and equity characteristics, since the investor has the right to convert the bond's nominal amount into a predefined number of shares at maturity (Bodie et al., 2009; Hull, 2009). In a simplified manner, the payoff of such a bond can be expressed as a straight bond with an embedded call option, whose fair value can be deduced from the time value of money combined with option pricing theory, provided by e.g. Black and Scholes (1973) and Merton (1973) (Ammann et al., 2008; De Spiegeleer et al., 2011; Hull, 2009). What distinguishes a CoCo from ordinary convertible capital is the dependence on a conversion trigger, where the trigger probability can for example be determined via an accounting value or a stock price that breaches a certain threshold (cf. section 2.3). Another distinctive fact is that the contemporaneous stock price at the date of conversion ultimately determines the payoff to the investor if the CoCo is converted into shares at the share price on the trigger date (cf. section 2.4.2). Due to the stochasticity of the share price (and/or accounting value) the payoff cannot be perfectly determined ex-ante and must therefore be approximated (Bürgi, 2013).

The pricing models that are introduced in this chapter includes a credit and equity derivative approach as proposed by De Spiegeleer and Schoutens (2011; 2012) - where the latter has been extended by Teneberg (2012) and

Corcuera et al. (2013) to incorporate fat tail behaviour - a structural approach that follows the implementation of Pennacchi (2010) and a credit default swap (CDS) approach that J.P. Morgan (Henriques and Doctor, 2011) has devised.

Irrelevant of which method is applied, the valuation is generally confronted with the determination of a triggering probability and the contemporaneous stock price at the time of conversion. All approaches therefore rely on assumptions regarding the stochastic process that governs the triggering probability and/or the stock price. The models are on the one hand presented in their original form where the returns from the underlying risky asset process are assumed to be normally distributed. Additionally, the behaviour of the models will also be investigated in a setting that allows for discontinuous returns. Specifically, this is done by imposing a jump-diffusion process as presented by e.g. Merton (1975) as return generating process.

At this point it must be noted that CoCos are securities that include non-tradeable risk drivers (e.g. the decision of a government body to force a conversion or the evolution of the CET1 ratio) and hence a perfect risk transfer by the investing agent is not possible. This generally leads to an incomplete market setting, which is also observed for many other financial and insurance products. In the classical application of financial engineering within a complete market setting (e.g. Black-Scholes) one can move from the physical probability space to a unique risk-neutral measure (the former is commonly referred to as $\mathbb{P}$ and the latter as $\mathbb{Q}$) via no-arbitrage / replicating conditions, arriving at a unique pricing kernel thus satisfying the first and second fundamental theorem of pricing (Birge and Linetsky, 2007; Björk, 2009). The consideration of a jump-diffusion process as underlying model induces market incompleteness, where a risk-neutral measure $\mathbb{Q}$ can still be achieved but with the caveat that it is non-unique and several parameter sets can lead to the same price (Björk, 2009; Joshi, 2003; Tankov, 2003).

Thus in incomplete markets the calibration of (in-)complete market models to observed security prices do not account for any costs generated through

hedging activities or any residual risk borne by the investing agent. The intrinsic assumption of a fictitious replicating portfolio strategy of (in-)complete market models wrongly appraises the non-hedgeable risk as though it could be diversified away (Birge and Linetsky, 2007). The observed pricing differences between the achieved model prices and the empirical prices must be interpreted within this setting.

3.1 Credit Derivative Model

In standard fixed income mathematics corporate debt is often priced using a reduced form approach, also referred to as intensity based credit modeling. It can be seen as a simplification of the Merton (1974) model, where instead of modeling an entire balance sheet only the default probability and the loss given default are involved. Combined with straight forward bond pricing methodologies results in the famous credit triangle, which is often encountered and applied in practice due to its simplicity and easy implementation (De Spiegeleer et al., 2011; Hull, 2009). The derivation mainly follows De Spiegeleer et al. (2011), De Spiegeleer and Schoutens (2011) and Duffie and Singleton (2003).

3.1.1 Intensity based credit risk approach

Proposed by e.g. Jarrow and Turnbull (1995), Duffie and Singleton (1997; 1999; 2003) or Madan and Unal (1998) and extensively covered in e.g. Lando (2009) or Duffie and Singleton (2003) the intensity based approach assumes that the default event is governed by an exogenously defined intensity process, which must not necessarily be correlated to the asset value of the company. This is in contrast to the structural models, where the default event is connected to the asset and debt levels of the company (cf. section 3.4). The default intensity directly relates to the hazard rate, which is the conditional default rate: define the default time τ as a non-negative random variable and assume that it has

a continuous density function f, then the probability of default up to time t is

$$P(\tau \leq t) = F(t) = 1 - S(t) = \int_0^t f(s)ds \tag{3.1}$$

where $S(t)$ is the survival function and $F(t)$ is the distribution function. The hazard rate $h(t)$ or correspondingly the default intensity $\lambda(t)$ is defined as

$$h(t) = \lim_{\Delta t \downarrow 0} \frac{1}{\Delta T} P(t \leq \tau < t + \Delta t) = \frac{f(t)}{S(t)} = \frac{f(t)}{1 - F(t)} = -\frac{d}{dt} \log(S(t)) \tag{3.2}$$

i.e. the rate of default conditional on the survival. The survival function $S(t)$ is then given by

$$S(t) = e\left\{ -\int_0^t \lambda(s)ds \right\} \tag{3.3}$$

The specification of $\lambda(t)$ is often treated as stochastic and usually term-structure models such as the Vasicek (1977) or Cox et al. (1985) model are applied.[1] The default intensity $\lambda(t)$ can also be modeled as a deterministic function of time, where $\lambda(t)$ can be constant or piecewise constant over time. This thesis treats the default intensity as a deterministic function of time, which is introduced subsequently both in constant and piecewise constant form.

By assuming that $\lambda(t)$ is a deterministic function of time t then the default probability can be expressed by combining equation (3.1) with (3.3) as

$$P(\tau \leq t) = 1 - e\left\{ -\int_0^t \lambda(s)ds \right\} \tag{3.4}$$

On the other hand, if $\lambda(t)$ is given piecewise constant between fixed time

---

[1]For more details on the technical definition in such a setting see e.g. Lando (2009).

points $t_1, t_2, ..., t_i$ as shown below

$$\lambda(t) = \begin{cases} \lambda_1 & \text{if } 0 < t \le t_1 \\ \lambda_2 & \text{if } t_1 < t \le t_2 \\ \vdots & \vdots \\ \lambda_i & \text{if } t_{i-1} < t \end{cases} \tag{3.5}$$

then the default probabilities using equation (3.4) can be expressed as

$$P(\tau \le t_i) = \begin{cases} 1 - e^{-\lambda_1 t} & \text{if } 0 < t \le t_1 \\ 1 - e^{-\lambda_1 t_1 - \lambda_2(t-t_1)} & \text{if } t_1 < t \le t_2 \\ \vdots & \vdots \\ 1 - e^{-\lambda_1 t_1 - \lambda_2(t_2-t_1)...\lambda_i(t-t_{i-1})} & \text{if } t_{i-1} < t \end{cases} \tag{3.6}$$

If a flat default intensity function is assumed for all maturities, the default probability reduces to

$$P(\tau \le t) = 1 - e^{-\lambda t} = 1 - P(\tau > t) \tag{3.7}$$

To illustrate the practical implication this simplification has, assume a single time step model, in which a zero-coupon bond can either survive and pay the full face value N at maturity T or it can default and pay a recovery rate $R \ge 0$, as illustrated in table 3.1. The expected zero-coupon bond value B

State	Value	Probability
No Default	$Ne^{-r_f T}$	$P(\tau > t)$
Default	$Ne^{-r_f T}R$	$1 - P(\tau > t)$

Table 3.1: *Zero-Coupon bond states.*

can then be computed by multiplying the value and the probability of the

respective state and discounting it with the risk-free rate r_f:

$$B = Ne^{-r_f T}[P(\tau > t) + (1 - P(\tau > t))R] \tag{3.8}$$

By substituting the survival probability $P(\tau > t) = e^{-\lambda t}$ with its first order approximation $1 - \lambda t$, the value of the zero coupon bond can be expressed as

$$B \approx Ne^{-r_f t}[1 - \lambda t + \lambda t R] = Ne^{-r_f t}[1 - \lambda t(1 - R)] \tag{3.9}$$

Combining equation (3.9) with the fact that a risky zero-coupon bond pays a certain credit spread s above the risk-free rate r_f, it is evident that there exists a link between the credit spread s, the default intensity λ and the recovery rate R. This is called the credit triangle (3.10) and is often used in practice as it provides a quick valuation method for bonds:

$$\lambda = \frac{s}{1 - R} \tag{3.10}$$

Equivalently, the credit spread can be expressed as

$$s = \lambda(1 - R) \tag{3.11}$$

This allows to determine the default probability from a credit spread or alternatively to calculate the credit spread for a given default intensity λ.

3.1.2   Application to CoCos

Recalling equation (2.3) the recovery rate R_{CoCo} is given by the choice of the conversion price C_p and the contemporaneous share price S_T^* at the trigger event

$$R_{CoCo} = \frac{S_T^*}{C_p} \tag{3.12}$$

In the case of CoCo's of primary interest is not necessarily the default intensity λ but the conversion intensity λ_{CoCo}, which will be greater than the former $\lambda_{CoCo} > \lambda$, as a conversion should happen before an actual default to secure the going-concern. Therefore, the CoCo credit spread s_{CoCo} with a constant default intensity λ_{CoCo} is

$$s_{CoCo} = \lambda_{CoCo}(1 - R_{CoCo}) \tag{3.13}$$

GBM Trigger Probability λ_{CoCo}
The conversion intensity λ_{CoCo} should reflect the probability of conversion up to a certain time T. The implementation outlined below allows to model the trigger event in terms of a market trigger, i.e. a trigger share price, as well as in terms of an accounting trigger. Specifically, the risk-neutral default probability within a first-passage-default model in a Black-Scholes setting as outlined by e.g. Black and Cox (1976) is defined as follows

$$p^*(T-t) = \phi \left(\frac{\log\left(\frac{S^*}{S_t}\right) - \mu(T-t)}{\sigma\sqrt{T-t}} \right) + \left(\frac{S^*}{S_t}\right)^{\frac{2\mu}{\sigma^2}} \phi \left(\frac{\log\left(\frac{S^*}{S_t}\right) + \mu(T-t)}{\sigma\sqrt{T-t}} \right) \tag{3.14}$$

Here, ϕ is the cumulative standard normal distribution, q is the continuous dividend yield, r_f is the continuous risk-free interest rate, σ is the volatility of the underlying and μ is given by $r_f - q - \frac{\sigma^2}{2}$. The equation coincides with the first time exit equation in a Black-Scholes setting used to price barrier options as it yields the probability that a geometric brownian motion with initial value S_0 touches a barrier S^* before time T (Derman and Iraj, 1996;

Su and Rieger, 2009).[2]

JGBM Trigger Probability λ_{CoCoJ}

There exist no closed form solutions for the first-passage-default probability under jump diffusion models (Abrahams, 1986; Zhou, 2001). Therefore, the trigger probability is computed by simulation. Specifically, the implementation follows the jump-diffusion process

$$\frac{dV_t}{V_t} = (\mu - q - \lambda k)dt + \sigma dW_t + (\Pi - 1)dY_t \qquad (3.15)$$

where μ is the expected return of the asset less the dividend yield q and where k, λ and σ are positive constants; W_t is a standard Brownian motion and dY is a Poisson process with intensity parameter λ; Π is the expected jump amplitude with $E(\Pi) = k-1$ where $k = e(\mu_\pi + \sigma_\pi^2/2) - 1$ under the assumption that $\ln(\Pi) \sim \phi(\mu_\pi, \sigma_\pi^2)$. Zhou (1997; 2001) then transforms (3.15) into the following form

$$X_t - X_{t_i} = x_i + y_i * \pi_i \qquad (3.16)$$

by letting $X_t = \ln(V_t)$ and with x_i, y_i and π_i being mutually and serially independent random variables drawn from

$$x_i \sim \phi((r_f - q - \frac{\sigma^2}{2} - \lambda k)\frac{T}{n}, \sigma^2 \frac{T}{n})$$

$$\pi_i \sim (\mu_\pi, \sigma_\pi^2)$$

$$y_i = \begin{cases} 0 & \text{with probability } 1 - \lambda\frac{T}{n} \\ 1 & \text{with probability } \lambda\frac{T}{n} \end{cases}$$

By discretizing T over n and finding the smallest integer $i \leq n$ for which X_{t_i} is smaller or equal than some threshold level $\ln(K)$ over a large number of simulations $j = 1, 2, \ldots, M$ for varying maturities allows to determine the

---

[2]For more details on barrier options please refer to section 3.2, where the topic is discussed in more detail within the equity derivative approach.

probability of default as

$$p_J^*(T) = \frac{\sum_{j=1}^{M} \mathbf{1}_{\{i=\tau^* \leq T\}}}{M} \tag{3.17}$$

A nice property of using a jump diffusion process is that it is capable of explaining credit spreads in short maturities, as there exists a probability in the short term that a non-continuous drop leads to default. However, the reverse is observable for longer maturities. This behaviour is shown in figure 3.1, where the cumulative default probability λ_{CoCo} and λ_{CoCoJ} is plotted as a function of maturity T. The basic intuition behind this is that when keeping the total process volatility constant the likelihood of a jump induced default is higher than a diffusion induced default for short maturities, whereas for longer maturities the opposite is true.[3] Of course the effect is more or less pronounced depending on the chosen parameter set and also if constant or piecewise constant conversion intensities are considered.

A further effect that plays a role is that the average recovery rate R_{CoCoJ} will be lower when adding the possibility of sudden jumps, because the trigger share price is not only approached continuously but discontinuous drops can induce a further loss. The recovery rate R_{CoCoJ} from the simulations can be determined by dividing the sum of the recovery rates by the number of observed defaults over the simulation runs $j = 1, 2, \ldots, M$

$$R_{CoCoJ} = \frac{\sum_{f=1}^{F} RR_f}{\sum_{j=1}^{M} \mathbf{1}_{\{i=\tau^* \leq T\}}} \tag{3.18}$$

Both of these reported effects are in line with the findings of Zhou (2001).

Naturally, this simulation approach is associated with an approximation error, which - at the cost of computational time - can be reduced by increasing

---

[3]As opposed to a geometric brownian motion, a jump diffusion process has a total variance of $\sigma_J^2 = \sigma^2 + \lambda(\mu_\pi^2 + \sigma_\pi^2)$ (Merton, 1975), which is kept constant in order to perform comparative analysis between jump and non-jump configurations. E.g. when adding jumps the diffusion volatility decreases by $\lambda(\mu_\pi^2 + \sigma_\pi^2)$.

the number of simulations. The standard error for 50'000 simulation runs is only about 3 basis points for a five year bond; the corresponding 95% confidence interval is given in brackets where applicable.
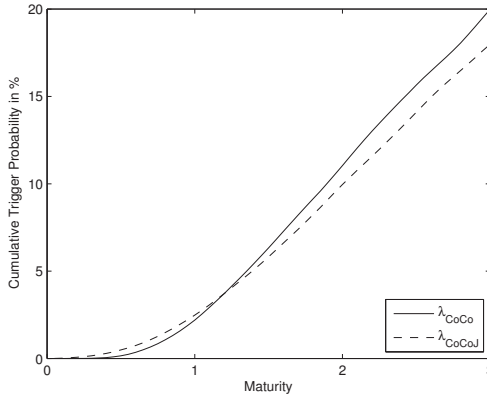
Figure 3.1: *Cumulative trigger probability λ_{CoCo} and λ_{CoCoJ} in the credit derivative approach as a function of maturity T. The parameters correspond to the generic CoCo parameters presented in table 3.3. The total process variance is kept constant in the evaluation. (based on: Zhou (2001))*

Calculation of the Credit Spread s_{CoCo}

Setting the probability of touching the barrier $p^*_{(J)}$ equal to the default probability from equation (3.7) allows to express $\lambda_{CoCo(J)}$ as a function of the underlying stock price process and maturity T (De Spiegeleer and Schoutens, 2011, 2012)

$$\lambda_{CoCo(J)} = \frac{\log(1 - p^*_{(J)}(T))}{T} \tag{3.19}$$

In combination with equation (3.13) yields the final CoCo spread in a Black-Scholes setting s_{CoCo} respectively the credit spread when returns include jumps s_{CoCoJ}. When dealing with piecewise constant default intensities the respective default probabilities $p^*_{(J)} = (p^*_{(J)}(t_1), p^*_{(J)}(t_2), \ldots, p^*_{(J)}(t_i))$ are computed for the respective time points t_i under consideration. The CoCo spread can then

be calculated using the simplified CDS pricing approach given by e.g. Hull (2009), Hull and White (2000) or Schönbucher (2003)

$$s(T) = \frac{(1 - R_{CoCo}) \sum_{i=1}^{T} e^{-rt_i} (F(t_i) - F(t_{i-1}))}{\sum_{i=1}^{T} e^{-rt_i} (1 - F(t_i))} \tag{3.20}$$

where $F(t_i)$ corresponds to the bootstrapped probabilities $P_{(J)}(\tau \leq t_i)$. Figure 3.2 shows the required coco yield, i.e. the credit spread s_{CoCo} plus the risk-free interest rate r_f, and the resulting bond price. What can be observed is that there are two main effects at play, which counteract each other. As the trigger price S^* decreases, the trigger probability decreases as well but on the other hand the loss to the investor increases, as the recovery rate R_{CoCo} is lowered. When the trigger price approaches the conversion price $C_p = 25$, the recovery rate increases to reach 100% and offsets the increasing trigger probability. For trigger levels above the conversion price, the CoCo holder would not suffer any loss and consequently the CoCo spread s_{CoCo} over the risk-free rate r_f is zero. What is also evident is that there is a double equilibrium price for different levels of the trigger price S^*.

3.1.3   Data Requirements and Calibration

With the aim to generate a time series in the context of the empirical analysis in chapter 5, the data sources and the calibration of the different parameters need to be defined. An overview of all the model parameters is provided in table 3.2.

GBM trigger probability (subtable 3.2b)
In a Black-Scholes setting the trigger probability is given by the standard deviation σ of the share price, the risk-free rate r_f, the dividend yield q as well as the current and trigger share price S_t respectively S^*. The diffusion parameter σ in this approach is calculated using the five year log returns of the respective underlying, which yields a representative value of the standard
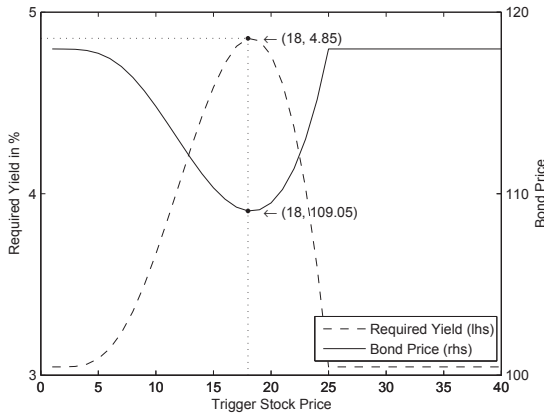
Figure 3.2: *This figure shows the required yield Y_{CoCo} on the left-hand side y-axis and the bond price CDC on the right-hand y-axis as a function of the trigger stock price S^*. The parameters correspond to the generic CoCo parameters presented in table 3.3. (based on: De Spiegeleer and Schoutens (2011))*

deviation. For the risk-free rate r_f the yield of a government bond of the same denomination and initial tenor as the bond will be used. The dividend yield q will be based on the five year average dividend yield prevailing the first pricing date of the CoCo bond but furthermore any firm specific policies or measures regarding their dividend payments will be taken into account.[4]

As a last element remains the unknown trigger level S^* at which the CoCo converts. Instead of arbitrarily choosing a stock price level, this value will be calibrated via minimization of the root mean squared error to meet the initial market price of the CoCo under consideration.

---

[4]As will be seen later on, Lloyds Banking Group was forced to seize any dividend payments starting from 2009 as part of their recapitalization scheme (Lloyds Banking Group, 2009b). In fact, Lloyds only very recently has applied to the Prudential Regulation Authority (PRA) to restart dividend payments (Lloyds Banking Group, 2009b, 2014).

JGBM trigger probability (subtable 3.2c)

Generally the estimation of the parameters inherent in (3.15) can for example be done via maximum likelihood estimation on the source data, which in turn yields those parameters which maximize the likelihood that the observed data has been generated with the respective process (Cochrane, 2009; Hull, 2009). However, when calibrating jump processes using this classical approach bears certain caveats, as it yields the most likely jumps and not the most pronounced jumps (Clewlow and Strickland, 2000). As the target in this thesis is to detect the most severe jumps - which are found in the tails of the return distribution - a threshold exceedance technique is applied to determine the jump distribution $\phi(\mu_\pi, \sigma_\pi^2)$.[5] In this case, the integer exceedance threshold k is determined by the assumed number of jumps λ per year multiplied by the length of the calibration period in years. The distribution is then determined on the sorted set of returns $x_n \leq \cdots \leq x_N$ and $k < N$ returns exceed the threshold. The positive jumps are found in the upper tail $x_{N-k} \leq \cdots \leq x_N$ and the negative jumps are in the lower tail $x_n \leq \cdots \leq x_{n+k}$. This implies that the largest negative and positive returns are used to construct the distribution, irrespective of the year when the jump happened.

Recovery ratio (subtable 3.2a)

To calculate the recovery ratio R_{CoCo} the conversion price C_p as well as the contemporaneous share price S_T^* at the trigger event is required. The conversion price C_p is (in most cases) readily available in the bond prospectus as they are usually set at the issue date of the bond. As already mentioned, the actual share price at the trigger event S_T^* is unknown and is given through the return dynamics of the model.

---

[5]Similar techniques are applied in e.g. extreme value theory (see e.g. McNeil et al. (2005a) or Embrechts et al. (1997)).

$$R_{CoCo} = \frac{S_T^*}{C_p}$$

Variable	Description	Data source	Usage
S_T^*	Share price at trigger event	Model dynamics	-
C_p	Conversion price	Bond prospectus	Static

(a) *Parameters to determine the recovery rate of the contingent convertible in the credit derivative model.*

$$p^*(T-t) = \phi\left(\frac{\log\left(\frac{S^*}{S_t}\right)-\mu(T-t)}{\sigma\sqrt{T-t}}\right) + \left(\frac{S^*}{S_t}\right)^{\frac{2\mu}{\sigma^2}} \phi\left(\frac{\log\left(\frac{S^*}{S_t}\right)+\mu(T-t)}{\sigma\sqrt{T-t}}\right), \ \mu = r_f - q - \frac{\sigma^2}{2}$$

Variable	Description	Data source	Usage
S^*	Trigger share price	Calibration	Static
S_t	Current share price	Market data	Dynamic
σ_t	Standard deviation of share price	Market data	Dynamic
r_f	Risk-free interest rate	Market data	Dynamic
q	Dividend yield	Market data	Static

(b) *Parameters to determine the trigger probability in the credit derivative model without jumps.*

Table 3.2: *Parameter overview credit model (continued)*

$$x_i \sim \phi\left(\left(r_f - q - \frac{\sigma^2}{2} - \lambda k\right)\frac{T}{n}, \sigma^2 \frac{T}{n}\right), \ \pi_i \sim (\mu_\pi, \sigma_\pi^2), \ y_i = \begin{cases} 0 & \text{with probability } 1 - \lambda\frac{T}{n} \\ 1 & \text{with probability } \lambda\frac{T}{n} \end{cases}$$

Variable	Description	Data source	Usage
r_f	Risk-free interest rate	Market data	Dynamic
q	Dividend yield	Market data	Static
σ_t	Standard deviation of the share price	Market data	Dynamic
λ	Jump intensity per year	Assumption	Static
μ_π	Mean jump size	Market data	Static
σ_π	Jump standard deviation	Market data	Static
n	Discretization factor	Assumption	Static

(c) *Parameters to determine the trigger probability in the credit derivative model including jumps.*

Table 3.2: *Parameter overview credit derivative model. (based on: Wilkens and Bethke (2014))*

3.1.4   Pricing Example

To put the theoretical framework into context this section provides an application on a generic CoCo bond presented in table 3.3. The individual steps will be outlined both assuming a constant (CDC) and a piecewise constant (CDP) conversion intensity to arrive at a final CoCo spread. The structure follows Alvemar and Ericson (2012).

Variable	Value	Description
N	100	Face value
T	5	Bond maturity in years
c_i	7%	Bond coupon rate, paid annually
α	1	Full conversion
S_0	40	Initial share price
S^*	20	Trigger share price
C_p	25	Conversion price
σ	30%	Annual standard deviation
r_f	3%	Risk-free rate
q	0%	Dividend yield
λ	1	Jump intensity
μ_π	0	Mean jump size
σ_π	20%	Jump standard deviation

Table 3.3: *Generic CoCo price parameters. (based on: Alvemar and Ericson (2012))*

Constant Conversion Intensity $\lambda_{CDC(J)}$

Recalling that the credit spread in a setting with a constant conversion intensity is given by equation (3.13), $s_{CDC(J)} = \lambda_{CDC(J)}(1 - R_{CoCo(J)})$, the first step involves the calculation of the conversion intensity $\lambda_{CDC(J)}$ using (3.19). Secondly, the recovery rate $R_{CoCo(J)}$ is expected to coincide with 80% in the GBM model, as the trigger share price S^* will not be broken but rather approached continuously such that $S_T^* = S^*$. In the case with jumps it should

be lower because on average $S_T^* < S^*$ due to discontinuous jumps.

In a Black-Scholes setting the trigger probability $p^*(T)$ is given by the first-passage default equation shown in (3.14). When considering jumps, the conversion probability $p_J^*(T)$ has to be approximated by simulating (3.16) and evaluating (3.17). The conversion intensity can then be calculated by plugging in the respective probability into equation (3.19).

The parameters from table 3.3 yield a likelihood of 33.83% that the stock price hits the barrier within five years in a standard Black-Scholes setting. When returns are discontinuous, the probability lowers to 31.78% and furthermore the recovery rate decreases slightly to 77.45% (which is in line with the previous findings). The resulting conversion intensities are $\lambda_{CDC} = 0.0826$ and $\lambda_{CDCJ} = 0.0764$. Table 3.4 summarizes these intermediary results.

Variable	Value	Description
$p^*(5)$	33.83%	CDC first-passage probability
$p_J^*(5)$	31.78%	CDCJ first-passage probability
λ_{CDC}	0.0826	CDC conversion intensity
λ_{CDCJ}	0.0764	CDCJ conversion intensity
R_{CDC}	80%	GBM Recovery rate
R_{CDCJ}	77.45%	JGBM Recovery rate

Table 3.4: *This table shows the trigger probabilities, the corresponding conversion intensities and the recovery rates of the credit derivative model with constant conversion intensity. (based on: Alvemar and Ericson (2012))*

The resulting CoCo spread is then given by

$$s_{CDC}(5) = 0.0826 \cdot (1 - 0.8) = 1.65\%$$
$$s_{CDCJ}(5) = 0.0764 \cdot (1 - 0.7745) = 1.72\% \ [1.70\%; 1.74\%]$$

There is only a slight pricing difference as the spread is about 7 basis points higher in the case when jumps in the returns are considered. The sensitivity analysis in chapter 4 will reveal further details on the behaviour of these

spreads. To arrive at the required yield the risk-free rate of 3% needs to be added

$$Y_{CoCo}(5) = 1.65\% + 3\% = 4.65\%$$

$$Y_{CoCoJ}(5) = 1.72\% + 3\% = 4.72\% \ [4.70\%; 4.74\%]$$

Piecewise Constant Conversion Intensity $\lambda_{CDP(J)}$

In the case of piecewise constant conversion intensities the probability of default is calculated for every year during the lifetime of the bond. In this case, the five year bond is split into five time points t_i and the corresponding cumulative default probability $p^*_{(J)}(t_i)$ is calculated. From this, the corresponding intra-period default intensities $p^*_{(J)}(t_i) - p^*_{(J)}(t_{i-1})$ are computed. This is illustrated in table 3.5. The CoCo spread is calculated using equation (3.20), which is

t_i	$p^*(t_i)$	$p^*(t_i) - p^*(t_{i-1})$	$p^*_J(t_i)$	$p^*_J(t_i) - p^*_J(t_{i-1})$
1	2.35%	2.35%	2.38%	2.38%
2	11.53%	9.18%	9.59%	7.21%
3	20.49%	8.97%	18.74%	9.15%
4	27.86%	7.37%	25.40%	6.60%
5	33.83%	5.98%	31.78%	6.38%

Table 3.5: *This table shows the piecewise constant default probabilities in the credit derivative model. (based on: Alvemar and Ericson (2012))*

presented again below

$$s(T) = \frac{(1 - R_{CoCo}) \sum_{i=1}^{T} e^{-rt_i} \left(p^*_{(J)}(t_i) - p^*_{(J)}(t_{i-1}) \right)}{\sum_{i=1}^{T} e^{-rt_i} \left(1 - p^*_{(J)}(t_i) \right)} \quad (3.21)$$

where the nominator corresponds to the sum of the discounted intra-period default probabilities multiplied by the loss given default and the denominator represents the sum of the discounted survival probabilities. In the case at

hand, the credit spread $s_{CoCo(J)}$ corresponds to

$$s_{CDP} = \frac{0.0617}{3.7209} = 1.66\%$$
$$s_{CDPJ} = \frac{0.0708}{3.8092} = 1.86\% \ [1.83\%; 1.89\%]$$

and the respective required yields are

$$Y_{CDP} = 1.66\% + 3\% = 4.66\%$$
$$Y_{CDPJ} = 1.86\% + 3\% = 4.86\% \ [4.83\%; 4.89\%]$$

In both cases the results are very similar to the case with constant default intensities. The difference is a bit more pronounced for the CDPJ model, as the higher default intensity for shorter maturities is reflected more accurately. This shows that the rule of thumb approach is quite accurate; however the difference will be more pronounced depending on the input parameters. The implied bond prices can be calculated by discounting the future cash flows CF_i with the yield rate.

Model	Price $= \sum_{i=1}^{T} CF_i e^{-Y_{CoCo(J)} \cdot t_i}$
CDC	110.02
CDCJ	109.69 [109.78; 109.59]
CDP	109.97
CDPJ	109.03 [109.17; 108.89]

Table 3.6: *This table shows the CoCo prices for the credit derivative model with constant and piecewise constant conversion intensity (CDC / CDP) as well as for the credit derivative model including jumps CDCJ and CDPJ respectively. (based on: Alvemar and Ericson (2012))*

3.2   Equity Derivative Model

The equity derivative model as proposed by De Spiegeleer and Schoutens (2011, 2012) tries to replicate the payoff structure of a CoCo by using existing equity derivative techniques. As the name implies, this approach is driven by a market trigger where a certain share price level S^* will determine the point of conversion. Recalling equation (2.5) the payoff of a CoCo in case of a conversion is given by $P_T = (1 - \alpha)N + C_r S_T^*$, which can be expanded differently such that it can be shown that the payoff can be decomposed into two components (it is assumed here that $S^* = S_T^*$) (Alvemar and Ericson, 2012; De Spiegeleer and Schoutens, 2011)

$$
\begin{aligned}
P_T &= \mathbf{1}_{\{\tau > T\}} N + \left[(1 - \alpha)N + \frac{\alpha N}{C_p S^*} \right] \mathbf{1}_{\{\tau \leq T\}} \\
&= N + \left[\frac{\alpha N}{C_p} S^* - \alpha N \right] \mathbf{1}_{\{\tau \leq T\}} \\
&= N + [C_r S^* - \alpha N] \mathbf{1}_{\{\tau \leq T\}} \\
&= N + C_r \left[S^* - \frac{\alpha N}{C_r} \right] \mathbf{1}_{\{\tau \leq T\}} \\
&= N + C_r [S^* - C_p] \mathbf{1}_{\{\tau \leq T\}}
\end{aligned}
\tag{3.22}
$$

The first component is the face value N of the bond and the second component is the implicit long position in C_r shares, which only generates a payoff if the trigger has materialized $\mathbf{1}_{\{\tau \leq T\}}$. Specifically, the second component can be thought of as a knock-in forward, where the strike price K equals the conversion price C_p and the barrier level equals the trigger share price S^*. The intuition is that at the point of the conversion the bond holder will use the face value N to exercise the forward contracts which commits the investor to buy the amount C_r shares for the price of C_p at maturity. Arguably, receiving a forward when the barrier is touched is not the same as receiving the actual share. The most notable difference is the omitted dividend which is accentuated if a conversion happens early during the lifetime of the CoCo.

However, De Spiegeleer and Schoutens (2011; 2012) find this to be a reasonable assumption since a company in distress will very likely (have to) be restrictive with their dividend payments.[6]

Furthermore, a third valuation component in connection to the corporate bond has to be evaluated that takes into account the foregone coupon payments should a conversion occur. This will reduce the value of the corporate bond and can be modeled with short positions in binary-down-and-in options (De Spiegeleer and Schoutens, 2011).

Subsequently the payoff structure will be disentangled and the theory behind it laid out to arrive at a closed form solution under standard Black-Scholes assumptions. A later section will then show how the same valuation can be done in a jump diffusion setting.[7]

3.2.1 Corporate Bond

The first component is a long position in a corporate bond of the issuing entity that mimics the properties of the bond profile before a possible conversion. The corporate bond with value V_t^{cb} has a face value N and pays a coupon c_i at time points t_i and can be priced through standard bond pricing (Hull, 2009)

$$V_t^{cb} = Ne^{-r_f(T-t)} + \sum_{i=t}^{T} c_i e^{-r_f t_i} \tag{3.23}$$

Notice that the corporate bond is discounted using the risk-free rate r_f as the potential loss in case of a trigger event is embedded in the down-and-in forward described below in section 3.2.3. The risk-free rate r_f in this case is assumed

---

[6]Recall e.g. the case of Lloyds Banking Group, who had to seize dividend payments altogether as part of their refinancing program (Lloyds Banking Group, 2009b, 2014). Similar cases include e.g. AIG, American International Group Inc., or UBS, Union Bank of Switzerland, who have not payed out any dividend at all or only very minor payments have been made since 2008 (American International Group, Inc., 2012; Reuters, 2012; UBS, 2012b).

[7]The author would like to thank Henrik Teneberg (2012), who generously provided key components of the program code to implement the equity derivative approach in a jump diffusion setting.

to be flat.[8] As noted before, including all the future coupon payments would not be correct since as soon as a conversion takes place, any future cash-flows are lost. The subsequent section 3.2.2 will present a binary option approach to capture this effect.

3.2.2   Binary Barrier Option

To take the effect of foregone coupon payments of the bond valued above into account, De Spiegeleer and Schoutens (2011; 2012) apply binary option techniques that partially or completely offset future coupon payments. Specifically, this can be achieved by taking a short position in a *down-and-in cash-or-nothing barrier option* for every coupon payment c_i of the CoCo. This type of option is a path dependent option and either pays a fixed amount of cash Q at maturity T if a predefined barrier level S^* has been breached during the lifetime of the option or zero otherwise (Derman and Iraj, 1996, 1997; Haug, 2006; Hull, 2009). Hence, the set of k down-and-in-cash-or-nothing binary barrier options can be used to add a negative rebate αc_i that partially or completely offsets the future coupon payments and accounts for the foregone cash flows once a trigger event has materialized. The barrier level S^* when the option gets activated corresponds to the overall conversion trigger of the CoCo and the maturities t_i of the binary barrier options are equal to the time points of the coupon payments c_i. Rubinstein and Reiner (1991) provide the following formula to derive the price of such an option in a Black-Scholes setting

$$
\begin{aligned}
V_{t_i}^{dibi}(c_i, S^*, t) = \alpha \sum_{i=1}^{k} c_i e^{-r_f t_i} [&\phi(-x_{1i} + \sigma\sqrt{t_i}) \\
+ &\left(\frac{S^*}{S}\right)^{2\lambda-2} \phi(y_{1i} - \sigma\sqrt{t_i})]
\end{aligned}
\tag{3.24}
$$

---

[8]The effect of incorporating daily yield curve data into the model is discussed in chapter 5.3.

with

$$x_{1i} = \frac{\log(\frac{S_t}{S^*})}{\sigma\sqrt{t_i}} + \lambda\sigma\sqrt{t_i}$$

$$y_{1i} = \frac{\log(\frac{S^*}{S_t})}{\sigma\sqrt{t_i}} + \lambda\sigma\sqrt{t_i}$$

$$\lambda = \frac{r_f - q + \frac{\sigma^2}{2}}{\sigma^2}$$

The formula shows that the value $V_{t_i}^{dibi}$ is the coupon amount c_i times the probability that the payment will take place. As the probability converges to one when approaching the barrier, the formula reduces to discounting a future cash flow payment. Indeed, the price of this option converges to the price of a zero-coupon bond as the probability of hitting the barrier increases (De Spiegeleer and Schoutens, 2011). This behaviour is illustrated in figure 3.3. It depicts the value of a binary barrier option which pays an amount of 1 at the expiry date if the barrier $S^* = 20$ is hit. The discounted value of a unit zero-coupon bond and a five year maturity is 0.86.
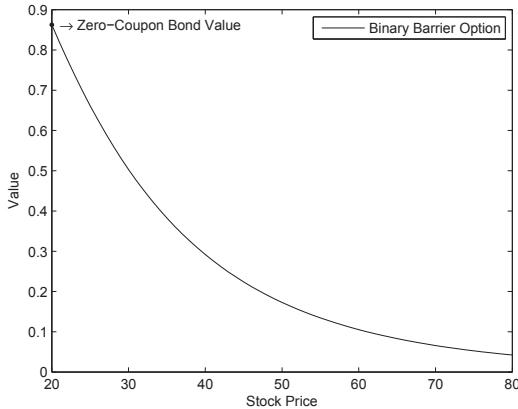
Figure 3.3: *Value of a five-year unit down-and-in binary barrier option as a function of the stock price. (based on: De Spiegeleer and Schoutens (2011))*

3.2.3   Down-And-In Forward

The remaining component is a long position in a down-and-in forward contract that replicates the long position in the shares once a trigger event occurs. Repeating the reasoning from above, a CoCo investor has the implicit obligation to buy C_r shares during the lifetime of the bond. After a conversion - respectively having the obligation to buy C_r shares - the CoCo investor is exposed to the upside potential of the stock as well as to a further deterioration of it until maturity. Following De Spiegeleer and Schoutens (2011; 2012) this component will be approximated using knock-in forwards on the underlying share.

It is well known that a synthetic forward contract on a stock can be replicated by a long position in a call option and a short position in a put option, both sharing the same strike K and the same maturity T (Hull, 2009). However, the specific down-and-in forward contract that needs to be modeled in this case must be path dependent. Therefore, vanilla options cannot be used to construct the synthetic forward but one has to resort to barrier options. Similarly to the binary barrier option above, a normal barrier option is a path dependent option where the payoff is a function of the underlying share price at maturity S_T and whether the share price S has breached a predefined barrier S^* during the lifetime of the option (Derman and Iraj, 1996, 1997; Haug, 2006; Hull, 2009). In case of a down-and-in option the barrier option gets activated once the threshold stock price S^* is hit. On the other hand, a down-and-out option ceases to exist once the barrier S^* is breached.

The payoff of a down-and-in call option (3.25) respectively of a down-and-in put option (3.26) can be specified as follows:

$$\max(S_T - K) \text{ if } \min_{0 \leq t \leq T}(S_T) \leq S^* \tag{3.25}$$

$$\max(K - S_T) \text{ if } \min_{0 \leq t \leq T}(S_T) \leq S^* \tag{3.26}$$

Assuming normality for returns, an assumption which will be relaxed in section

3.2.4, there exist closed form solutions for the described barrier options as presented by Merton (1973) for a down-and-in call

$$
\begin{aligned}
V_t^{dic}(S_t, S^*, K) = S_t e^{-q(T-t)} \left(\frac{S^*}{S_t}\right)^{2\lambda} \phi(y) \\
- K e^{-r_f(T-t)} \left(\frac{S^*}{S_t}\right)^{2\lambda-2} \phi(y - \sigma\sqrt{T-t})
\end{aligned}
\tag{3.27}
$$

with

$$
y = \frac{\log(\frac{S_*^2}{S_t K})}{\sigma\sqrt{T-t}} + \lambda\sigma\sqrt{T-t}
$$

$$
\lambda = \frac{r_f - q + \frac{\sigma^2}{2}}{\sigma^2}
$$

or for a down-and-in put

$$
\begin{aligned}
V_t^{dip}(S_t, S^*, K) = S_t e^{-q(T-t)} \left(\frac{S^*}{S_t}\right)^{2\lambda} (\phi(y) - \phi(y1)) \\
- K e^{-r_f(T-t)} \left(\frac{S^*}{S_t}\right)^{2\lambda-2} (\phi(y - \sigma\sqrt{T-t}) \\
- \phi(y1 - \sigma\sqrt{T-t})) + K e^{-r_f(T-t)} \phi(x1 + \sigma\sqrt{T-t}) \\
- S_t e^{-q(T-t)} \phi(-x1)
\end{aligned}
\tag{3.28}
$$

with

$$
x1 = \frac{\log(\frac{S_t}{S^*})}{\sigma\sqrt{T-t}} + \lambda\sigma\sqrt{T-t}
$$

$$
y1 = \frac{\log(\frac{S^*}{S_t})}{\sigma\sqrt{T-t}} + \lambda\sigma\sqrt{T-t}
$$

Interestingly the down-and-in call as well as the down-and-in put converge to the standard Black and Scholes European option prices as the share price S approaches the barrier S^*. This convergence is illustrated in figure 3.4. It can be observed that the down-and-in call has a negative delta, as its value

increases as the share price approaches the barrier. This is due to the fact that it can only generate a payoff once the call is activated, which is more likely the closer the stock price is to the barrier (Derman and Iraj, 1996, 1997). Similarly
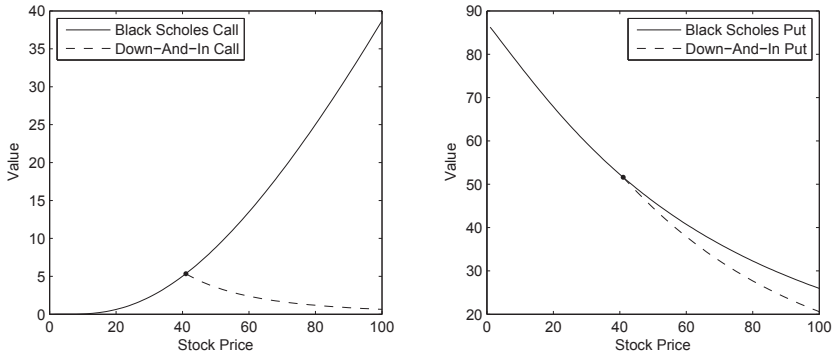
Figure 3.4: *Convergence of barrier options to Black and Scholes option value. (based on: De Spiegeleer and Schoutens (2011))*

to the synthetic forward contract a down-and-in forward can be constructed by buying a down-and-in call option and selling a down-and-in put option with the same strike price K, the same maturity T and additionally the same knock-in barrier S^*. The payoff of such a down-and-in forward is defined as follows (Hull, 2009)

$$\min(S_t) \leq S^* : P_T = S_T - K = \max(S_T - K) - \max(K - S_T) \qquad (3.29)$$

$$\min(S_t) > S^* : P_T = 0 \qquad (3.30)$$

As soon as the barrier is hit, the option holder is paying the price K for one share. Depending on the terminal share price S_T either the down-and-in call or the down-and-in put component is in the money and the investor is either gaining or losing money as in equation (3.29). On the other hand, if the barrier is not breached during the lifetime of the down-and-in forward, the payoff is zero as in equation (3.30). The further away the barrier S^* is from the strike price K, the less likely it is that the share price is going to recover to a level

where the down-and-in call is in the money once it is activated. It is clear that the conditional distribution of the payoff, once the down-and-in forward is activated, is crucial to evaluate its value.

The final down-and-in forward can be constructed using equation (3.27) and (3.28), where C_r indicates how many down-and-in forward contracts the investor is exposed to in case of conversion (cf. section 2.4.2) and ϕ stands for the cumulative normal distribution function:

$$
\begin{aligned}
V_t^{difwd}(S_t, S^*, K) = C_r[&Se^{-q(T-t)} \left(\frac{S^*}{S} \right)^{2\lambda} \phi(y_1) - Ke^{-r_f(T-t)} \left(\frac{S^*}{S} \right)^{2\lambda-2} \\
&\phi(y_1 - \sigma\sqrt{T-t}) - Ke^{-r_f(T-t)}\phi(-x_1 + \sigma\sqrt{T-t}) \\
&+ Se^{-q(T-t)}\phi(-x_1)]
\end{aligned}
$$

(3.31)

with

$$
x_1 = \frac{\log(\frac{S}{S^*})}{\sigma\sqrt{T-t}} + \lambda\sigma\sqrt{T-t}
$$

$$
y_1 = \frac{\log(\frac{S^*}{S})}{\sigma\sqrt{T-t}} + \lambda\sigma\sqrt{T-t}
$$

$$
\lambda = \frac{r_f - q + \frac{\sigma^2}{2}}{\sigma^2}
$$

Similarly to De Spiegeleer and Schoutens (2011), a Monte Carlo simulation has been run with a geometric brownian motion as return generating process to show the payoff of a down-and-in forward contract. The results are plotted in figure 3.5. The volatility of the stock has been set to 40% and the risk-free interest rate is assumed to be 5% whereas the dividend yield is set to 0%. Moreover, the initial share price S is 100 and the barrier S^* lies at 40. The result of 50'000 simulations over a three year maturity reveals a probability of about 21% that the barrier was breached and the down-and-in forward activated. Since the barrier is far below the strike price, the share price seldom succeeds to recover above the strike price; it is much more likely that the short

put component is in the money and generates a loss. The conditional expected payoff $E(P_T)$ equals -58.09 whereas the unconditional expected payoff equals -12.49.
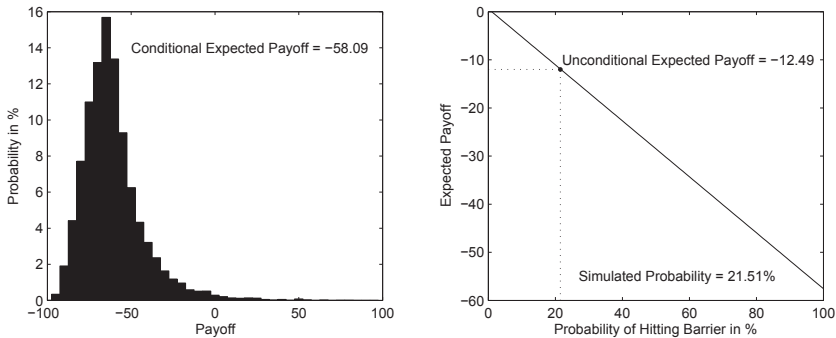
Figure 3.5: *Down-and-in forward conditional expected payoff and unconditional expected payoff. (based on: De Spiegeleer and Schoutens (2011))*

Also the down-and-in forward convergences to a standard forward contract as the share price S approaches the knock-in barrier S^*. This is shown in figure 3.6. The dashed line indicates the value of the down-and-in forward component for different levels of the stock price S. In combination with the conversion ratio $C_r = \frac{\alpha N}{C_p}$ the value of the down-and-in forward component can be calculated.

The final value of the CoCo in the equity derivative model is then derived as

$$\text{ED}_t = V_t^{cb} - V_{t_i}^{dibi} + V_t^{difwd} \tag{3.32}$$

3.2.4   Jump Diffusion setting

The corporate bond component is not affected by the change from a GBM to a JGBM setting and is evaluated according to (3.23). However, the calculation of the binary barrier options and the forward position is not available in a closed form anymore and must be approximated to accommodate the jump
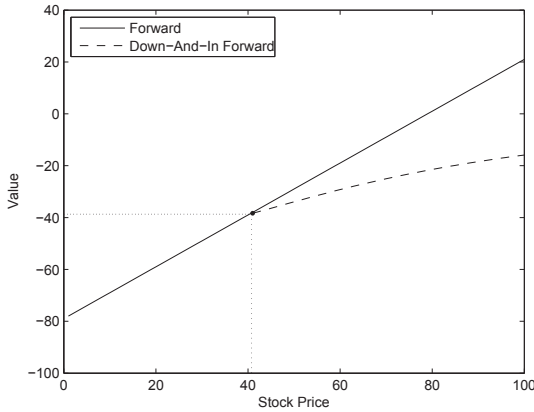
Figure 3.6: *Down-and-in forward convergence to a normal forward contract. (based on: De Spiegeleer and Schoutens (2011))*

diffusion process. The implementation and valuation is achieved within a trinomial tree as shown by e.g. Hull (2009) or more specifically in a jump diffusion setting shown by Albert et al. (2006). Furthermore, to decrease the inherent non-linearity error the Ritchken (2005) technique is applied, which introduces a stretch parameter into the lattice, that ensures that a tree node falls on the barrier level.

As it is easier to set up the lower boundary conditions for down-and-out rather than for down-and-in options in a trinomial tree, the former are priced in the tree and the in-out-parity of barrier options is exploited to calculate the down-and-in option value. The parity shown in equation (3.33) establishes a relationship between the vanilla option and the down-and-in respectively down-and-out option values and holds for European style options without rebate (Derman and Iraj, 1996, 1997; Hull, 2009).

$$
\begin{aligned}
V_t^{pJ} &= V_t^{dipJ} + V_t^{dopJ} \\
V_t^{cJ} &= V_t^{dicJ} + V_t^{docJ}
\end{aligned}
\tag{3.33}
$$

The down-and-in forward in a jump diffusion setting can then be expressed by

$$V_t^{difwdJ}(S_t, S^*, K) = [(V_t^{cJ} - V_t^{docJ}) - (V_t^{pJ} - V_t^{dopJ})] \qquad (3.34)$$

The value of the vanilla call V_t^{cJ} and put V_t^{pJ} in a JGBM setting is given in semi-closed form as shown by Merton (1975) for normally distributed jumps

$$V_t^{cJ/pJ} = \sum_{n=0}^{\infty} \frac{e^{\lambda(1+k)(T-t)n}}{n!} V_t^{c/p} \qquad (3.35)$$

where λ is the average number of jumps per year and $k = e(\mu_\pi + \sigma_\pi^2/2) - 1$. The Black-Scholes option value $V_t^{c/p}$ is given subsequently in equation (3.36) for a call and for a put (Black and Scholes, 1973; Hull, 2009).

$$\begin{aligned} V_t^c &= S\phi(d_1) - Ke^{-\bar{r}(T-t)}\phi(d_2) \\ V_t^p &= Ke^{-\bar{r}(T-t)}\phi(-d_2) - S\phi(-d_1) \end{aligned} \qquad (3.36)$$

with

$$d_1 = \frac{\log \frac{S}{K} + (\bar{r} + \frac{\bar{\sigma}^2}{2}(T-t))}{\bar{\sigma}\sqrt{(T-t)}}$$

$$d_2 = d_1 - \sigma\sqrt{(T-t)}$$

In this particular case Merton (1975) adjusts the interest rate to $\bar{r} = r_f - \lambda k + \frac{n\mu_\pi}{(T-t)}$ and the variance rate to $\bar{\sigma}^2 = \sigma^2 + \frac{n*\sigma_\pi^2}{(T-t)}$; the counter n is bounded to 100.[9] It is evident that if the jump parameters λ, μ_π and σ_π are zero, the formula collapses to a standard Black-Scholes value.

The binary option package $V_{t_i}^{dibiJ}$ is calculated by subtracting the value of a down-and-out binary option from its own payoff, i.e. one, as the value of the down-and-out binary option equals the probability of being knocked-out and is mutually exclusive to the event of being knocked-in (Derman and Iraj,

---

[9]The interested reader is referred to Merton (1975), where he provides a rationale for the changes in interest rate and variance.

1996, 1997; Teneberg, 2012).

$$V_{t_i}^{dibiJ}(c_i, S^*, t) = \alpha \sum_{i=1}^{k} (1 - e^{-r_f t_i} - V_{t_i}^{dobiJ}) \qquad (3.37)$$

By setting the jump parameters λ, μ_π and σ_π to zero, the convergence between the analytical and approximated CoCo price can be studied. The convergence in figure 3.7 shows the well-known sawtooth behaviour when approximating options in a tree setting (see e.g. Boyle and Lau (1994)). The oscillation effect is somewhat dampened by the fact that different options with different error developments are combined. The annotations in the graph represent the Ritchken (2005) optimal points.

Similar to 3.32, the final value of the CoCo in the equity derivative model including jumps is

$$\mathrm{ED}_t = V_t^{cb} - V_{t_i}^{dibiJ} + V_t^{difwdJ} \qquad (3.38)$$
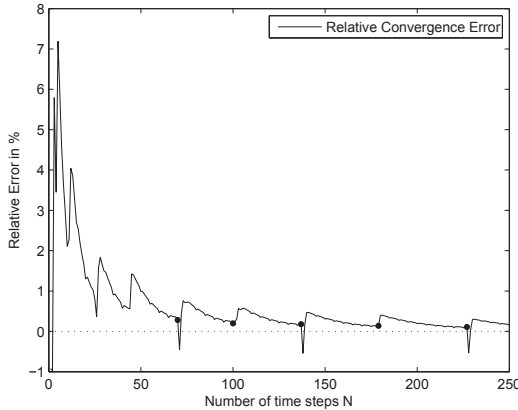
Figure 3.7: *Total CoCo convergence error in the equity derivative approach. The markers indicate the Ritchken (2005) optimal points. (based on: Teneberg (2012))*

3.2.5   Data Requirements and Calibration

The required input parameters of the equity derivative model are presented in table 3.7, along with the respective data source and if the value is updated dynamically or remains fixed over time.

Corporate Bond V_t^{cb} (subtable 3.7a)

The information concerning the bond specifics are readily available in the respective prospectus and do not change over time. The risk-free rate r_f is proxied by a government bond in the same denomination and with the same initial tenor as the CoCo bond to be valued.

Binary barrier option $V_{t_i}^{dibi(J)}$ and down-and-in forward $V_t^{difwd(J)}$ (subtable 3.7b)

The volatility σ to calculate the option values follows the same methodology as mentioned in subsection 3.1.3 of the credit derivative approach and uses the five year historic log-returns of the underlying share price as basis to calculate an annual standard deviation. The strike price K of the options correspond to the conversion price C_p and the share price S_t feeds into the model on a daily basis. The jump parameters λ, μ_π and σ_π are calibrated using the threshold exceedance method as described in section 3.1.3 of the credit derivative approach. Having parametrized the model, the trigger share price S^* is fitted by minimizing the root mean squared error to match the issuance price of the instrument and is thereafter kept constant.

$$V_t^{cb} = Ne^{-r_f(T-t)} + \sum_{i=t}^{T} c_i e^{-r_f t_i}$$

Variable	Description	Data source	Usage
N	Bond face value	Bond prospectus	Static
c_i	Coupon payments	Bond prospectus	Static
r_f	Risk-free rate	Market data	Dynamic
f	Coupon frequency	Bond prospectus	Static

(a) *Parameters to determine the corporate bond value in the equity derivative model.*

Table 3.7: *Parameter overview equity derivative model (continued)*

$$V_{t_i}^{dibi(J)}, V_t^{difwd(J)}$$

Variable	Description	Data source	Usage
α	Conversion fraction	Bond prospectus	Static
c_i	Coupon payments	Bond prospectus	Static
f	Coupon frequency	Bond prospectus	Static
r_f	Risk-free rate	Market data	Dynamic
q	Dividend yield	Market data	Static
S_t	Share price at time t	Market data	Dynamic
S^*	Trigger share price	Calibrated	Static
K	Strike price (equals conversion price)	Bond prospectus	Static
σ	Standard deviation of share price	Market data	Dynamic
λ	Jump intensity	Assumption	Static
μ_π	Mean jump size	Market data	Static
σ_π	Jump standard deviation	Market data	Static

(b) *Parameters to determine the binary barrier options and the down-and-in forward in the equity derivative model.*

Table 3.7: *Parameter overview equity derivative model. (based on: Wilkens and Bethke (2014))*

3.2.6 Pricing Example

Similarly to the pricing example provided in section 3.1.4 for the credit derivative approach also the yield and price in the equity derivative model for the same CoCo parameters shown in table 3.3 are computed.

For a five year maturity corporate bond V_t^{cb} with an annual coupon frequency and a coupon of 7%, the resulting present value is 118.09. The cash-flow array c_i, the respective discount factors $e^{-r_f t_i}$ and the present values $V_{t_i}^{cb}$ are shown in table 3.8. Furthermore, table 3.8 also shows the

t_i	c_i	N	$e^{-r_f t_i}$	$V_{t_i}^{cb}$	$V_{t_i}^{dibi}$	$V_{t_i}^{dibiJ}$
1	7		0.97	6.79	0.16	0.06
2	7		0.94	6.59	0.76	0.57
3	7		0.91	6.40	1.31	1.11
4	7		0.89	6.21	1.72	1.54
5	7	100	0.86	92.10	2.03	1.87
			$\sum$	**118.09**	**5.98**	**5.15**

Table 3.8: *This table shows the bond cash-flow array $V_{t_i}^{cb}$ and the value of the down-and-in binary options $V_{t_i}^{dibi(J)}$ in the equity derivative approach. (based on: De Spiegeleer and Schoutens (2011))*

corresponding binary barrier options $V_{t_i}^{dibi(J)}$ that are deducted from the individual coupon payments. The total value of V_t^{dibi} is 5.98 and 5.15 for V_t^{dibiJ} respectively. The down-and-in forward contract for this generic bond V_t^{difwd} equals $\frac{1 \cdot 100}{25} \cdot -1.03 = -4.12$ in a GBM setting and $V_t^{difwdJ} = \frac{1 \cdot 100}{25} \cdot -0.74 = -2.96$ in a JGBM setting. Interestingly, the value of the binary option package is slightly lower and the forward value is slightly higher in a jump setting than in a standard Black-Scholes setting. This is due to the fact that the variance has been kept constant in the JGBM model to be able to study the jump impact explicitly. Specifically V_t^{cJ} and V_t^{pJ} of the down-and-in forward package decrease slightly and V_t^{docJ} decreases as well, as the price of the down-

and-out call is very close to that of a standard call and lower diffusion volatility levels lower the price in spite of adding jumps (Joshi, 2003). In contrast the down-and-out put V_t^{dopJ} is worth a lot less than the standard put as it seizes to exist at levels when the standard put is deep in the money, therefore it actually profits from lower diffusion volatility levels and its price increases slightly (Derman and Iraj, 1996, 1997). The combined effect leads to slightly higher overall prices (i.e. less negative) for V_t^{difwdJ}. Similarly, the value of the down-and-out binary barrier option V_t^{dobiJ} increases with decreasing diffusion volatility, as the probability of being knocked-out decreases; as consequence the value of V_t^{dibiJ} decreases.

Figure 3.8 shows the values of the risk-free corporate bond, the binary options and the down-and-in forward. Clearly the value of the bond of 118.09 accounts for most of the final CoCo price whereas the binary option package provides a rebate of -5.98 / -5.15 and the down-and-in forward amounts to -4.12 / -2.96. The final CoCo price is 107.99 and 109.98 respectively. This results in a yield of $Y_{ED} = 5.02\%$ and $Y_{EDJ} = 4.63\%$.
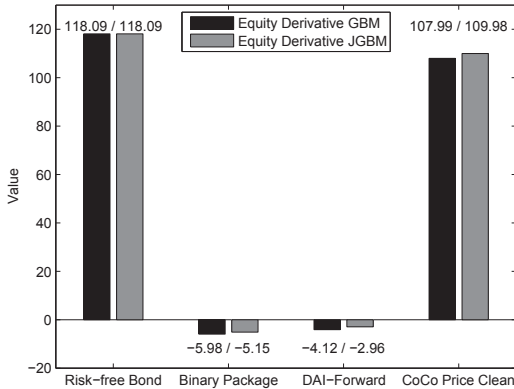
Figure 3.8: *This figure shows the decomposition of the CoCo price under the equity derivative approach as the sum of a risk-free corporate bond, a binary option package and a down-and-in forward.*

3.3   J.P. Morgan Model

The investment bank J.P. Morgan was among the first to address the issue of pricing contingent convertible capital. Henriques and Doctor (2011) propose a pricing approach that is based on CDS- and option-pricing methodologies, as they decompose a CoCo bond into a zero recovery portion that gets written down to zero and an amount that gets converted into equity upon a trigger event. The derivation follows Henriques and Doctor (2011).

Specifically, they consider a CoCo bond to be a bond, where the issuer has a long position in an option from the bondholder. The option is exercised at the occurrence of a trigger event such that the face value of the bond is (partly) converted into equity at a predetermined strike K (i.e. the conversion price). Depending on the trigger stock price S^* the bond holder might have to bear a write-down that equals the difference between the strike price K and the trigger stock price S^*, whereas the remaining amount is converted into equity. Table 3.9 illustrates this. For example if the bond notional N equals 100 and

$S^*/K\%$	$(K - S^*/K)\%$
Conversion to equity	Zero recovery / write-down

Table 3.9: *CoCo value decomposition in the J.P. Morgan approach. (source: Henriques and Doctor (2011))*

the strike K lies at 50 (i.e. $K\% = 50/100 = 0.5$) with a barrier stock price of $S^* = 40$, then an amount of $S^*/K\% = 40/0.5 = 80$ of the notional is converted into equity, whereas the remainder $(K - S^*)/K\% = (50 - 40)/0.5 = 20$ is written down to zero.

3.3.1   Zero Recovery Part $(K - S^*/K)\%$

The zero recovery portion is priced by combining quoted CDS spreads with option pricing methodologies to infer information of the underlying stock distribution. Using traded CDS spreads the cost for a CDS with no running

spread but only an upfront payment is calculated. Furthermore, by scaling up the recovery amount to 100% this can then be interpreted as paying upfront for a CDS that pays 100% in case of a default event and 0% otherwise. The next step involves backing out the implied volatility of a binary put option that pays 100% if the strike price K is hit and whose price is equivalent to aforementioned upfront CDS premium. The implied volatility computed in said step can then be used to price a binary put option that pays 100% in the case that the stock falls below a defined barrier S^*. As a final step, the cost of this option is converted into a running spread again using CDS pricing methodologies. This then yields the spread of the zero recovery part of the CoCo. In summary, Henriques and Doctor (2011) propose the following four steps to arrive at the final running spread:

1. Calculation of the up-front CDS payment

2. Backing out of the implied volatility of a binary put option

3. Pricing of a binary put option at the conversion threshold

4. Conversion of the cost of the binary put option into an implied running spread

Step one: Calculation of the up-front CDS payment
The calculation of the equivalent up-front CDS payment from a quoted running spread involves much of the same calculations as outlined already in section 3.1.1 of the credit derivative approach. Specifically, the credit triangle of equation (3.10) is used to determine a flat hazard rate, which is then utilized to calculate the unconditional default probabilities using (3.7) to appropriately discount the protection leg, i.e. the nominator of equation (3.20) of the CDS contract. The standard recovery rate R for subordinated corporate bonds equals 20% and must therefore be scaled up to 100% to reflect a full insurance contract.[10] Henriques and Doctor (2011) simply scale up the calculated

---

[10]E.g. the International Swaps and Derivatives Association (ISDA, 2013) assumes a 20% recovery rate in their standard model for European and North American corporate subordinated CDS contracts.

upfront premium by dividing it with $1 - R$. For example if the calculated upfront premium for a CDS that provides 60% indemnity in the case of a credit event is 10%, the payment for a CDS that provides full protection is $10\%/60\% = 16.6\%$. Figure 3.9 depicts the relationship between the quoted CDS spread and the required upfront payment for a recovery rate of 40% and 100%.
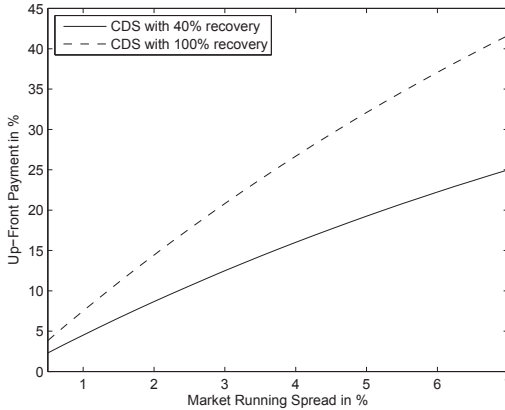
Figure 3.9: *This figure shows the up-front payment of a 5-year CDS contract with a recovery ratio of 40% and 100% as a function of the quoted running spread.*

Step two: Implied volatility at default

A key assumption that Henriques and Doctor (2011) make is that the implied volatility at default is equal to the implied volatility at the time of conversion. For this they set the level at which a default occurs to 5% of the current stock price.[11] The option of interest is a binary put option that pays out a fixed amount of one if the asset price is below the strike price at maturity. The value of such an option as shown by e.g. Hull (2009) is $V_t^{bip} = e^{-r_f(T-t)}\phi(-d_2)$, where d_2 is given as part of equation (3.36) in section

---

[11]Corcuera et al. (2013) find a similar default level of 6% by computing the weighted average of fifty EuroStoxxs CDS quotes and translating them into zero-recovery upfront premia, which they then compare with a range of digital put prices at different strike price levels.

3.2.4. Using the calculated upfront premium in step one as the price of the digital option with the strike set to 5% of the current stock price allows to back out the implied volatility of a T maturity binary put option. Figure 3.10 shows the implied volatility of a digital put as a function of the required CDS upfront payment from step one. The resulting volatility of this approximation serves as the assumed volatility that will prevail at the point of default.
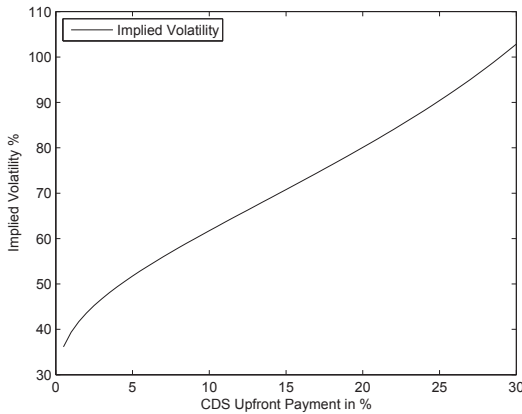
Figure 3.10: *This figure shows the implied volatility of a digital put option as a function of the CDS up-front payment.*

Step three: Pricing of a digital option at the conversion threshold
Given the volatility at default computed in step two another digital put option is priced at the conversion threshold S^*. Henriques and Doctor (2011) suggest that the trigger level S^* of the CoCo ought to be a function of the required loss that the solvency variable has to suffer, e.g. the CET1 ratio, in order to hit the trigger. This implies a linear relationship between the share price and the solvency variable. I.e. if the issuer has a minimum CET1 ratio of 10%, then the trigger level of the high-trigger CoCo tranche should be 30% and the low-trigger CoCo tranche at 50% below the share price at is-

suance. As will be seen later on, the trigger level S^* will be calibrated such that the model price meets the initial market price of the CoCo under consideration.

Step four: Conversion of the cost of the digital put option into an implied running spread

Step three results in the upfront price of a digital put option, whose strike lies at S^* and that pays 100% if it hits the strike. This upfront premium is again translated back into a running spread.

After this four step process the zero recovery component has been priced. The pricing of the remaining component that is converted into equity is described in the following subsection.

3.3.2 Equity Conversion Part $S^*/K\%$

Henriques and Doctor (2011) assume that the portion that gets converted into equity can be hedged with a CDS contract with zero recovery. This implies that if the conversion price is set to the contemporaneous stock price at the time of conversion, then the CoCo spread would coincide with the spread on a zero recovery CDS contract. Henriques and Doctor (2011) use the traded market spread of the same CDS contract that was used in step one above and scale it down to reflect a zero recovery CDS.

3.3.3 Jump Diffusion setting

The only difference in a JGBM setting to the approach outlined above involves step three, where the price of the binary put option is evaluated in a JGBM setting as opposed to a normal GBM setting at the implied volatility calculated in step two. Specifically, the price of the binary put option is evaluated as given in equation (3.35) in section 3.2.4 where V_t^{bip} corresponds to the normal GBM value with adjusted risk-free rate and variance as given by Merton (1975). For

ease of reference, the formula is given again below in equation (3.39)

$$V_t^{bipJ} = \sum_{n=0}^{\infty} \frac{e^{\lambda(1+k)(T-t)}n}{n!} V_t^{bip} \qquad (3.39)$$

and $V_t^{bip} = e^{-\bar{r}(T-t)}\phi(-d_2)$ with d_2 given in equation (3.36) in section 3.2.4.

3.3.4   Data Requirements and Calibration

The required parameters for the J.P. Morgan model are represented in table 3.10. The data sources and the calibration of the parameters is discussed subsequently in light of chapter 5, where a daily time series is generated as part of the empirical analysis.

Hazard rate λ_t (subtable 3.10a)
As primary input to calculate the upfront CDS premium of step one serves the hazard rate λ_t, which is extracted from market traded CDS spreads s_t. With the aim to generate a daily time series in chapter 5, the daily CDS spread s_t of an equivalent maturity subordinated bond of the issuer under consideration serves as input to generate daily updated hazard rates λ_t. The recovery rate R is kept constant over time.

Binary put value $V_t^{bip(J)}$ (subtable 3.10b)
To compute the implied volatility and subsequently the cost of a binary put option, the daily share price S_t, along with the upfront payment calculated from the hazard rate λ_t in step one, serves as primary input to the calculation. The assumed level of the share price at which default occurs is kept constant at 5%, as proposed by Henriques and Doctor (2011) and validated by Corcuera et al. (2013). Furthermore, the risk-free rate r_f is proxied by an equivalent maturity government bond of the same denomination as the CoCo bond. The dividend yield q is assumed to be constant and is estimated based on the five year dividend history of the company respecting any firm specific constraints as

mentioned in section 3.1.3. The conversion threshold S^* is calibrated once to match the initial market price of the CoCo bond and thereafter kept constant. The jump parameters λ_π, μ_π and σ_π are again extracted by means of the threshold exceedance method mentioned in section 3.1.3 of the credit derivative approach.

$$\lambda_t = \frac{s_t}{1-R}$$

Variable	Description	Data source	Usage
s_t	Quoted CDS spread	Market data	Dynamic
R	Recovery rate	Assumption	Static

(a) *Parameters to determine the upfront CDS spread in the J.P. Morgan model.*

$$V_t^{bip} = e^{-r_f(T-t)}\phi(-d_2), \quad V_t^{bipJ} = \sum_{n=0}^{\infty} \frac{e^{\lambda(1+k)(T-t)}{}_n}{n!} V_t^{bip}$$

Variable	Description	Data source	Usage
S^*	Trigger share price	Calibrated	Static
S_t	Share price at time t	Market data	Dynamic
σ_t	Implied standard deviation at $(S_t \cdot 5\%)$	Model dynamics	Dynamic
r_f	Risk-free interest rate	Market data	Dynamic
q	Dividend yield	Market data	Static
λ	Jump intensity	Assumption	Static
μ_π	Mean jump size	Market data	Static
σ_π	Jump standard deviation	Market data	Static

(b) *Parameters to determine the digital put price in the J.P. Morgan model.*

Table 3.10: *Parameter overview J.P. Morgan model. (based on: Wilkens and Bethke (2014))*

3.3.5   Pricing Example

The generic CoCo parameters lined out in table 3.3 in section 3.1.4 serve as input to compute a CoCo spread in the J.P. Morgan model by Henriques and Doctor (2011). As a further component, the CDS spread on a five year subordinated bond is assumed to be 2.5%.

Using the credit triangle of equation (3.10) and assuming a recovery rate of 20%, the implied hazard rate λ equals $\frac{0.025}{(1-0.2)} \cdot 100 = 3.13\%$. Using (3.7) the values in the second column of table 3.11 are calculated, which are then used to calculate the nominator of the CDS pricing formula in (3.20), where the time points t_i match the timing of the coupon payments. Therefore, for a contract

t_i	$p^*(t_i)$	$p^*(t_i) - p^*(t_{i-1})$	Contingent Leg
1	3.12%	3.12%	0.0242
2	6.15%	3.03%	0.0228
3	9.08%	2.93%	0.0214
4	11.91%	2.83%	0.0202
5	14.66%	2.75%	0.0190
		$\sum$	**0.1076**

Table 3.11: *Calculation of the CDS upfront premium in step one of the J.P. Morgan approach. (based on: Hull (2009))*

that pays 20% recovery in case of default the upfront cost is 10.76%. Scaling this to a contract that pays 100% in case of default yields $\frac{0.1076}{(1-0.2)} \cdot 100 = 13.45\%$. In a second step the implied volatility of a digital put option with a strike at 5% of the current spot price S that costs 13.45% is computed, which equals 75.22%. The price of a digital put with a volatility of 75.22% and a strike equal to $S^* = 20$ is 0.5480, which comprises the third step. Finally, the binary put value is converted into a running spread, which amounts to 17.68%.

The equity conversion part is calculated by dividing the initial CDS spread of 2.5% by 80% to reflect a zero recovery CDS contract. This amounts to

3.125%.

Since the trigger level $S^* = 20$ lies at 80% of the conversion price $C_p = 25$, the combined spread is $20\% \cdot 17.68\% + 80\% \cdot 3.125\% = 6.04\%$. Table 3.12 summarizes the different steps and also shows the digital put value as calculated in a JGBM setting. As expected, the digital put value is slightly lower when keeping the total variance constant. The resulting spread is almost the same for both approaches in this example; however, the values will differ more for different parameters and equity- / zero-recovery portions (cf. chapter 4). The

Instrument	Metric	Level	LevelJ	Step
CDS	5y spread	2.5%		Step 1
	Upfront	10.76%		
	Scaled Upfront	13.45%		
Equity	Implied volatility	75.22%		Step 2
	Digital put@S^*	0.549	0.546	Step 3
CoCo	Implied running spread	17.68%	17.59%	Step 4
	Zero recovery portion	20%		
	Zero recovery spread	3.125%		
	Equity portion	80%		
	CoCo spread	6.04%	6.02%	
	Risk-free rate	3%		
	CoCo yield	9.04%	9.02%	

Table 3.12: *This table shows the individual steps involved to calculate the CoCo spread in the J.P. Morgan model. (based on: Henriques and Doctor (2011))*

bond price calculated with $\sum_{i=1}^{T} CF_i e^{-Y_{CoCo(J)} \cdot t_i}$ amounts to JPM = 89.74 and JPMJ = 89.83 respectively; there is only a marginal price difference in the two approaches for this generic CoCo bond.

3.4 Structural Model

This section introduces a structural credit risk concept which has its roots in the famous Merton model that was introduced in 1974. The model postulates a default mechanism that depends on the relationship between the assets and liabilities at the end of a time period. The default event is therefore modeled endogenously as opposed to the credit derivative approach, which in itself can be seen as a reduced structural model, where default is determined exogenously. Specifically, a structural model considers a bank's balance sheet that is composed of assets, equity and debt where the assets follow a stochastic process and default occurs if the value of assets fall below the value of liabilities (Black and Scholes, 1973; McNeil et al., 2005b; Merton, 1974). E.g. Ingersoll (1977) applied this concept to value convertible securities.

The model that will be introduced is based on Pennacchi (2010), who modifies the structural model to incorporate equity, short-term deposits, subordinated debt and contingent capital.

3.4.1 Synthetic Balance Sheet

Asset Returns

The banks assets are funded with short-term deposits, long-term debt in the form of contingent capital or standard non-convertible subordinated debt and shareholders' equity. The total change in the quantity of assets is comprised of cash-in respectively cash-out flows plus the rate of return achieved on the investment. The assets can be invested in various positions that generate a return which follow a mixed jump-diffusion process as introduced previously in section 3.1.2. For ease of reference and to provide more details on how the process is incorporated into this model, the dynamics are repeated again below (Glasserman, 2004; Hull, 2009; Merton, 1975; Seydel, 2009).

$$\frac{dA_t^r}{A_t^r} = (r_t - q - \lambda k)dt + \sigma dW_t + (\Pi - 1)dY_t \qquad (3.40)$$

The superscript r indicates asset fluctuations exclusively due to changes in the return. Furthermore, dW_t is a Brownian motion, Π is an identically and independently distributed random variable drawn from $\ln(\Pi) \sim \phi(\mu_\pi, \sigma_\pi^2)$ at time t where μ_π is the mean jump size and σ_π the standard deviation of the jumps and dY_t is a Poisson counting process. The counting process Y_t is either zero when no Poisson event occurs or it augments by one whenever a jump occurs. The risk-neutral probability that a jump occurs and that Y_t increases by one is $\lambda_t dt$, where λ_t is the intensity of the jump process (Hull, 2009). Depending if the random variable is either greater or smaller than one there is an upward respectively a downward jump in the bank's asset value. For example Duffie and Lando (2001) interpret these discrete time points when finite jumps occur as times when newly available information has a higher than marginal impact on the asset value. Lastly, the risk-neutral expected proportional jump is defined as $E(\Pi) = k - 1$ where $k = e(\mu_\pi + \sigma_\pi^2/2)$ and the jump intensity and the risk neutral jump probability are assumed to be independent, then the change in the return over the time interval dt caused by the jump element $(\Pi - 1)dY_t$ is $\lambda_t k_t dt$ (Hull, 2009; Merton, 1975).

In order to include the payment of premiums to deposit holders h_t and coupon payments to debt holders $c_t^{c/f}$, as specified later on, Pennacchi (2010) adjusts the asset process in equation (3.40) to follow

$$dA_t = [(r_r - \lambda k_t)A_t - (r_t + h_t)D_t - c_t^{c/f}B]dt + \sigma A_t dz + (Y_t - 1)A_t dq \quad (3.41)$$

To include the deposit-growth process $g(\hat{x} - x_t)$ of equation (3.58), as defined later on, Pennacchi (2010) restates equation (3.41) and substitutes with $x_t = A_t/D_t$, which leads to[12]

$$\frac{dA_t}{A_t} = \left[(r_t - \lambda k) - \frac{r_t + h_t + c_t^{c/f} b_t}{x_t} \right] dt + \sigma dz + (Y_t - 1)dq_t \quad (3.42)$$

---

[12]Notice that the superscript r is no longer needed, as the asset process now not only includes value changes due to returns but also due to cash in- and outflows.

which now allows to include the deposit growth process of equation (3.58) by defining

$$
\begin{aligned}
\frac{dx_t}{x_t} &= \frac{dA_t}{A_t} - \frac{dD_t}{d_t} \\
&= \left[(r_t - \lambda k) - \frac{r_t + h_t + c_t^{c/f} b_t}{x_t} - g(x_t - \hat{x}) \right] dt + \sigma dz + (Y_t - 1)dq_t
\end{aligned}
$$

(3.43)

Finally, an application of Itô's lemma then allows Pennacchi (2010) to model the stochastic dynamics of this process as

$$
\begin{aligned}
dln(x_t) = &\left[(r_t - \lambda k) - \frac{r_t + h_t + c_t^{c/f} b_t}{x_t} - g(x_t - \hat{x}) - \frac{1}{2}\sigma^2 \right] dt \\
&+ \sigma dz + lnY_t dq_t
\end{aligned}
$$

(3.44)

Default-Free Term Structure

This model considers a stochastic interest rate environment to price both fixed- and floating-rate coupons for contingent capital.[13] Furthermore, the instantaneous maturity interest rate is the minimum interest rate that deposit holders receive, as will be shown later on, and it is used to discount the future cash-flows of the evaluated bond. To accurately reflect this, the equilibrium term structure model of Cox et al. (1985) is incorporated. It can be understood as an extension to the one factor model introduced in 1977 by Vasicek but which additionally includes a square-root diffusion term to prevent the interest rate r_t from becoming negative. Specifically, the risk adjusted dynamics of the instantaneous interest rate are defined by the following stochastic differential equation as shown by Cox et al. (1985)

$$
dr_t = \kappa(\bar{r} - r_t)dt + \sigma_r \sqrt{r_t}dW_t
$$

(3.45)

---

[13]Within this thesis only fixed coupon bonds are evaluated.

Where κ is the speed of convergence, $\bar{r}$ is the long-run equilibrium interest rate, r_t is the continuous short-term interest rate, σ_r is the instantaneous volatility and W_t is a Wiener Process. As stated above, the square root diffusion term $\sigma_r \sqrt{r_t}$ prevents the undesirable feature that r_t can become negative by linking the instantaneous volatility σ_t to the interest rate r_t, therewith converging to zero when r_t approaches the initial rate (Brigo and Mercurio, 2006; Carmona and Tehranchi, 2006). A sample evolution of the instantaneous maturity interest rate as well as three ten-year term structures with different initial rates r_0 have been plotted in figure 3.11 respectively figure 3.12.

To allow for comparative analysis with a default-free bond, consider the evaluation of a T-maturity unit discount bond $P(r,T)$ via (Cox et al., 1985)

$$P(r,T) = A(T)e^{-B(T)r} \tag{3.46}$$

with

$$A(t,T) = \left(\frac{xe^{y(T-t)}}{y(e^{x(T-t)} - 1) + x} \right)^z \tag{3.47}$$

$$B(t,T) = \left(\frac{e^{x(T-t)} - 1}{y(e^{x(T-t)} - 1) + x} \right) \tag{3.48}$$

$$x = \sqrt{\kappa^2 + 2\sigma_r^2} \tag{3.49}$$

$$y = \frac{\kappa + x}{2} \tag{3.50}$$

$$z = \frac{2\kappa\bar{r}}{\sigma_r^2} \tag{3.51}$$

A coupon bond can then be replicated as a portfolio of pure discount bonds of different maturities, and in turn a riskless coupon bearing bond $B(c,r,T)$ is the weighted sum of unit discount bonds (Longstaff, 1993)

$$B(c,r,T) = \sum_{i=1}^{N} c_i D(r,T_i) \tag{3.52}$$

where T_i represent the coupon payment dates in the amount of $c_i \geq 0$, with the last coupon payment including the face value. The par yield to maturity for a default free coupon bearing bond that matures in T years issued at date t is

$$c_r = \frac{1 - A(t,T)e^{-B(t,T)r_t}}{\int_0^{(t,T)} A(s)e^{-B(s)r_t}ds} \qquad (3.53)$$

$$\approx \frac{1 - A(t,T)e^{-B(t,T)r_t}}{\sum_{i=1}^{i=(T/dt)} A(dt \times i)e^{-B(dt \times i)r_t}dt} \qquad (3.54)$$
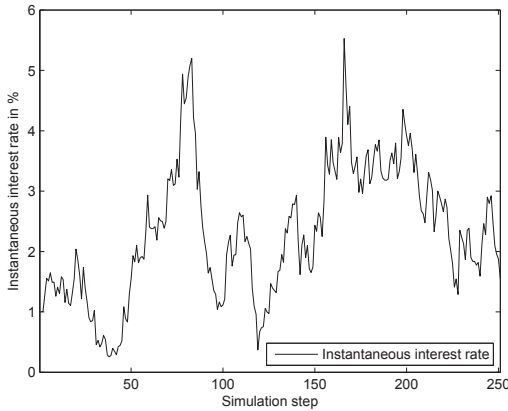
Figure 3.11: *This figure shows a sample evolution of the instantaneous maturity interest rate using the Cox et al. (1985) model with $\kappa = 0.0455, \bar{r} = 0.0483$ and $\sigma = 0.0746$.*

Deposits

The most senior source of funding of the bank are deposits D_t, which have an instantaneous maturity (i.e. overnight funds) and Pennacchi (2010) assumes that they are either partially or fully insured by e.g. a government insurer. The deposit holders receive the competitive instantaneous maturity default-free interest rate r_t. Furthermore, the instantaneous insurance premium h_t accounts for the risk-neutral expected loss per dollar of deposit. Deposit
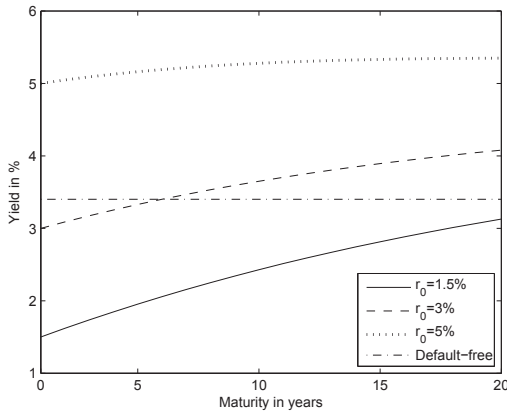
Figure 3.12: *This figure shows a Cox et al. (1985) 10-year term structure with different starting values r_0. The remaining parameters are $\kappa = 0.0455, \bar{r} = 0.0483$ and $\sigma = 0.0746$.*

holders can only suffer a loss if the asset value of the bank falls below the value of the deposits $A_t < D_t$ or equivalently $x_t < 1$, i.e. when bankruptcy occurs. This implies that only a discontinuous movement (i.e. a downward jump) in the asset value can impose a loss to the depositors. Hence the credit risk premium h_t must incorporate the risk-neutral expectation of the instantaneous proportional loss incurred to deposits if such a jump occurs $(D_t - Y_t A_t / D_t)$. Pennacchi (2010) goes on to show that h_t changes continuously depending on the asset-to-deposit ratio x_t

$$h_t = \lambda \left[\phi(-d_1) - x_t e^{(\mu_\pi + 0.5\sigma_\pi^2)} \phi(-d_2) \right] \tag{3.55}$$

$$d_1 = \frac{\log(x_t) + \mu_\pi}{\sigma_\pi} \tag{3.56}$$

$$d_2 = d_1 + \sigma_\pi \tag{3.57}$$

For non-insured deposits the insurance premium h_t can be understood as a credit risk premium in favor of the deposit holder. Therefore, the total cost of

deposits amounts to $(r_t + h_t)D_t dt$ (Pennacchi, 2010).

Studies by e.g. Adrian and Shin (2010), Memmel and Rapauch (2010), Flannery and Rangan (2008) or Collin-Dufresne and Goldstein (2001) show that banks have a certain target leverage ratio and that deposit growth is positively correlated to the amount of capital. Furthermore, within the Basel III framework and the Swiss finish banks have to adhere to a minimum amount of capital-to-assets. Within this model, the target leverage ratio is expressed as an asset-to-deposit ratio $x_t \equiv \frac{A_t}{D_t}$. To incorporate the positive correlation between the amount of capital and deposits, Pennacchi (2010) links the deposit growth to the asset-to-deposit ratio as shown in equation (3.58).

$$\frac{dD_t}{D_t} = g(\hat{x} - x_t)dt \qquad (3.58)$$

The reversion to the target asset-to-deposit ratio $\hat{x} > 1$ happens at the speed of $g > 0$. For example if $x_t > \hat{x}$ the bank would increase its deposits D_t and hence increase its leverage to converge to its target asset-to-deposit ratio $\hat{x}$ at a rate of g in each time step dt.

Contingent Convertible Capital

Alternatively to subordinated debt the banks' long-term financing can take the form of contingent convertible capital that has a par value B and pays a continuous coupon $c_t B dt$ during its lifetime. The coupon rate can either be a fixed-rate $c_t^c = c$ or a floating-rate coupon $c_t^f = r + s$, where s denotes a fixed spread over the instantaneous maturity interest rate r_t (Pennacchi, 2010). Conversion into common shareholders' equity occurs at a prespecified asset-to-deposit ratio $x_t \leq x^*$ or equivalently total capital-to-assets of $(1 - 1/x^* = (A_t - D_t)/A_t)$. The value of contingent capital at the date of conversion V_{t_c} depends on the banks' remaining equity capital $A_{t_c} - D_{t_c}$. Similarly to Wilkens and Bethke (2014) the fact that most CoCo issuances have a specified conversion price is incorporated via the conversion ratio p, which reflects the conversion fraction of the CoCo bond. Using the fact that the stock price S_{c-}

as well as the number of shares prior to conversion N_{c-} is known and due to the specified conversion price C_p the newly created number of shares N_c is also known, the following relationship holds

$$N_0 S_{c-} + N_c S_c = (N_0 + N_c) S_{c+} \tag{3.59}$$

Therefore, one can work out the adjusted share price after the conversion S_{c+}, giving the conversion fraction $p = \frac{S_{c+}}{C_p}$. To determine the CoCo price, the coupon payments c_i and the nominal value B are discounted using the risk-free discount rate r_f from the Cox et al. (1985) process (Cochrane, 2009; Hull, 2009)

$$V_0 = E_0 \left[\int_0^T e^{-\int_0^t r_f \, dt} v(t) dt \right] \tag{3.60}$$

and compared to the par value B. Coupon payments are continuously paid up to the point of conversion t_c, where a one time cash flow equal to pB takes place; subsequently for all $t > t_c$, $v(t) = 0$.

3.4.2   Data Requirements and Calibration

The model requires a list of parameters, which mostly are not directly observable and thus have to be approximated or otherwise assumed. Furthermore if modeling a time series of CoCo prices some parameters remain constant over time and some have a dynamic nature. An overview of the parameters is provided in table 3.13.

Asset return process (subtable 3.13a)
The model simulates the evolution of the assets as well as the deposits by linking the latter to a target asset-to-deposit ratio. Hence both the amount of assets as well as the amount of deposits is required to evaluate the current asset-to-deposit ratio. In line with Wilkens and Bethke (2014) and Bürgi (2013) the values for the assets A_t are represented as the sum of the daily

total liabilities D_t and the daily market capitalization E_t of the company; the latter is readily available on a daily basis whereas the former is linearly interpolated between reporting periods to arrive at daily values. Assuming an efficient market should ensure that effects of divergence between market and book values of assets are reflected in the market capitalization (Bini and Penman, 2013; Bürgi, 2013). In keeping with the assumption of a correlation between the market capitalization and the total asset value, the asset volatility is calculated as

$$\sigma_{A_t} = \sigma_{E_t} \frac{E_t}{A_t} = \sigma_{E_t} \frac{E_t}{D_t + E_t} \tag{3.61}$$

which is based on the boundary conditions of Merton (1974). Finally the jump intensity λ and the parameters of the jump distribution $\phi(\mu_\pi, \sigma_\pi)$ result from the threshold exceedance method as explained in section 3.1.3 of the credit derivative model.

Interest rate process (subtable 3.13b)

Following Duan and Simonato (1999) the parameters for the term structure process are calibrated using a Kalman-Filter.[14] The calibration takes monthly yield series with maturities of 3, 6, 12 and 60 months as input and calibrates the speed of conversion κ, the equilibrium interest rate $\bar{r}$ and the standard deviation σ_r accordingly, which serve as input to equation 3.45. The associated standard errors are determined via the inverse of the negative Hessian matrix. This is ideally done on the yield series of the base currency of the bond, i.e. for a USD denominated bond the monthly U.S. treasury bill yield series are used.

Deposit growth process (subtable 3.13c)

The mean reversion speed g of the deposit growth process in equation (3.58) is set to 0.5. This means that it would take the bank around three years to

---

[14]See e.g. Harvey (1990) for more details on Kalman-Filtering in combination with econometric and time series concepts.

reach its target asset-to-deposit ratio $\hat{x}$. The initial asset-to-deposit ratio x_t is determined from the daily asset values V_t and the interpolated liabilities D_t as explained above. The target asset-to-deposit ratio $\hat{x}$ can be interpreted as the newly imposed minimum leverage ratio of Basel III, to which banks have to adhere to. Details on the parametrization are described as part of the empirical analysis in chapter 5.

$$\frac{dA_t^r}{A_t^r} = (r_t - q - \lambda k)dt + \sigma dW_t + (\Pi - 1)dY_t$$

Variable	Description	Data source	Usage
r_0	Initial risk-free interest rate	Market data	Dynamic
r_t	Instantaneous maturity interest rate	Interest-rate process	Dynamic
σ_{V_t}	Volatility of asset returns (annual)	Market data	Dynamic
λ	Risk-neutral frequency of jumps	Assumption	Static
μ_π	Risk neutral mean jump size	Market data	Static
σ_π	Standard deviation of jumps	Market data	Static

(a) *Parameters of the jump diffusion process for asset returns (for simplicity the pure return process is shown here).*

$$dr_t = \kappa(\bar{r} - r_t)dt + \sigma_r\sqrt{r_t}dW_t$$

κ	Speed of convergence	Calibrated	Static
$\bar{r}$	Long-term interest rate	Calibrated	Static
r_t	Instantaneous maturity interest rate	Interest-rate process	Dynamic
σ_r	Standard deviation of interest rate	Calibrated	Static

(b) *Parameters of the Cox et al. (1985) term structure process.*

Table 3.13: *Parameter overview structural model* (continued)

$$\frac{dD_t}{D_t} = g(\hat{x} - x_t)dt$$

Variable	Description	Data source	Usage
g	Speed of convergence	Assumption	Static
$\hat{x}$	Target asset-to-deposit ratio	Balance sheet	Static
x_t	Current asset-to-deposit ratio	Asset return process	Dynamic
V_t	Asset value	Market data	Dynamic
D_t	Debt value	Market data	Dynamic

(c) *Parameters of the deposit growth process.*

Table 3.13: *Parameter overview structural model. (based on: Wilkens and Bethke (2014))*

3.4.3 Pricing Example

Also for the structural approach the generic CoCo bond parameters from table 3.3 serve to calculate a pricing example. Due to the model's complexity a number of additional parameters as outlined in table 3.14 below must be set. As a base case the starting assets V_0 are set to 1000 and the starting

Variable	Description	Value
V_0	Asset value	1000
D_0	Debt value	880
E_0	Equity value	120
N_0	Number of original shares	3
B	CoCo value	25
N_c	Number of new shares	1
$\hat{x}$	Target asset-to-deposit ratio	112%
x^*	Trigger asset-to-deposit ratio	106.82%
σ_V	Volatility of asset returns	3.33%
μ_y	Risk neutral mean jump size	0%
σ_y	Standard deviation of jumps	0.024%
κ	CIR Speed of convergence	0.0413
		(0.0109)
$\bar{r}$	Long-term interest rate	7.42%
		(0.0192)
σ_r	Standard deviation of interest rate	4.81%
		(0.0019)
g	Deposit-growth speed of convergence	0.5

Table 3.14: *This table presents the additional CoCo price parameters to price the generic CoCo outlined in table 3.3 in the structural model.*

equity E_0 to 120, which is the share price S_0 of 40 multiplied by an assumed amount of outstanding shares N_0 of 3. This leaves the debt value (including the CoCo value) at $D_0 = 880$. This results in a starting capital-to-asset

ratio of $\frac{120}{1000} \cdot 100 = 12\%$, or equivalently an asset-to-deposit ratio x_0 of $\frac{1000}{880} \cdot 100 = 113.64\%$ and a capital-to-deposit ratio of $\frac{120}{880} \cdot 100 = 13.64\%$. The conversion is triggered when the asset value falls to 940, i.e. at a critical asset-to-deposit ratio x^* of $\frac{940}{880} \cdot 100 = 106.82\%$. The target asset-to-deposit ratio $\hat{x}$ is set at 112%, which means that the bank starts out slightly overcapitalized.

To translate the equity volatility $\sigma_E = 30\%$ into an equivalent asset volatility σ_V, the equity volatility σ_E of 30% is de-levered by rearranging equation (3.61) for σ_V, which results in $\sigma_V = \frac{\sigma_E E_0}{V_0} = \frac{0.3*120}{1000} \cdot 100 = 3.33\%$. Similarly the jump component is de-levered in the same way, which yields a jump volatility of 0.024%. In line with the other pricing examples, the total volatility is kept constant at 3.33% according to equation (3.62).

$$\sigma_J^2 = \sigma^2 + \lambda(\mu_\pi^2 + \sigma_\pi^2) \tag{3.62}$$

In this pricing example, the number of newly created shares in case of a conversion is given by the CoCo amount B divided by the conversion price C_p of 25, which equals exactly one share. At the trigger level of x^* the assets are worth 940, leaving the equity worth 60 and the stock price prior to conversion S_{c-} 20. After conversion, equity is worth 85 with 4 shares outstanding, leaving the adjusted share price after conversion S_{c+} at 21.25. As the single CoCo holder paid 25 for the stock, there is a value shift from the CoCo holder to the shareholder, as the former takes an immediate loss of 15%. This is assuming that x^* is approached continuously. When allowing for discontinuous drops in the asset values, the recovery rate is expected to be lower, which is what could be observed in the credit derivative model as well.

Running the simulation with these parameters yields a price of 107.95 [107.75, 108.13] and 106.41 [106.24, 106.65] when including jumps. The 95% confidence interval is given in brackets. This corresponds to a yield of 5.18% [5.14%, 5.22%] and 5.52% [5.46%, 5.55%].

3.5   Intermediary Conclusion

Clearly CoCos already form an integral part of the debt markets and issuances
are foreseen to grow stronger, as the new capital requirements by Basel III and
particularly the case for Switzerland allow that the higher capital requirements
can be partially met with contingent convertible capital. Furthermore it has
been shown, that the CoCo specific conversion designs allow for very different
implementations, which can have a substantial impact on the associated risk-
profile from a share- respectively a bondholder perspective. As the qualitative
discussion would suggest to optimally use a market trigger as indication for
the conversion event, the regulators and therefore the issuers are clearly opting
for accounting based triggers, mostly in connection with a regulatory trigger
as well. Such an implementation makes valuation more difficult, as the clarity,
objectivity and transparency of the trigger event is attached with uncertainties.

The implementation of the pricing models revealed key differences with
respect to their complexity, parametrization and price examples. Reverting to
the four main value drivers as outlined in section 2.2, the following conclusions
can be drawn: None of the models include all value drivers, most importantly
though, the bond price components, i.e. the coupon and final principal, are
included in all models. In the J.P. Morgan approach, this is implicitly included
in the CDS spread (indicated as '(o)' in table 3.15), as this product reflects
the insurance premium on a regular corporate bond with all its associated
cash-flows. If a conversion takes place, none of the models include the dividend
payments that a shareholder is entitled to. The final equity value is only
included in the equity derivative model through the down-and-in forward
contract. Those findings are summarized in table 3.15, where 'o' indicates that
the value driver is included in the model, whereas 'x' indicates that it is not
included.

As shown in table 3.16 the prices of the generic CoCo bond are rather
closely distributed for all models except for the J.P. Morgan model, which
indicates a much higher yield. However, the CDS level at 250 basis points has

been chosen rather high, which is reflected in the price.

Clearly the complexity of the implementation is highest in the equity deriva-
tive model with discontinuous returns, as the barrier options must be evaluated
with advanced numerical techniques. The easiest to implement certainly is
the credit derivative model in a normal Black-Scholes setting, as the closed
form solutions are quickly implemented. Furthermore, all closed-form solutions
naturally lead to computationally more efficient prices, whereas the applied
simulation techniques take a toll on computational time, sometimes taking
multiple minutes to calculate one price.

It will be interesting to see how on the one hand the models react to
different initial parameters as shown in the subsequent chapter 4 and on the
other hand how significantly this will impact the empirical time series analysis
of chapter 5.

Value Driver	CD	ED	JPM	ST
Coupons	o	o	(o)	o
Principal	o	o	(o)	o
Dividends	x	x	x	x
Equity value	x	o	x	x

Table 3.15: *This table shows the value drivers that are included in the models. CD stands for the credit derivative model, ED for the equity derivative model, JPM for the J.P. Morgan model and ST for the structural model. 'o' indicates that the respective value driver is included in the model, whereas 'x' indicates that it is not included; '(o)' stands for an implicit inclusion.*

Model	Price	Yield
CDC	110.02	4.65%
CDCJ	109.69 [109.59, 109.78]	4.72% [4.70%, 4.74%]
CDP	109.97	4.66%
CDPJ	109.03 [108.89, 109.17]	4.86% [4.83%, 4.89%]
ED	107.99	5.02%
EDJ	109.98	4.63%
JPM	89.74	9.04%
JPMJ	89.83	9.02%
ST	107.95 [107.75, 108.13]	5.18% [5.14%, 5.22%]
STJ	106.41 [106.24; 106.65]	5.52% [5.46%; 5.55%]

Table 3.16: *This table shows the prices and yields obtained in the different models for the generic CoCo bond. CD(C/P) stands for the credit derivative model with (piecewise-)constant conversion intensity, ED for the equity derivative model, JPM for the J.P. Morgan model and ST for the structural model. The indicator J stands for the models including jumps. The values in brackets stand for the 95% confidence interval.*

This page intentionally left blank.

Chapter 4

Dynamics and Sensitivity Analysis

Chapter 3 has provided the theoretical setting of the different pricing models and has also introduced preliminary pricing examples. Furthermore, the different pricing parameters and therewith the necessary data requirements have been outlined. This chapter investigates the sensitivity of the models with respect to their primary input parameters. This will allow to assess the price impact a single variable has, while keeping the remaining parameters constant. Specifically, the four models are analysed towards changes in the underlying share price $\Delta = \frac{\delta V}{\delta S}$, the volatility of the share price $\kappa = \frac{\delta V}{\delta \sigma}$, the risk-free interest rate $\rho = \frac{\delta V}{\delta r}$ and the maturity $\Theta = \frac{\delta V}{\delta \tau}$ (Hull, 2009). Moreover, to honour the CoCo specific parameters, changes in the conversion price C_p and the trigger level S^* are also investigated. To discriminate between the models that allow for discontinuous returns versus the closed-form models, different jump intensities λ will be checked. Unless otherwise indicated, the model parameters correspond to the base parameters as outlined in the previous chapter in table 3.3 for the credit and equity derivative model as well as the J.P. Morgan model and the additional base parameter set in table 3.14 for the structural model.

4.1   Credit Derivative Model

The left-hand side diagram in figure 4.1 displays how the CoCo price reacts to changes in the stock price S at different volatility levels σ. What can be observed is that with an increasing stock price the CoCo price increases as well, respectively the required CoCo yield decreases. As the current stock price S moves further away from the trigger level S^*, the probability of conversion decreases, therefore decreasing the required yield. On the other hand, an increase in the volatility level σ has a countering effect, as this increases the conversion probability, thus lowering the overall CoCo price. On the right-hand side in figure 4.1 the CoCo price as a function of maturity T is depicted for different risk-free interest rates r_f. Increasing the risk-free rate has a two-fold effect on the final price of the CoCo: Due to the increased growth rate the probability of conversion decreases but at the same time the required yield - including the risk-free rate - by the CoCo investor increases. For longer maturities the former effect outweighs the latter, but there is a slight dip for shorter maturities at a level of 5% for the risk-free rate. Figure 4.2 shows the same analysis for piecewise constant conversion intensities with very similar patterns. The only discernable difference can be observed for stock price levels close to the trigger level, where the piecewise constant model reacts more sensitive to changes and exhibits a larger delta.

Figure 4.3 shows the CoCo price as a function of the trigger price S^* for different conversion price levels C_p on the left-hand side and the CoCo price as a function of the stock price S when returns are discontinuous at different levels of the jump intensity λ. As the recovery ratio R_{CoCo} in the credit derivative approach results from the division of the trigger price S^* by the conversion price C_p, the closer the trigger price is to the conversion price, the higher is the recovery ratio and the CoCo price. However, as the trigger price gets closer to the current stock price, the trigger probability increases, reducing the CoCo price. This opposing effect can lead to a double equilibrium price (De Spiegeleer and Schoutens, 2011). Adding the possibility of discountinuous

Figure 4.1: *The plot on the left shows the sensitivity of the credit derivative approach with constant conversion intensity towards changes in the stock price S for different levels of volatility σ. The plot on the right shows the sensitivity of the credit derivative approach with constant conversion intensity for different maturities T at different risk-free interest rate levels r_f.*

Figure 4.2: *The plot on the left shows the sensitivity of the credit derivative approach with piecewise constant conversion intensity towards changes in the stock price S for different levels of volatility σ. The plot on the right shows the sensitivity of the credit derivative approach with piecewise constant conversion intensity for different maturities T at different risk-free interest rate levels r_f.*
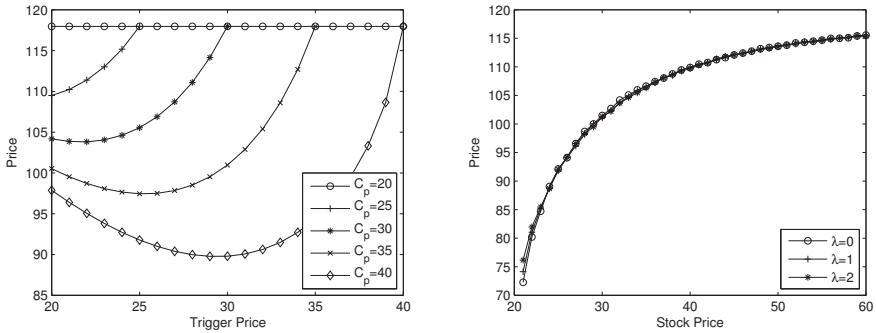
Figure 4.3: *The plot on the left shows the sensitivity of the credit derivative approach with constant conversion intensity towards changes in the trigger price S^* for different levels of the conversion price C_p. The plot on the right shows the sensitivity of the credit derivative approach with constant conversion intensity when introducing jumps λ at different stock price levels S.*

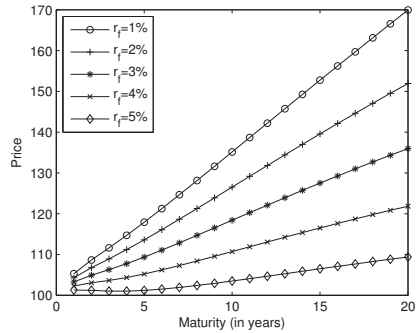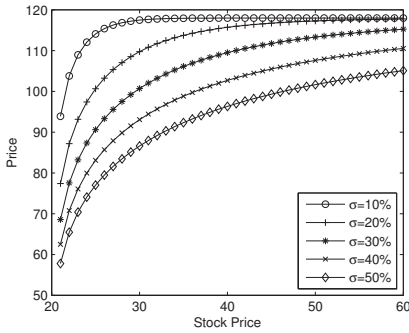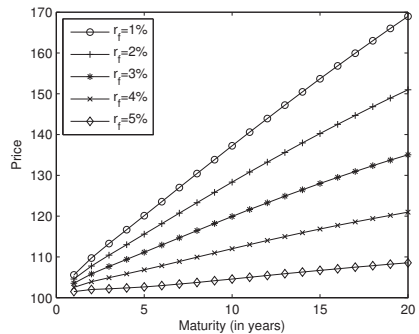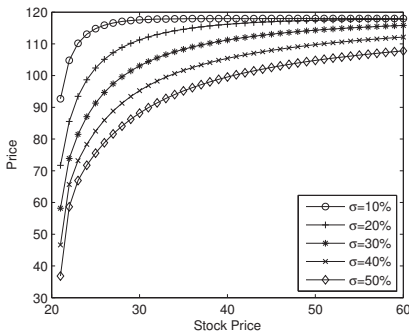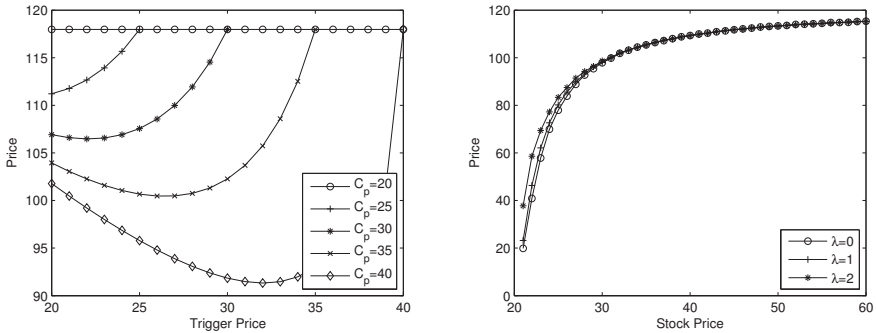**Figure 4.4:** *The plot on the left shows the sensitivity of the credit derivative approach with piecewise constant conversion intensity towards changes in the trigger price S^* for different levels of the conversion price C_p. The plot on the right shows the sensitivity of the credit derivative approach with piecewise constant conversion intensity when introducing jumps λ at different stock price levels S.*

returns through the jump diffusion process leads to almost the same CoCo prices, where the only discernable difference is for stock price levels close to the trigger level. For higher stock price levels, the effect of the overall lower conversion probability and the lower recovery ratio seem to offset each other, ultimately leading to the same CoCo prices irrespective of the amount of jumps. An effect which could already be observed in the pricing example in section 3.1.4. Again the same analysis is also shown for the credit derivative model with piecewise constant conversion intensities in the right-hand side graph of figure 4.4, where the difference is slightly more outspoken for stock price levels close to the trigger price.

4.2 Equity Derivative Model

Performing the same analysis for the equity derivative model yields qualitatively similar results to the credit derivative model. The left-hand side diagram in figure 4.5 shows the CoCo price as a function of the stock price S at different volatility levels σ, whereas the right-hand side graph shows the CoCo price as a function of maturity T for different risk-free interest rate levels r_f. Again the price increases the further away the stock price is from the trigger price S^* until eventually the CoCo price reaches the price of a risk-free bond. Interestingly, independent of the volatility level all prices converge when the stock price approaches the trigger level $S^* = 20$ as the knock-out options and the down-and-in forward reach the same value because they share the same strike and maturity structure. With increasing volatility, the down-and-in forward as well as the binary option package gets more expensive and therefore reduces the price. The right-hand side diagram looks very similar to the case of the credit derivative approach. The main price driver in the equity derivative model is the corporate bond value, which is discounted using the risk-free rate. Therefore, with increasing r_f and considering higher discount factors for increasing maturities, the overall CoCo bond value decreases at higher levels of r_f. Obviously, with increasing maturity a larger cash-flow stream from the

coupon payments is expected, which raises the price for longer maturity bonds.

Figure 4.6 shows the CoCo bond price as a function of the trigger level S^* for different conversion price levels C_p on the left-hand side. The right-hand side graph shows the CoCo bond price as a function of the stock price when introducing different jump intensities λ. As long as the trigger price S^* is below the conversion price C_p, which corresponds to the strike price K of the option package, the short put of the synthetic forward is in the money whereas the long call is out of the money. This reduces the overall CoCo price. A low conversion price C_p would therefore be favorable to the investor, which is reflected in the higher prices for lower conversion price levels (Alvemar and Ericson, 2012). Interestingly for high levels of the conversion price also the equity derivative model is challenged with a double equilibrium problem, as two levels of the trigger price lead to the same CoCo value. Introducing jumps at different levels of the stock price in the equity derivative approach has a counterintuitive effect at first sight, as the price increases when adding jumps. This effect can be explained by the fact that the total process variance is kept constant, therefore reducing the volatility of the continuous diffusion process at the cost of adding jump induced volatility, with the effect that the down-and-in forward and the binary option package provide less of a rebate. The same effect was shown in the pricing example in section 3.2.6 and is in line with observations by Teneberg (2012), who evaluates different ranges of jump intensities and jump standard deviations.

4.3   J.P. Morgan Model

Figure 4.7 shows the J.P. Morgan CoCo price as a function of the CDS price s_t for different stock price levels S in the left-hand graph as well as the impact of varying maturities T and risk-free interest rates r_f in the right-hand side graph. In general, an increase in the CDS level leads to an increase in the spread of the equity portion, which is what can be observed in the left-hand diagram in figure 4.7. Furthermore, a higher initial CDS spread increases the

Figure 4.5: *The plot on the left shows the sensitivity of the equity derivative approach towards changes in the stock price S for different levels of volatility σ. The plot on the right shows the sensitivity of the equity derivative approach for different maturities T at different risk-free interest rate levels r_f.*
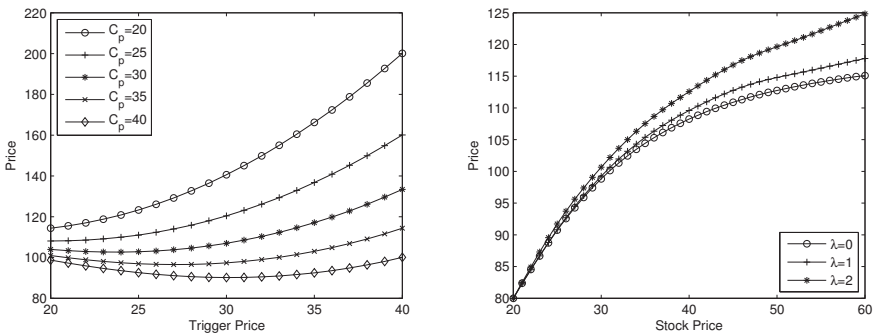
Figure 4.6: *The plot on the left shows the sensitivity of the equity derivative approach towards changes in the trigger level S^* for different levels of the conversion price C_p. The plot on the right shows the sensitivity of the equity derivative approach when introducing jumps λ at different stock price levels S.*

level of the implied volatility and as a result the spread on the zero recovery portion increases as well, leading to lower CoCo prices. Recalling that the spot price in combination with the assumed strike level of 5% determines the OTM-level (out-of-the-moneyness) at which the implied volatility is calculated, it becomes clear that lower spot prices result in deeper out-of-the-money levels at which the implied volatilities are calculated and ultimately lead to higher spreads and lower prices (Henriques and Doctor, 2011).

The right-hand side graph in figure 4.7 shows that an increasing maturity generally leads to higher required upfront payments for the CDS contract, which is more pronounced for lower interest rates as the discounting effect is lower. This ultimately reduces the spread on the zero recovery portion, thus increasing the CoCo price. For higher risk-free interest rates, this effect is offset by the fact that the required CoCo yield, i.e. the CoCo spread including the risk-free rate, increases more in proportion.

Figure 4.8 shows the CoCo price as a function of the trigger price S^* for different conversion price levels C_p in the left-hand diagram. As the trigger price divided by the conversion price determines the equity respectively the zero recovery portion, it can be observed that as soon as the trigger price is above the conversion price, the CoCo price is solely set by the spread on the equity portion. Contrarily, as the trigger price decreases, the zero recovery portion increases, ceteris paribus decreasing the price. At lower trigger levels not shown here, the value of the binary put would continue to decrease as it moves further out of the money, which ultimately would lead to a convex evolution of the price curve and raise the issue of a double equilibrium, as encountered with the credit derivative approach.

The right-hand diagram in figure 4.8 shows the CoCo price evolution as a function of the OTM level when adding jumps. The OTM level corresponds to the different strike levels at which the implied volatility of the digital option is evaluated. Thus, the lower the strike level (the higher the OTM level) the higher is the implied volatility of the digital option, which in turn increases the CoCo spread and lowers the CoCo price. As already seen in the pricing

example in chapter 3.3, the addition of jumps has virtually no impact on the resulting price in the J.P. Morgan model. The only influence it has is on the binary put price, which almost stays the same in a setting where the total variance is kept constant.
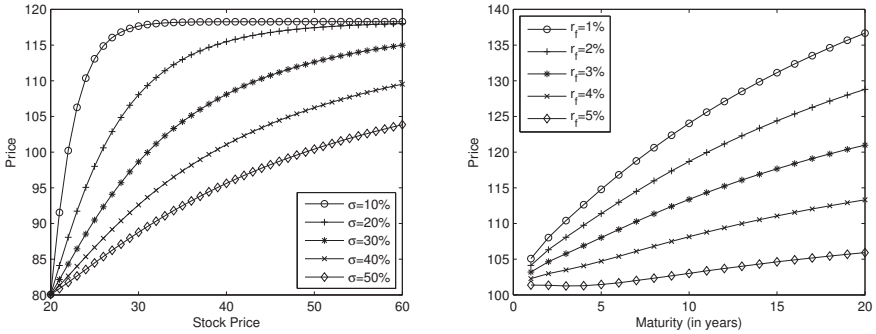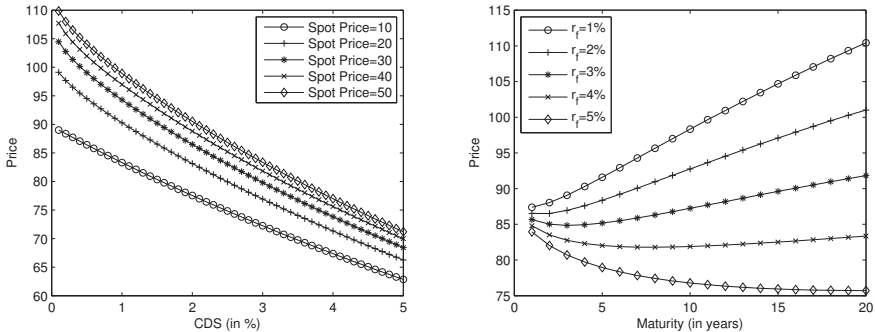

Figure 4.7: *The plot on the left shows the sensitivity of the J.P. Morgan approach towards changes in the CDS price level for different levels of the spot stock price S. The plot on the right shows the sensitivity of the J.P. Morgan approach for different maturities T at different risk-free interest rate levels r_f.*

## 4.4 Structural Model

The same analysis is conducted for the structural model. Figure 4.9 shows the CoCo price as a function of the starting value of assets to deposits x_0 at different volatility levels σ on the left-hand side and the CoCo price as a function of maturity T for different risk-free interest rate levels r_f on the right-hand side. With an increasing starting level of assets to deposits x_0 the likelihood that the conversion threshold is going to be hit decreases, therefore increasing the CoCo price. Expectably, if the volatility of the asset process increases the evolution of the asset to deposit ratio is more volatile, which increases the probability of hitting the threshold thus reducing the price level.

Increasing the maturity generally has a positive effect on the CoCo price, as
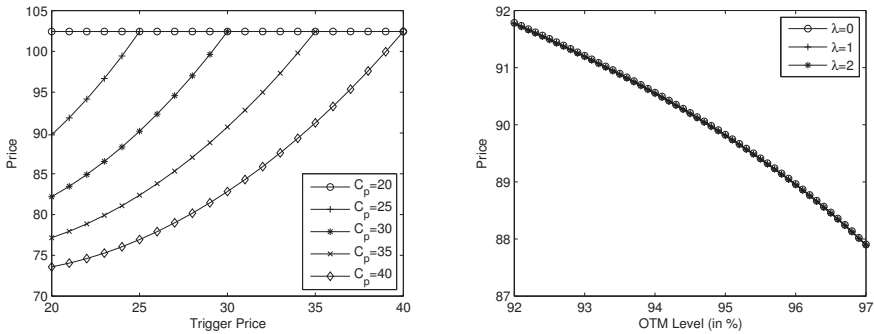
Figure 4.8: *The plot on the left shows the sensitivity of the J.P. Morgan approach towards changes in the trigger level S^* for different levels of the conversion price C_p. The plot on the right shows the sensitivity of the J.P. Morgan approach when introducing jumps λ at different OTM levels.*

the number of the discounted coupon payments increase and the likelihood of a conversion remains relatively low. For well capitalized banks (as is the case here) the required yield would approach the default free yield as calculated in the Cox et al. (1985) term structure process (Pennacchi, 2010). A familiar picture presents itself when increasing the risk-free interest rate r_f, which increases the discount factors but on the other hand increases the growth rate of the asset process as well. However the former effect outweighs the latter, especially so because the bank is well capitalized.

The left-hand side diagram in figure 4.10 shows the CoCo price as a function of the starting asset to deposit ratio x_0 for different conversion threshold levels x_c. The right-hand side graph shows the effect of adding jumps λ for different starting asset to deposit values x_0. As to be expected, raising the trigger threshold x_c increases the probability that the CoCo is converted early on and therefore reduces the price. Even though the probability of conversion is at its lowest at a level of conversion of 106% of assets to deposits, the price practically coincides with the conversion level of 107%. This can be explained by the fact that at lower conversion levels the possibility increases that not the

entire CoCo value can be converted and the CoCo investor faces a loss at the trigger event (i.e. the recovery amount decreases), which poses a counteracting effect.

It is evident in the right-hand graph of figure 4.10 that increasing the jump intensity increases the probability of a conversion and therefore decreases the price level of the CoCo. Further to increasing the conversion probability also the recovery rate is on average lower with discontinuous asset returns. For asset to deposit ratios close to and far away from x^*, the difference is less outspoken as the trigger probability is high in the first case and low in the second case, where the addition of jumps shows less of an impact.

Finally, figure 4.11 shows the CoCo price for different starting values of assets to deposits x_0 at different conversion price levels C_p. As the conversion price increases, the loss that a CoCo investor might face at the trigger event is higher than with a lower conversion price. Obviously, for lower asset to deposit ratios this is accentuated because the probability of a conversion is increased.
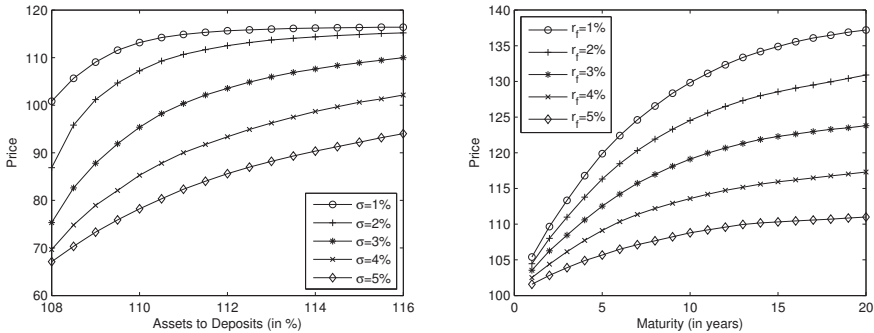
Figure 4.9: *The plot on the left shows the sensitivity of the structural model towards changes in the starting level of assets to deposits x_0 for different levels of the asset process volatility σ. The plot on the right shows the sensitivity of the structural model for different maturities T at different risk-free interest rate levels r_f.*

Evidently the models show a similar behaviour for variables like the ma-
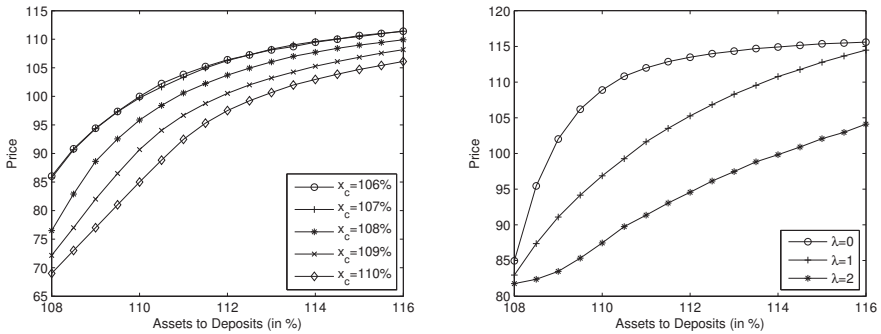
Figure 4.10: *The plot on the left shows the sensitivity of the structural model towards changes in the starting level of assets to deposits x_0 for different levels of the conversion threshold x_c. The plot on the right shows the sensitivity of the structural model for different starting asset to deposit ratios x_0 with different jump intensities λ.*
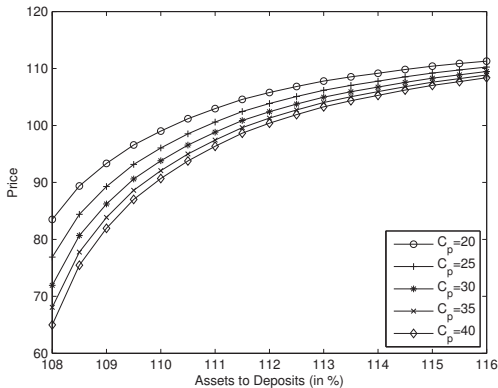
Figure 4.11: *The plot shows the sensitivity of the structural model towards changes in the starting level of assets to deposits x_0 for different levels of the conversion price C_p.*

turity, the risk-free rate, and the volatility. An increasing maturity generally leads to higher prices, whereas higher risk-free interest rates universally lead to lower prices. Increasing the diffusion volatility also shows lower prices in all models, as the conversion probability is increased. However the delta, i.e. the change in the value of the CoCo per unit change of the underlying stock price, shows distinct model differences. I.e. in the credit derivative approach, the model with piecewise constant conversion intensity shows a higher sensitivity when the stock price get close to the trigger level, as opposed to the constant conversion intensity model. The equity derivative model shows a higher delta when the diffusion volatility is lower and ultimately converges to the same CoCo price if the stock price is at the trigger level. The structural model overall shows quite low levels of sensitivity when the threshold is approached.

Furthermore, the credit derivative, J.P. Morgan and equity derivative model are all challenged with a double equilibrium problem, as they present a convex price curve for varying trigger levels. This makes it more challenging to judge which trigger level might be the correct one.

The inclusion of jumps while keeping the total process variance constant shows to have a very minor effect on the credit derivative and J.P. Morgan approach. In the equity derivative model there is a clear difference for higher levels of the stock price. Where it is clearly evident that jumps have an impact is in the structural model, where a jump in the assets has an accentuated effect on the equity through the high leverage ratio.

Subsequently, the models are implemented in the empirical time series analysis, where the combined effects will play a role.

This page intentionally left blank.

Chapter 5

Empirical Analysis and Model Comparison

This chapter investigates to what extent the different models are capable to reflect the (clean) observed market prices of a set of traded CoCo bonds. The focus lies on contingent convertible bonds, which are converted into ordinary shares once a trigger event materializes. Specifically, two CoCo bonds from Credit Suisse (CS) and two CoCo bonds from Lloyds Banking Group (LBG) are evaluated in the different models. For each model, a time series is generated using the data and calibration procedures outlined in chapter 3 to match the observation period of the respective CoCo bond. Applying different error measures such as the root mean squared error (RMSE), the mean absolute scaled error (MASE) and the relative tracking time (TT) allows to scrutinize between models and across CoCo series.

In a first part the specifics of the CoCo's are outlined, followed by the parametrization of the models to obtain a time series. In a third part, the results are compared and discussed in a qualitative and quantitative assessment.

5.1   Data Description

As the focus of the work lies on the traditional contingent capital bond that converts into equity, bonds of this class have been chosen to conduct the empirical analysis. Furthermore, to allow a comparison across different issuers and to enable a judgement of different CoCo designs for the same issuer, two CoCos of Lloyds Banking Group and two CoCos of Credit Suisse are investigated. The chosen bonds represent the longest time series available and have shown to have a high liquidity compared to other CoCo issuances. Furthermore, three of these bonds have also been investigated by Wilkens and Bethke (2014) in their empirical assessment, which will allow a comparison of the results.

5.1.1   Credit Suisse

Up to the end of 2013, Credit Suisse Group in Switzerland had issued six CoCo bonds in denominations of USD, CHF and EUR. Four qualify as tier 2 bonds and two as tier 1 bonds. Three of these bonds are equity conversion bonds, whereas the other three are write-off bonds. Subsequently two pure equity conversion bonds are introduced, which form part of the empirical analysis.

CS1 ISIN XS0595225318

The first CoCo under consideration in the case of Credit Suisse was issued on February 24th 2011 (cf. table 1.1) and the first registered quote was March 16th 2011. The first closing price recorded was USD 102.05. The time series spans 704 trading days up to December 31st 2013. The maturity of the bond as outlined in the bond prospectus is 30 years and it is callable the first time on August 24th 2016 and semi-annually afterwards. Due to the call feature, the bonds upside potential will be limited to its redemption value after the first call date, as the issuer would otherwise call the bond (Brennan and Schwartz, 1977). Thus the assumed maturity of the bond corresponds to the

call protection period and is 5.5 years.[1] The face value N of the bond is USD 1000 and it has semi-annual coupon payments of 7.875%. The CoCo is converted into ordinary shares if the core equity tier 1 ratio of Credit Suisse falls below 7% or at the discretion of the Swiss Financial Market Supervisory Authority (FINMA) (Credit Suisse, 2011).

Due to the fact that the CoCo bond is denominated in USD but a conversion takes place in CHF at a conversion price of $C_p = \max(20\text{CHF}, 20\text{USD}, \bar{S})$, the CoCo investor is exposed to a potential exchange rate risk as well (Credit Suisse, 2011). Specifically, if the USD to CHF exchange rate is higher than one on the date of conversion, the effective conversion price will be higher than USD 20. As table 5.4c shows, the exchange rate was always above one during the observation period, ranging from a minimum of 1.01 USD per CHF up to 1.37 USD per CHF. This fact is incorporated into the model by converting the conversion floor price of CHF 20 into the USD equivalent using the USD/CHF exchange rate FX_t on the respective trading day. $\bar{S}$ corresponds to the volume weighted average share price in CHF of the 30 trading days preceding the conversion. However, as the model implied trigger prices are all below the conversion floor price, it can be assumed that the conversion price can be simplified to $\max(20\text{CHF}, 20\text{USD})$ with a negligible impact. The conversion prices C_p therefore range from 21.19 up to 27.49 USD.

The mean empirical price as shown in table 5.4c of the CS1 CoCo lies at USD 101.33, with a standard deviation of the price of USD 5.71. The CoCo shows a rather large price span, as the minimum price is as low as USD 86.58 and the maximum price lies at USD 110.73.

CS2 ISIN CH0181115681

The second Credit Suisse CoCo was issued on March 22nd 2012 (cf. table 1.1) with a first registered quote of CHF 101.2 on the same date. The time series spans 464 trading days up to December 31st 2013. The bond has a maturity

---

[1]This assumption is in line with e.g. Wilkens and Bethke (2014), De Spiegeleer and Schoutens (2011) or Bürgi (2013).

of 20 years and is also callable after five years on March 22nd 2017 however without any further specified optional redemption dates (Credit Suisse, 2012a). For the same reasoning as above, the initial maturity is chosen to be five years to match the call protection period. The face value N of the bond is CHF 1000 with a coupon rate of 7.125% paid annually. Like the CS1 CoCo the full face value is converted into ordinary shares but in this case at a floor of $C_p = \max(20\text{CHF}, \bar{S})$, if the core equity tier 1 ratio of Credit Suisse falls below 7% or at the discretion of the Swiss Financial Market Supervisory Authority (FINMA) (Credit Suisse, 2012a).

Table 5.5c shows a mean price level of the CS2 CoCo of CHF 104.99, with a price standard deviation of CHF 3.54. With a minimum / maximum price of CHF 97.1 / CHF 111.3, the span is not as large as for the CS1 CoCo; however this is mainly attributable to the different observation period.

The evolution of the CS1 and CS2 CoCo price, the Credit Suisse stock price, the core equity tier 1 ratio and the CDS price on a five year subordinated bond is depicted in figure 5.1.

5.1.2   Lloyds Banking Group

As part of their refinancing program to exit the asset protection scheme put in place by the UK Treasury, Lloyds Banking Group has issued a series of 21 contingent convertible bonds at the end of 2009, generating approximately 7.5 billion GBP of contingent core capital (National Audit Office, 2010). Two of the larger CoCo issues are part of the subsequent empirical analysis.

LBG1 ISIN XS0459086582
The first Lloyds Banking Group CoCo was issued on December 1st 2009 with a maturity date of May 12th 2020 without any optional redemption dates (cf. table 1.1 and table A.1). This results in an initial maturity of approximately 10.5 years. The time series under consideration encompasses 1065 trading days

until December 31st 2013. The CoCo pays a semi-annual coupon of 7.5884% and has a face value of GBP 1000. It is fully converted into ordinary shares at a predetermined price of GBp 59 if the core equity tier one ratio falls below 5% (Lloyds Banking Group, 2009a).

Table 5.6c shows a mean price for LBG1 of GBP 91.29, with a standard deviation of the price of GBP 10.55. The relatively large price span is shown via a minimum price of GBP 68.82 and a maximum price of GBP 109.15.

LBG2 ISIN XS0459089255

The second Lloyds Banking Group CoCo was also issued on December 1st 2009 and has a maturity date of December 21st 2019. It features a 15% coupon, that is paid semi-annually and it has a face value of GBP 1000. The conversion price is GBp 59 and a conversion into ordinary shares occurs at a core equity tier one ratio of 5%. Until December 31st 2013, 1030 quotes are available. Both bonds do not have a call feature (Lloyds Banking Group, 2009a).

The mean price of this CoCo lies at a high level of GBP 129.77, with a lowest price level of GBP 103.89 and a peak of GBP 148.15. The price standard deviation is GBP 11.39 (cf. table 5.7c).

Also for Lloyds Banking Group, the evolution of the LBG1 and LBG2 CoCo price, the stock price, the core equity tier 1 ratio and the CDS price on a ten year subordinated bond is depicted in figure 5.2.

5.2   Model Parametrization

Following the calibration procedures outlined in chapter 3 the different model parameters are determined to reflect the specifics of the CoCos and the issuers. The only degree of freedom remaining in the models is the trigger share price S^* for the credit and equity derivative model as well as the J.P. Morgan model and the trigger threshold x^* for the structural model. This parameter is calibrated via minimization of the mean squared error between the model

price and the initial market price of the respective CoCo.[2]

Credit Derivative Model

Recalling the required parameter set outlined in table 3.2 and following the calibration procedures described in section 3.1.3 leads to the descriptive statistics shown in table 5.4 and 5.5 for CS1 and CS2 and in table 5.6 and 5.7 for LBG1 and LBG2 respectively. Specifically, the equity volatility σ_E has been calculated with a rolling window over 1250 trading days preceding the pricing date, i.e. five years, on the stock price of Credit Suisse and Lloyds Banking Group. E.g. for the CS1 CoCo this encompasses 1955 closing prices from March 5th 2005 to December 31st 2013 to yield 1954 daily returns and 704 rolling standard deviations. As the volatility is one of the main uncertainties feeding into the models, the standard error of the estimate is assessed via bootstrap sampling over the respective return period and translated into a 95% confidence band. The evolution of the volatility is shown in diagram three of figure 5.1 for Credit Suisse and in diagram three of figure 5.2 for Lloyds Banking Group. For Credit Suisse, the average volatility over the entire observation period lies at 56.03% and for Lloyds Banking Group the mean is at an astoundingly high level of 71.15%. The high standard deviation is also clearly reflected in the span of the share prices S_t, which feed into the model. The lowest share price for the CS1 CoCo corresponds to USD 15.81 and the highest price is at USD 44.41, with an average price level of USD 27.47. For the LBG issues, the mean price level is at GBp 52.12, with a minimum price almost 60% lower at GBp 21.84 and the peak lies at GBp 80.37, which is roughly 50% higher than the mean price.

As the CS1 bond is denominated in USD, the risk free interest rate r_f corresponds to the five year US-treasury yield, whereas for the CS2 bond the yield on a five year Swiss government bond is chosen. For the LBG issues,

---

[2]In a comparable analysis, Wilkens and Bethke (2014) assess the overall model fit in their paper and calibrate the trigger level on the entire period of the CoCo. For the structural approach, they furthermore calibrate the asset process parameters σ, λ, μ_π and σ_π.

the yield on a ten year UK government bond is applied. The applicable five year US yield rate has a mean level of 1.13%, with a lowest level of 0.62% and a peak level of 2.36% over the observation period of the CS1 bond. The yield on Swiss government bonds for the CS2 CoCo is even lower, with a mean level of 0.18%, a standard deviation of 0.16% and a lowest level of 0%. The risk-free interest levels on ten-year UK bonds show an average of 2.8%, with a maximum of 4.09% and minimum of 1.64%. Overall the flat levels clearly reflect the low interest rate policies of the national banks.

The trigger share price S^* is calibrated by minimizing the mean squared error between the model price and the initial CoCo price and is thereafter kept constant. Recall that an inherent problem to this model is the double equilibrium price as encountered in figure 3.2 and 4.3, the calibration procedure is therefore constrained to yield the lower trigger price.

The generated time series is shown in figure 5.4 to 5.7 for CS1, figure 5.14 to 5.17 for CS2, figure 5.24 to 5.27 for LBG1 and figure 5.34 to 5.37 for LBG2.

Equity Derivative Model

The equity derivative model relies largely on the same input parameters as outlined above for the credit derivative approach. The only additional parameter is the strike price K for the down-and-in forward and barrier options, which corresponds to the conversion price C_p. For the CS1 issue this also includes the adjustments due to the changes in the USD to CHF exchange rate. As above, the trigger share price S^* is calibrated to meet the first market price via minimization of the root mean squared error of the model price and the market price.

The parameters for the equity derivative model are summarized in table 5.4 for CS1, table 5.5 for CS2 and table 5.6 and 5.7 for LBG1 and LBG2 respectively. The generated time series can be found in figure 5.8 to 5.9 for CS1, figure 5.18 to 5.19 for CS2, figure 5.28 to 5.29 for LBG1 and 5.38 to 5.39 for LBG2.

J.P. Morgan Model

The J.P. Morgan model relies on quoted CDS spreads s_t as main input along with the stock price S_t. To reflect the approximate five year maturity of the CS1 and CS2 bond, the CDS spread on a five year subordinated corporate bond from Credit Suisse is used. In the case of the LBG1 and LBG2 issue, a ten year CDS spread on a subordinated bond on Lloyds Banking Group is used. Referring to table 5.4c and 5.5c the mean CDS level is at 2.09% for Credit Suisse over the CS1 observation period and at a mean level of 1.98% over the period of the CS2 bond. The spreads exhibit a rather large standard deviation of roughly 0.7%. The first CDS price surge leads to a highest level for the CS1 bond at 3.74%, whereas for the CS2 bond it is at 3.46%. Naturally, the spreads on a ten-year subordinated bond for LBG are higher, with a mean level of 3.95% and a peak spread of 7.72%, as shown in table 5.6c and table 5.7c. As the standard deviation is not part of the required parameters and the model is available in closed / semi-closed form, there is no confidence band reported.

The parameters for the J.P. Morgan model are summarized in table 5.4 for CS1, table 5.5 for CS2 and table 5.6 and 5.7 for LBG1 and LBG2 respectively. The generated time series can be found in figure 5.10 to 5.11 for CS1, figure 5.20 to 5.21 for CS2, figure 5.30 to 5.31 for LBG1 and figure 5.40 to 5.41 for LBG2.

Structural Model

In order to calculate daily asset values A_t, the total liabilities D_t are inferred from the balance sheet and linearly interpolated between fiscal quarters to get daily values, to which the daily market capitalization E_t is added. From this the evolution of the asset-to-deposit ratio x_t can be inferred. The relatively low levels for both Credit Suisse and Lloyds Banking Group clearly reflect the high leverage that they have. The mean asset-to-deposit ratio of Credit Suisse over the entire observation period ranges from 102.01% up to 105.67%,

with a mean level of 103.66%. For Lloyds the mean asset-to-deposit ratio is at 103.95%, with a minimum level of 101.61% and a highest level of 106.87%. This is coherent with the recent monitoring exercise by the Basel Committee on Banking Supervision (2013), who report a weighted average leverage ratio of 3.8% across a sample of 223 participating banks.[3]

Based on the rolling volatility window as explained beforehand, the annual asset volatility σ_{A_t} is calculated using the procedure outlined in section 3.4.2. This leads to a mean asset volatility for Lloyds Banking Group of 2.87% and a span from 1.19% up to 4.97%. The Credit Suisse assets are slightly less volatile, at a mean level of 2.08%, a peak level of 3.05% and a lowest value of 1.2%. This is in line with e.g. Crosbie and Bohn (2003), who report annualized asset volatilities of 1% up to 5% for financial institutions.

The parameters κ, $\bar{r}$ and σ_r for the term-structure process are calibrated on monthly time series of 3, 6, 12 and 60 month treasury bill yields in the respective denomination of the CoCo, each covering a time frame from January 1993 to December 2013. E.g. for the CS2 bond denominated in CHF the twenty year yield series on Swiss government bonds is used. The calibrated long-term interest rate $\bar{r}$ is highest for the US government yields at 7.42%, followed by the UK yields at an equilibrium level of 3.87% and the lowest levels are observed for Swiss government yields at a steady state of 3.28%.

The target asset-to-deposit ratio $\hat{x}$ can be regarded as the newly imposed minimum leverage ratio by Basel III. Under regular Basel III provisions, the minimum leverage ratio is still to be calibrated until 2017 but for testing purposes is set to 3% (Basel Committee on Banking Supervision, 2011a). As Lloyds Banking Group is already well above that (i.e. at 4.4% at year-end 2013), the minimum is set to 4% for LBG1 and LBG2. In Switzerland the capital adequacy ordinance ("Eigenmittelverordnung") prescribes that the leverage ratio, i.e. the non-risk-weighted capital adequacy requirements, must amount to 24% of the total capital requirements (Swiss Federal Council, 2013).

---

[3]Note that the final calculation procedure of the new Basel III leverage ratio is still under discussion at the time of writing.

E.g. for the target of 19% capital requirements outlined in the capital adequacy ordinance, the according leverage ratio is 4.56%.[4] This ratio is then translated into a target asset-to-deposit ratio of 104.77% for Credit Suisse and 104.17% for Lloyds Banking Group.

The critical conversion threshold in terms of assets-to-deposits x^* is calibrated via minimization of the root mean squared error to meet the initial CoCo price. As there is a linear relationship between the assets, deposits and the market capitalization this trigger threshold is also translated into a trigger share price S^*, as in the other models.

All the descriptive statistics for the parameters in the structural model are summarized in table 5.4 and in table 5.5 for CS1 and CS2 and in table 5.6 and 5.7 for LBG1 and LBG2 respectively. Figure 5.12 to 5.13 and figure 5.22 to 5.23 show the generated time series for CS1 and CS2, whereas figure 5.32 to 5.33 and figure 5.42 to 5.43 shows the time series for LBG1 and LBG2.

Jump Parameters

The threshold exceedance method as introduced in chapter 3 is applied on a twenty year return history spanning the years 1993 to 2013 of both Credit Suisse and Lloyds Banking Group. Assuming one jump per year, i.e. $\lambda = 1$, determines the exceedance threshold and yields a jump distribution of 40 jumps, containing large negative as well as large positive returns. The descriptive statistics (cf. table 5.4a / 5.5a for Credit Suisse and table 5.6a / 5.7a for Lloyds) reveal that large negative jumps seem to be almost offset by positive jumps of the same magnitude, as the mean jump size μ_π is close to zero with a high standard error (calculated via bootstrap sampling) for both Credit Suisse and Lloyds Banking Group. The jump standard deviation σ_π is highly significant in both cases and with $\sigma_\pi = 18.74\%$ versus $\sigma_\pi = 14.03\%$ larger for Lloyds Banking Group than for Credit Suisse, which matches its overall higher

---

[4]Credit Suisse (2014) assumes that their total capital requirements will be at 16.66% in 2019, which would translate into a leverage ratio of 4%. Due to the uncertainty attached to the final capital requirements, the target is set to 4.56%.

standard deviation of the stock price vis-à-vis the Credit Suisse stock price.

5.3   Model Comparison

Firstly the models are assessed in a qualitative analysis, in which the observation period is split into three windows and the generated time series are discussed. In a second part, a quantitative analysis measures and compares the root mean squared error, the mean absolute scaled error and the tracking time of the models; furthermore, the implied trigger prices are assessed.

5.3.1   Qualitative Analysis

As the CoCos of Credit Suisse and Lloyds Banking Group respectively show qualitatively the same price evolution the remarks below can be generalized. In both cases the time under observation is divided into three sub-periods, as shown in figure 5.1 for Credit Suisse and figure 5.2 for Lloyds Banking Group. The first period for Credit Suisse only applies to the CS1 CoCo, whereas the observations for period two and three apply to both. As both Lloyds CoCos have been issued on the same date, the qualitative assessment applies for all three periods to both bonds.

What can be taken away beforehand is that due to the fact that the trigger price is calibrated to meet the initial CoCo price, the price error defined as $e_t = y_t - \hat{y}_t$, where y_t is the empirical price, starts off at zero for all models; this is also the main reason why the jump versus non-jump time series are almost indistinguishable as the different risk-characteristic is mainly captured in the trigger level.

Credit Suisse
Over the entire observation period from April 2011 to December 2013 the CET1 ratio of Credit Suisse has steadily increased to reach 16% at the end of 2013. The stock price during the same period has been highly volatile,

dropping from USD 40 to below USD 20 during the first year, only to recover slightly and showing a sideways movement until December 2013. Comparing the CS1 CoCo to the evolution of the stock price, there seems to be a clear connection as the CS1 CoCo follows the sharp decline of the stock price in period one. Even the short lived recovery of the stock price in October 2011 is clearly reflected in the CoCo price.[5] Subsequently, the stock price recovers slightly to reach the end of period one. Afterwards, it further declines to reach its low in July 2012 at a level of USD 15.8, thereafter recovering to around the same level at the start of the second time window. Interestingly, during the same time frame the CET1 ratio (which is reported quarterly) improves from 10% in April 2011 to roughly 15% at the end of June 2012 and continues to improve to 16% at the end of 2013. This development also seems to be reflected in the CoCo prices, as the mean price level of CS1 and CS2 steadily increases (albeit with a slight correction in period three). This makes intuitive sense as the trigger of both CoCos is linked to the CET1 ratio.

At the start of the first period, the price models are calibrated to meet the initial market price and all models start with no price error. During the first couple of weeks, the CS1 CoCo as well as the model prices remain steady until the stock price starts dropping in the second half of period one. Referring to figures 5.4 to 5.13, this is when all the model prices start exhibiting positive pricing errors (i.e. the model price is below the empirical CoCo price) and mostly outside the confidence interval, as the model prices react more sensitive to the decline in the stock price. Furthermore there is a noticeable increase in the level of the rolling volatility, as shown in diagram three of figure 5.1, which stays high until the end of period three. The brief recovery until the start of period two still leaves the model prices below the actual CS1 price and barely within the confidence interval of the credit derivative model with piecewise constant conversion intensity (jump and non-jump) and the structural model. A similar picture presents itself for the J.P. Morgan model, as the CDS prices

---

[5]Wilkens and Bethke (2014) report a significant correlation of one-day and five-day returns between the individual stock and CoCo for Credit Suisse and Lloyds Banking Group.

almost double in period one, the price decreases over-proportionally versus the actual CoCo price, leading to the positive price error presented in diagram three of figure 5.10 and 5.11.

The second period is dominated by a further decline in the stock price and overall high levels of the CDS spread. The high sensitivity of the models to the stock price movements further accentuate the pricing errors, as the empirical CS1 and CS2 CoCo's reaction is not as volatile. Even for the CS2 CoCo, whose price error is zero at the beginning of period two, the divergence of the model price to the actual price increases quickly. What can be noticed during period two is the high increase in the CET1 ratio, along with a general increase in the price level of the CS1 and CS2 CoCo. During the second period the risk-free interest rate level is also at its lowest, where the risk-free rate for Swiss government bonds even reach zero percent. This should lead to slightly higher prices in the models as seen in the dynamics and sensitivity analysis of chapter 4. Even though the CDS spread tightens towards the end of period two, the J.P. Morgan model still exhibits quite a large price difference for CS1 (cf. figure 5.10 and 5.11) and CS2 (cf. figure 5.20 and 5.21). The final period features a slight recovery of the stock price and a further increase in the CET1 ratio. What can also be observed is the level of the rolling volatility, which decreases approximately ten percentage points towards the end of period three. This is due to the fact that the most turbulent times of the financial crisis are not included in the rolling window anymore. The combined effect of increasing stock prices and lower volatility levels gradually reduce the pricing error of the credit derivative models, as well as the equity derivative and structural approach. Overall, the lower volatility levels towards the end result in narrower confidence bands in the models. Whereas the price errors remain positive for the CS1 bond, towards the end of period three the price error turns negative for the CS2 CoCo. In the case of the structural model there is a sudden increase in the model price in the first half of period three, which is due to the fact that fresh capital was injected via a mandatory conversion of CHF 3.8 billion of mandatory and contingent convertible securities (MACCS), which were issued
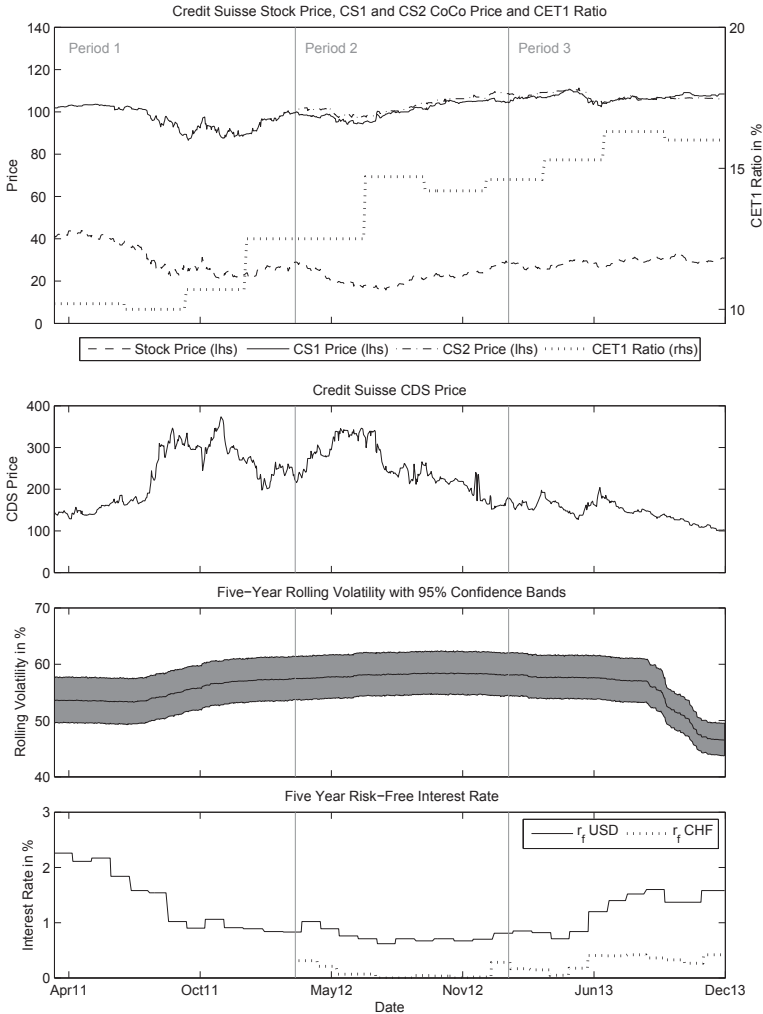
Figure 5.1: *The first diagram shows the stock price of Credit Suisse along with the investigated CoCos CS1 and CS2 on the left-hand y-axis and the evolution of the CET1 ratio on the right-hand y-axis. The second diagram shows the CDS price on a five year subordinated corporate bond of Credit Suisse. Diagram three shows the five-year rolling volatility on the Credit Suisse stock. The confidence band is computed using bootstrap sampling. The final diagram shows the evolution of the five-year risk-free interest rates.*

in July 2012, into 233.5 million shares at a conversion price of CHF 16.29 (Credit Suisse, 2013). This essentially boosts the asset-to-deposit ratio and reduces the pricing error and the structural model tracks the CS1 CoCo quite well towards the end. The price error of the J.P. Morgan model remains almost the same through period three although the CDS price steadily decreases.

The descriptive statistics in table 5.4c show that the JPM and the JPMJ prices show a similar standard deviation of 5.49 and 5.41 compared to the empirical CS1 CoCo, which itself shows a standard deviation of 5.71. The JPM model is closely followed by the structural models ST and STJ, with a standard deviation of 6.57 and 6.66 respectively. The credit derivative models all show comparatively high standard deviations in terms of the price of around 11, as they are quite sensitive to changes in the stock prices. Also the equity derivative models ED and EDJ exhibit a high standard deviation of the prices. A similar picture paints itself for the CS2 bond (cf. table 5.5c), where the standard deviation this time is lowest and closest to the empirical price standard deviation in the structural models ST and STJ. Interestingly, the mean prices lie quite closely together for the structural, J.P. Morgan and credit derivative model with piecewise constant conversion intensity and are comparable to the empirical mean price of the CS2 CoCo. This is partly attributable to the shorter observation period.

Lloyds Banking Group
Also in the case of Lloyds Banking Group the entire observation period is divided into three sub-periods as shown in figure 5.2. Generally, the CET1 ratio steadily increases over all three periods to reach a level of 14% from a starting value of 6.3%. However, also the stock price of Lloyds suffers a depression during the second period reaching a low of 21.84 GBp in November 2011 and therewith increasing CDS spreads on a ten year subordinated bond of up to 772.25 basis points, before recovering again in the third period. The five-year rolling volatility level is extremely high with a mean level of 71.15%

and rather wide confidence bands. Both empirical CoCo prices react to the changes in the stock price, which is especially pronounced in period one and two, whereas towards the end of period three the overall price level of LBG1 and LBG2 increases along with the rising CET1 ratio.

Due to the calibration of the trigger price to match the initial price, the price error between the model prices and the actual price are again zero at the beginning of period one. As seen in figure 5.24 to figure 5.27 for LBG1 and figure 5.34 to 5.37 for LBG2, the credit derivative models are able to track the price evolution quite nicely during the first period, with the price error only outside the confidence interval towards the end of period one. The equity derivative model also performs well as the price error develops similarly to the credit derivative models, as shown in figure 5.28 to figure 5.29 and figure 5.38 to 5.39. The J.P. Morgan model shows a slightly negative pricing error (i.e. the model price is above the actual CoCo price) before the CDS price almost doubles within a short time period, which decreases the model price significantly and leads to a positive pricing error. The structural model shows a slight overestimation of the price during the first half of period one before leading to a short period of a negative price error but subsequently the model prices decline again, ending period one with a positive pricing error for both LBG1 and LBG2.

The second period is dominated by low share prices and high CDS spreads, as mentioned above. This leads to lower prices in all of the models and also the empirical CoCo prices of LBG1 and LBG2 drop. However, due to the higher sensitivity of the model prices to the decline in the stock and CDS prices, they underestimate the price, which leads to a positive price error for all of the models and for both bonds during this time window. The price error is somewhat more pronounced for the equity derivative model than in the credit derivative approach, while the J.P. Morgan models' price error stays more or less constant, as seen in figure 5.30 to 5.31 and figure 5.40 to 5.41. Only the structural model shows a negative price error during a short time-frame in period two.

In period three the stock price and the CDS price recover again, while the CET1 ratio steadily increases. Hence the prices for all models start to increase to reach their highest price levels at the end of the third period. The price error decreases towards the end of period three for both LBG1 and LBG2 and for all models to end up almost at a level of zero. Also the rolling volatility of Lloyds decreases slightly in the last few months of the observation period to reach approximately the same level as at the start of period one. The positive error of the structural model - depicted in figure 5.32 to 5.33 and figure 5.42 to 5.43 - stays relatively constant in the last part of period three and does not pull back to zero like the other models.

The descriptive statistics in table 5.6c and 5.7c show that only the structural model (ST / STJ) exhibits more or less the same mean price of 86.87 / 85.73 for the LBG1 bond and 125.81 / 124.50 for the LBG2 bond, which themselves show a mean price of 91.29 / 129.77. The remaining models show lower average prices, ranging from 75.79 for the CDCJ model to 82.08 for the JPM approach. Interestingly, the structural model exhibits a lower price standard deviation than LBG1, with a level of 7.56 versus 10.55. This is even more pronounced for the LBG2 bond, which shows a price standard deviation of 11.39, whereas the structural model including jumps (STJ) shows a deviation in the price of 5.24. For the LBG1 bond, the credit derivative, equity derivative and J.P. Morgan approach show similar standard deviations to the empirical value between 10.7 and 12.89. In the case of the LBG2 bond, said models exhibit a higher price deviation than the empirical value with values ranging from 12.93 up to 17.14.

Based on the qualitative analysis it is evident that none of the models are able to accurately track the actual price evolution of the CoCos under consideration. However, only knowing about the severity of the pricing errors will allow to conclude which of the models performs best under the given circumstances.
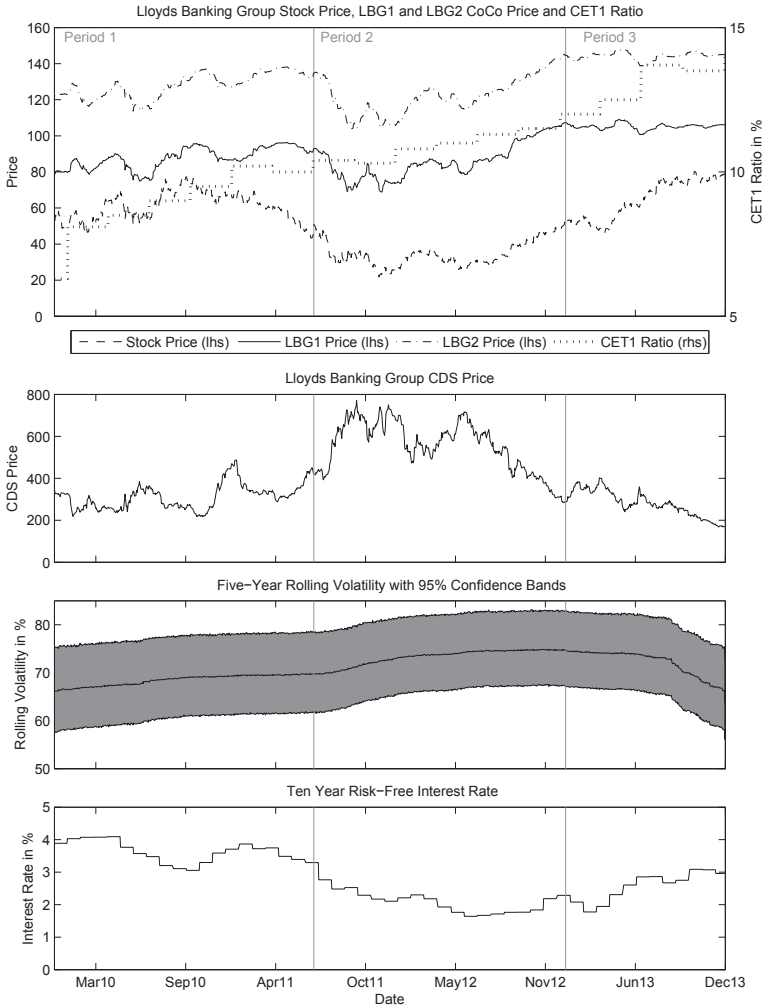
Figure 5.2: *The first diagram shows the stock price of Lloyds Banking Group along with the investigated CoCos LBG1 and LBG2 on the left-hand y-axis and the evolution of the CET1 ratio on the right-hand y-axis. The second diagram shows the CDS price on a ten year subordinated corporate bond of Lloyds Banking Group. Diagram three shows the five-year rolling volatility on the Lloyds Banking Group stock. The confidence band is computed using bootstrap sampling. The final diagram shows the evolution of the ten-year UK risk-free interest rates.*

5.3.2 Quantitative Analysis

As a standard measure the root mean squared error (RMSE) is used to compare the goodness and forecasting accuracy of the different models. Let y_t denote the observation and $\hat{y}_t$ the forecast at time $t \in \{1, ..., N\}$, then the RMSE is defined as (Kirchgässner and Wolters, 2008)

$$\text{RMSE} = \sqrt{\frac{1}{N} \sum_{t=1}^{N} (y_t - \hat{y}_t)^2} \tag{5.1}$$

A smaller RMSE is desirable as it indicates a better fit. Furthermore, the mean absolute scaled error (MASE) is investigated, which enables to compare the results across time series and models (Hyndman and Koehler, 2006). The error is defined as the forecast errors $e_t = y_t - \hat{y}_t$ as in the RMSE but scaled by the mean error of the naïve forecast (i.e. random walk)

$$q_t = \frac{e_t}{\frac{1}{N-1} \sum_{t=2}^{N} |y_t - y_{t-1}|} \tag{5.2}$$

The MASE is then simply the mean of the absolute scaled error

$$\text{MASE} = \text{mean}(|q_t|) \tag{5.3}$$

To get an indication of the accuracy of the models taking into account their confidence bands, the relative tracking time (TT) is computed by dividing the joint number of observations that $e_t^{95} = y_t - \hat{y}_t^{95}$ is above zero and $e_t^5 = y_t - \hat{y}_t^5$ is below zero by the total number of observations N

$$\text{TT} = \frac{\sum_{t=1}^{N} \mathbf{1}_{\{e_t^{95} > 0\}} \cap \mathbf{1}_{\{e_t^5 < 0\}}}{N} \tag{5.4}$$

The superscript 95 stands for the price calculated using the upper volatility confidence band and vice versa the superscript 5 equals the price calculated with the lower confidence band of the rolling volatility.

Table 5.1 provides an overview of the RMSE, the MASE as well as the tracking time of the models for the different CoCos. The root mean squared error and the mean absolute scaled error are calculated using the mean price $(\hat{y}^{50})$ of the models. Note that interpreting the tracking time on a standalone basis might be misleading, as larger values might seem desirable. As the tracking time represents the time that the models forecast error bounded by the lower and upper confidence band is indistinguishable from zero, models with larger confidence bands will perform better and have a larger tracking time. However, large confidence bands do not speak for the accuracy of the model. Therefore, the tracking time is best interpreted in conjunction with the RMSE or the MASE. For example, the credit derivative model with piecewise constant conversion intensity including jumps (CDPJ) for the CS1 bond has a low RMSE and the lowest MASE of the group, but its TT is largest with 0.365. Hence the RMSE and MASE might be as low as the CDP model, but at the cost of larger inaccuracies.

Looking at the CS1 CoCo the lowest RMSE and MASE is clearly achieved by the structural model with values of 0.067 and 0.139 respectively, closely followed by the J.P. Morgan model with a RMSE of 0.071 and a MASE of 0.169. The structural model furthermore shows the lowest tracking time, which is due to the fact that it has very narrow confidence bands (cf. figure 5.12). The credit derivative model with piecewise constant conversion intensity slightly outperforms its counterparts with constant conversion intensity, as the RMSE and the MASE are lower for the former with 0.124 / 0.253 for the CDPJ model versus 0.133 / 0.284 in the CDC model. As the confidence bands for the credit derivative models with jumps are slightly higher, the tracking time is increased as well. E.g. the CDP and the CDPJ model show the same RMSE, but the CDPJ specification exhibits a higher tracking time. The equity derivative model without jumps shows comparable levels of the RMSE, MASE and tracking time to the credit derivative representation, whereas the EDJ specification shows overall higher error measures than without jumps.

In the case of the CS2 bond, the lowest RMSE and MASE is achieved

by the JPM models, where the JPMJ configuration slightly outperforms the JPM model with values of 0.031 / 0.105 versus 0.032 / 0.109 for the RMSE and MASE respectively. A similar picture paints itself for the equity derivative model, where the ED configuration shows lower error levels (0.086 / 0.314) than its jump counterpart EDJ (0.095 / 0.346). The credit derivative implementations do not show any large differences in any of the error measures and are at levels of 0.088 to 0.09 for the RMSE and 0.312 to 0.322 for the MASE. As a runner up to the J.P. Morgan model is the structural approach, with a RMSE of 0.037 and a MASE of 0.137.

Mostly due to the larger observation period, the average error levels are higher for the LBG bonds as compared to the Credit Suisse issues. Nevertheless, also for the LBG1 CoCo the structural and the J.P. Morgan models clearly outperform the equity and credit derivative approaches. Specifically, the ST model edges out the JPMJ approach, with a RMSE and MASE of 0.097 / 0.201 versus 0.117 / 0.259 respectively. The credit derivative models all perform in the same range with RMSE's reaching from 0.162 to 0.169 and MASE's from 0.348 to 0.352, with overall high levels of the tracking time. Again, this is mainly attributable to the large confidence bands attached. Both the ED and EDJ models fare slightly worse than the CD implementation.

Focusing on the LBG2 bond, the overall error levels are slightly elevated compared to the LBG1 bond, except for the structural model, where the fit becomes slightly better. Considering that the two CoCos have almost the same specification, this is mainly attributable to the different coupon structure, where LBG1 features a 7.5884% coupon the LBG2 bond pays 15%. The gap between the structural and J.P. Morgan model is almost doubled, with an RMSE of 0.079 versus 0.152 and a MASE of 0.161 as opposed to 0.337. The credit derivative implementations follow the JPM model, with average RMSE levels close to 0.2 and MASE levels of 0.4. Also for the LBG2 bond, the equity derivative model fares worst.

Finally, the overall comparison of the RMSE for each CoCo clearly favors the structural model (ST and STJ) as it shows the lowest RMSE across all

models for all CoCos, closely tracked by the J.P. Morgan model. The overall average RMSE of 0.071 however is clearly lowest for the structural model, whereas the JPMJ implementation shows a level of 0.093. Looking at the MASE leads to the same conclusion, as it is also lowest for the structural model, where the average lies at 0.161 versus 0.281 in the JPMJ implementation. The credit derivative models show equal averages for the root mean squared error and the mean absolute scaled error and are almost twice as high as in the structural approach. The worst performance in this setting is shown by the equity derivative approach, with an average RMSE and MASE of 0.171 / 0.393 in the EDJ configuration.

The error statistics presented in table 5.3 underpin the previously made findings. The structural model ST(J) shows the lowest average price error across all bonds, ranging from 0.58 for the CS2 bond to 7.21 for the LBG1 bond, with a price deviation of 3.66 and 6.51 respectively. It is closely followed by the JPM(J) model, which shows the smallest mean error for CS2 of 1.77 with a deviation of 2.53 and the largest mean error for LBG2 of 10.99 with a deviation of 10.52. The credit and equity derivative models fare less well, where the credit derivative approach manages to slightly outperform the equity derivative models. The former shows mean errors between 0.31 for the CS2 bond up to 16.25 for the LBG2 bond, whereas the latter shows a minimum average error of 4.13 for the CS2 bond and a maximum average error of 18.33 for the LBG2 bond.

Although Wilkens and Bethke (2014) use a different calibration method and have a much shorter observation period, they also find that the equity derivative model performs worst in their model fitting analysis as measured by the RMSE, across all three bonds that they investigate. They report an RMSE of the equity derivative model ranging from 0.0633 for the Credit Suisse bond, which corresponds to the CS1 bond, to 0.1842 for the first Lloyds Banking Group bond, which matches the LBG2 bond of the work at hand. This is compared to a reported RMSE of 0.0268 and 0.1422 for the CS1 and LBG2 equivalents for the structural model in their work.

Note that comparing the values between the jump and non-jump models only makes limited sense, as the main model difference will already have been captured in the initial calibration of the trigger threshold S^*, which will be investigated subsequently. Notably, the values for the RMSE, MASE and TT are almost the same for the credit derivative and the J.P. Morgan model in a jump vs. a non-jump setting. Only the equity derivative model shows a discernable difference, where the non-jump model fares better for all bonds.

	CS1			CS2			LBG1			LBG2			Average	
	RMSE	MASE	TT	RMSE	MASE	TT	RMSE	MASE	TT	RMSE	MASE	TT	RMSE	MASE
CDC	0.133	0.284	0.279	0.088	0.322	0.362	0.162	0.348	0.457	0.199	0.404	0.425	0.146	0.339
CDCJ	0.129	0.277	0.288	0.085	0.312	0.379	0.164	0.352	0.427	0.195	0.395	0.443	0.148	0.344
CDP	0.124	0.257	0.339	0.090	0.320	0.362	0.165	0.348	0.446	0.200	0.404	0.398	0.145	0.332
CDPJ	0.124	0.253	0.365	0.089	0.316	0.375	0.169	0.358	0.434	0.199	0.403	0.399	0.145	0.333
ED	0.129	0.283	0.256	0.086	0.314	0.334	0.178	0.383	0.379	0.224	0.454	0.360	0.154	0.359
EDJ	0.157	0.344	0.188	0.095	0.346	0.338	0.196	0.411	0.405	0.235	0.470	0.400	0.171	0.393
JPM	0.075	0.179	-	0.032	0.109	-	0.117	0.261	-	0.153	0.339	-	0.094	0.222
JPMJ	0.071	0.169	-	*0.031*	*0.105*	-	0.117	0.259	-	0.152	0.337	-	0.093	0.218
ST	*0.067*	*0.139*	0.195	0.037	0.137	0.181	*0.097*	*0.201*	0.156	0.083	0.166	0.221	*0.071*	*0.161*
STJ	0.068	*0.139*	0.197	0.038	0.138	0.179	0.100	0.210	0.143	*0.079*	*0.161*	0.213	*0.071*	*0.162*

Table 5.1: *This table provides an overview of the root mean squared error (RMSE), the mean absolute scaled error (MASE) as well as the tracking time (TT) of the models for each CoCo. The RMSE and the MASE are calculated based on the model price using the 50 percentile rolling standard deviation. The smallest RMSE and MASE values are emphasized in italic.*

A further indication to compare the models is presented in figure 5.3, where the calibrated implied trigger stock price level S^* is plotted for each CoCo and each model. The diagram reveals that for each CoCo the implied trigger levels are relatively tightly distributed with exception of the structural model, which indicates slightly higher trigger levels and the J.P. Morgan model with slightly lower implied trigger levels. E.g. for LBG1, the prices range from GBp 3.58 to GBp 4.06 for the J.P. Morgan approach, whereas the structural model implies prices of GBp 13.23 to GBp 14.67. Considering the initial market price was at GBp 54.14 for Lloyds, this corresponds to a level of 6.61% up to 27.10%. Moreover, based on a conversion price of GBp 59, this would lead to average recovery rates for the LBG1 CoCo of 6.07% in the JPM model and an average recovery rate of 24.86% in the structural model without jumps.[6] Table 5.2 shows an overview of the trigger levels relative to the initial share price $\bar{S}^*$ and the model implied recovery rates $\bar{R}$. Interestingly, for the Credit Suisse CS1 CoCo the average recovery rate $\bar{R}$ lies between 22.21% for the JPMJ model up to 62.71% for the structural model, however, higher recovery rates are joined by the fact that the trigger level in terms of the initial share price $\bar{S}^*$ is also elevated at levels between 11.1% (JPMJ) and 31.12% (ST), suggesting a higher likelihood of a trigger event. The Lloyds CoCos show a slightly different picture, as the recovery rates $\bar{R}$ are rather low between 6.12% in the JPMJ model and 24.93% in the ST approach for the LBG1 bond. These values are accompanied with low implied trigger levels $\bar{S}^*$ as well, ranging from 6.62% to 27.11% for the LBG1 bond.

What can further be observed in figure 5.3 and table 5.2 is that the trigger levels are also very similar across CoCos. Especially as the LBG1 and LBG2 bond were issued on the same date, the values are directly comparable and the differences are very minor between the two bonds. This confirms the models' abilities to reflect different CoCo variations of the same issuer. Finally, the difference of the trigger stock price S^* for the jump versus the non-jump models is usually small. For all pricing models the trigger price including

---

[6]These results are comparable to those reported by Wilkens and Bethke (2014).

jumps is slightly higher except in the case of the JPM model and the structural approach, where it is slightly lower when including jumps.[7]

As mentioned in section 3.2, the impact of adding daily yield curve data into the equity derivative model has been assessed for the LBG1 bond. For this, daily UK government yield curve data is obtained reflecting one to ten year maturities. To specifically gauge the contribution of adding yield curve data to the model, it is not re-calibrated and the trigger level S^* of the ED model is used. Doing the same error analysis shows that the mean price error $e_{ED|LBG1}$ of 15.13 as reported in table 5.3b is reduced to 10.34, with a standard deviation of 9.03. The RMSE and MASE are reduced from 0.178 and 0.383 to 0.137 and 0.279 respectively.[8]

Closely linked to the implied trigger levels S^* are the risk-neutral conversion probabilities that the different models suggest. The results presented in table 5.2 reflect the risk-neutral conversion probabilities at the time of calibration (i.e. at the time of issuance of the bonds) for three different time horizons. Expectedly, the conversion probabilities increase with an increasing investment horizon, as the one year probabilities are practically zero for all models and all bonds, except for the structural model ST(J), which indicates conversion probabilities ranging from 0.057 (ST) for the CS1 bond and 0.173 (STJ) for the LBG2 bond. On a five year horizon, the highest conversion probability is observed for the structural model STJ for the CS2 bond with 0.375 and the lowest for the ST model with 0.244 for LBG1. Naturally, the conversion probabilities would change over time as the input parameters change as well. E.g. for CS2 versus CS1 one can observe higher conversion probabilities for the former, quite possibly due to the higher contemporaneous volatility level at the time of issuance of the CS2 bond. For the two Lloyds Banking Group bonds LBG1 and LBG2 the probability levels are within close range, as the

---

[7]Corcuera et al. (2013) report similar findings for the equity derivative approach under a smile conform model using a special class of a β-process from the Lévy process family.

[8]When re-calibrating, the trigger level S^* would increase from originally 5.36 to 6.62, as the calculated CoCo prices are lower than with a flat yield rate. The error measures would remain practically the same with a higher trigger level, as the effect would be captured almost entirely in the higher trigger level.

only difference can be attributed to the slightly different implied trigger stock level S^*. The addition of jumps into the risk-dynamics of the models shows overall higher conversion probabilities for the credit derivative models CDCJ and CDPJ as well as for the structural model STJ. Due to the ambiguous impact on the option values the equity derivative model EDJ shows overall slightly lower conversion probabilities than the non-jump counterpart ED. The same can be observed for the JPM model.

Overall though these values underpin the findings from chapter 2, that a CoCo on average has a low probability of a trigger event happening, but at a great cost if a conversion takes place.
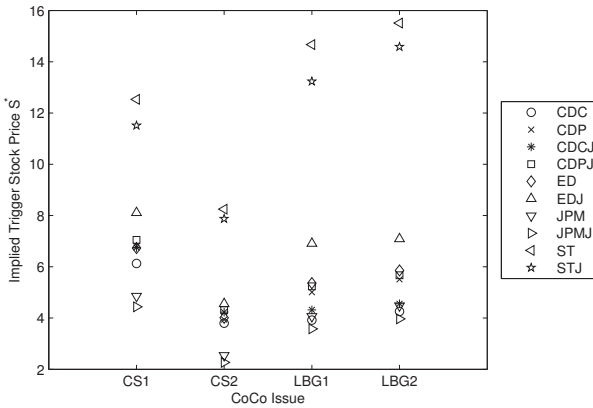
Figure 5.3: *This diagram shows the implied trigger stock price levels S^* of the different models as a result of the calibration to the initial CoCo market price. For CS1 and CS2 the trigger stock price is to be interpreted in USD and for LBG1 and LBG2 in GBp.*

	CS1		CS2		LBG1		LBG2	
	$\bar{S}^*$	$\bar{R}$	$\bar{S}^*$	$\bar{R}$	$\bar{S}^*$	$\bar{R}$	$\bar{S}^*$	$\bar{R}$
CDC	0.152	0.307	0.137	0.190	0.072	0.066	0.079	0.072
CDCJ	0.168	0.338	0.152	0.212	0.079	0.073	0.084	0.073
CDP	0.169	0.341	0.146	0.197	0.093	0.085	0.102	0.093
CDPJ	0.175	0.353	0.155	0.216	0.097	0.089	0.105	0.096
ED	0.167	0.337	0.144	0.201	0.099	0.091	0.108	0.099
EDJ	0.201	0.406	0.164	0.228	0.128	0.117	0.131	0.120
JPM	0.120	0.243	0.091	0.127	0.075	0.069	0.083	0.076
JPMJ	0.110	0.222	0.082	0.115	0.066	0.061	0.073	0.067
ST	0.311	0.627	0.297	0.413	0.271	0.249	0.287	0.263
STJ	0.286	0.576	0.283	0.394	0.244	0.224	0.269	0.247

Table 5.2: *This table provides an overview of the implied trigger share price levels $\bar{S}^*$ and recovery rates $\bar{R}$ relative to the initial stock price levels of USD 40.25 for CS1, USD 27.82 for CS2 and GBp 54.14 for LBG1/2. The base conversion prices C_p to calculate the recovery rates are USD 20 for CS1/2 and GBp 59 for LBG1/2.*

	CS1			CS2		
	1yr	3yr	5yr	1yr	3yr	5yr
CDC	0.001	0.107	0.279	0.002	0.127	0.319
CDCJ	0.001	0.110	0.281	0.001	0.123	0.321
CDP	0.002	0.133	0.314	0.002	0.136	0.331
CDPJ	0.002	0.132	0.307	0.001	0.123	0.331
ED	0.002	0.123	0.281	0.002	0.138	0.332
EDJ	0.002	0.115	0.269	0.002	0.132	0.321
JPM	0.000	0.109	0.193	0.000	0.095	0.197
JPMJ	0.000	0.098	0.185	0.000	0.088	0.192
ST	0.057	0.150	0.249	0.062	0.165	0.263
STJ	0.086	0.193	0.333	0.093	0.198	0.375

(a) *Risk-neutral conversion probabilities for Credit Suisse.*

	LBG1			LBG2		
	1yr	3yr	5yr	1yr	3yr	5yr
CDC	0.000	0.012	0.193	0.000	0.066	0.211
CDCJ	0.003	0.054	0.212	0.001	0.065	0.215
CDP	0.001	0.089	0.249	0.000	0.105	0.274
CDPJ	0.004	0.091	0.247	0.006	0.107	0.273
ED	0.001	0.093	0.224	0.002	0.108	0.244
EDJ	0.000	0.075	0.196	0.001	0.100	0.229
JPM	0.000	0.097	0.210	0.000	0.110	0.226
JPMJ	0.000	0.086	0.201	0.000	0.099	0.218
ST	0.102	0.203	0.244	0.117	0.224	0.276
STJ	0.154	0.279	0.344	0.173	0.286	0.365

(b) *Risk-neutral conversion probabilities for Lloyds Banking Group.*

Table 5.2: *This table provides an overview of the risk-neutral conversion probabilities for the Credit Suisse and Lloyds Banking Group bonds evaluated in the different models at the time of issuance. 1yr, 3yr and 5yr stand for the investment horizon under consideration.*

Variable	Mean	Std.	Min.	Q. 1	Md.	Q. 3	Max.
$e_{CDC|CS1}$	10.22	8.45	-2.49	3.14	9.06	15.58	32.94
$e_{CDCJ|CS1}$	9.92	8.42	-2.49	2.72	8.89	15.17	33.33
$e_{CDP|CS1}$	8.01	9.40	-8.74	0.37	7.01	14.01	31.02
$e_{CDPJ|CS1}$	8.49	8.98	-6.04	0.94	7.06	13.90	31.43
$e_{ED|CS1}$	10.31	7.92	-2.26	3.95	9.33	15.91	30.71
$e_{EDJ|CS1}$	12.70	8.46	-1.46	6.11	12.11	18.86	34.23
$e_{JPM|CS1}$	6.56	3.61	-2.65	3.45	7.69	9.11	13.31
$e_{JPMJ|CS1}$	6.11	3.48	-2.98	3.23	7.19	8.58	12.65
$e_{ST|CS1}$	4.91	4.51	-5.52	1.26	3.66	8.64	15.06
$e_{STJ|CS1}$	5.02	4.53	-4.89	1.34	3.89	9.54	16.04
$e_{CDC|CS2}$	3.91	7.93	-12.03	-1.59	4.21	10.37	21.12
$e_{CDCJ|CS2}$	3.49	7.79	-11.99	-1.80	3.96	9.51	20.41
$e_{CDP|CS2}$	0.31	9.02	-17.36	-7.43	0.32	6.57	18.43
$e_{CDPJ|CS2}$	1.11	8.86	-17.87	-8.18	-0.29	5.67	16.93
$e_{ED|CS2}$	4.13	7.52	-11.55	-0.87	4.92	9.98	20.61
$e_{EDJ|CS2}$	4.57	8.29	-12.45	-1.09	5.07	11.16	22.74
$e_{JPM|CS2}$	1.95	2.56	-2.93	0.21	1.59	3.92	7.69
$e_{JPMJ|CS2}$	1.77	2.53	-3.09	0.02	1.49	3.73	7.38
$e_{ST|CS2}$	0.58	3.66	-4.88	-3.16	0.51	3.98	8.51
$e_{STJ|CS2}$	0.97	3.66	-4.48	-2.76	0.91	4.38	8.91

(a) *This table presents the error statistics of the different models for the CS1 and CS2 bond. 'Std.' stands for standard deviation, 'Min.' for minimum, 'Q. 1' for the first quantile, 'Md.' for median, 'Q. 3' for the third quantile and 'Max.' for maximum.*

Table 5.3: *Error statistics CS1/2, LBG1/2 (continued)*

Variable	Mean	Std.	Min.	Q. 1	Md.	Q. 3	Max.
$e_{CDC|LBG1}$	13.69	8.72	-5.43	5.82	14.49	21.06	29.52
$e_{CDCJ|LBG1}$	15.05	9.88	-5.76	6.42	15.98	24.78	34.05
$e_{CDP|LBG1}$	13.65	9.28	-6.62	5.15	14.38	22.07	30.85
$e_{CDPJ|LBG1}$	14.09	9.32	-5.62	5.72	14.68	22.57	31.77
$e_{ED|LBG1}$	15.13	9.33	-5.12	6.85	15.95	23.09	31.44
$e_{EDJ|LBG1}$	16.16	11.12	-5.87	5.84	16.93	26.29	36.02
$e_{JPM|LBG1}$	9.22	7.22	-9.01	3.84	11.77	14.65	20.05
$e_{JPMJ|LBG1}$	9.29	7.08	-8.53	4.15	11.76	14.59	20.01
$e_{ST|LBG1}$	7.21	6.51	-8.15	2.21	6.91	12.83	19.19
$e_{STJ|LBG1}$	7.71	6.51	-7.65	2.71	7.41	13.33	19.69
$e_{CDC|LBG2}$	16.25	11.52	-8.19	5.89	18.23	26.84	34.99
$e_{CDCJ|LBG2}$	15.78	11.51	-9.33	5.63	17.81	26.37	35.03
$e_{CDP|LBG2}$	15.72	12.38	-10.13	4.65	18.19	26.32	36.59
$e_{CDPJ|LBG2}$	15.63	12.39	-9.98	4.33	18.05	26.22	36.16
$e_{ED|LBG2}$	18.33	12.85	-8.01	6.25	20.72	30.32	38.14
$e_{EDJ|LBG2}$	18.21	14.85	-10.77	4.36	19.49	32.08	41.48
$e_{JPM|LBG2}$	10.89	10.71	-14.75	7.88	15.19	18.29	26.67
$e_{JPMJ|LBG2}$	10.99	10.52	-14.09	7.77	15.29	18.22	26.69
$e_{ST|LBG2}$	3.97	7.29	-16.18	-1.37	4.39	10.07	17.95
$e_{STJ|LBG2}$	3.27	7.29	-16.88	-2.07	3.69	9.38	17.25

(b) *This table presents the error statistics of the different models for the LBG1 and LBG2 bond. 'Std.' stands for standard deviation, 'Min.' for minimum, 'Q. 1' for the first quantile, 'Md.' for median, 'Q. 3' for the third quantile and 'Max.' for maximum.*

Table 5.3: *Error statistics CS1/2, LBG1/2.*

Descriptive Statistics and Time Series

The subsequent pages present the descriptive statistics and time series figures of the different pricing models for the four CoCos under consideration.

Credit Suisse CS1

Variable	Value	Description
N	1000	Face value
c_i	7.875%	Bond coupon rate, semi-annual
α	1	Full conversion
q	2.96%	Dividend yield
λ	1	Jump intensity per year
μ_π	-0.49%	Mean jump size
	(0.0067)	
σ_π	14.03%	Jump standard deviation
	(0.0073)	
S^*_{CDC}	6.13	Implied trigger share price CDC
	(0.0011)	
S^*_{CDP}	6.82	Implied trigger share price CDP
	(0.0331)	
S^*_{CDCJ}	6.75	Implied trigger share price CDCJ
	(0.0002)	
S^*_{CDPJ}	7.05	Implied trigger share price CDPJ
	(0.0004)	
S^*_{ED}	6.73	Implied trigger share price ED
	(0.2280)	
S^*_{EDJ}	8.11	Implied trigger share price EDJ
	(0.1750)	
S^*_{JPM}	4.85	Implied trigger share price JPM
	(0.0068)	
S^*_{JPMJ}	4.44	Implied trigger share price JPMJ
	(0.0046)	

(a) *This table presents the static parameters of the credit, equity derivative and J.P. Morgan model to price the CS1 CoCo. The standard errors of the jump distribution $\phi(\mu_\pi, \sigma_\pi)$ reported in brackets are calculated via bootstrap sampling. The standard error of S^* reported in brackets is calculated via the square root of the inverse of the hessian matrix.*

Table 5.4: *Descriptive statistics CS1 (continued)*

Variable	Value	Description
N	1000	Face value
c_i	7.875%	Bond coupon rate, semi-annual
α	1	Full conversion
q	2.96%	Dividend yield
λ	1	Jump intensity per year
μ_π	-0.49%	Mean jump size
	(0.0067)	
σ_π	14.03%	Jump standard deviation
	(0.0073)	
κ	0.0413	CIR Speed of convergence
	(0.0109)	
$\bar{r}$	7.42%	Long-term interest rate
	(0.0192)	
σ_r	4.81%	Standard deviation of interest rate
	(0.0019)	
g	0.5	Deposit-growth speed of convergence
$\hat{x}$	104.78%	Target asset-to-deposit ratio
b_0	0.19%	Initial CoCo-to-deposit ratio
x^*_{ST}	101.42%	Implied trigger asset-to-deposit ratio ST
	(0.0012)	
S^*_{ST}	12.53	Implied trigger share price ST
x^*_{STJ}	101.30%	Implied trigger asset-to-deposit ratio STJ
	(0.0015)	
S^*_{STJ}	11.51	Implied trigger share price STJ

(b) *This table presents the static parameters of the structural model to price the CS1 CoCo. The standard errors of the jump distribution $\phi(\mu_\pi, \sigma_\pi)$ reported in brackets are calculated via bootstrap sampling. The standard error of x^* reported in brackets is calculated via the square root of the inverse of the hessian matrix.*

Table 5.4: *Descriptive statistics CS1 (continued)*

Variable	Mean	Std.	Min.	Q. 1	Md.	Q. 3	Max.
t_i (years)	4.05	-	2.65	3.34	4.05	4.75	5.5
S_t	27.47	6.38	15.81	23.05	26.85	29.8	44.41
CDS_t^{sub5}	209.78	69.44	100.8	150.96	185.93	266.21	373.59
A_t	1067.88	67.45	969.18	993.7	1083.15	1125.19	1170.56
D_t	1030.64	70.83	927.44	951.39	1059.7	1085.63	1131.79
E_t	37.24	9.09	21.39	29.92	35	46.23	53.96
σ_{A_t} (%)	2.08	0.53	1.2	1.62	1.99	2.57	3.05
x_t (%)	103.66	1.03	102.01	102.8	103.4	104.75	105.67
$CET1$ (%)	13.31	2.23	10	10.7	14.2	15.3	16.3
σ_t (%)	56.03	2.81	46.54	54.15	57.28	58.02	58.45
C_t^p	21.91	1.09	20.13	21.28	21.69	22.14	27.49
r_t^{f5} (%)	1.13	0.46	0.62	0.76	0.9	1.52	2.26
FX_t	1.1	0.05	1.01	1.06	1.08	1.11	1.37
V_{CS1}	101.33	5.71	86.58	97.21	102.65	106.14	110.73
V_{CDC}	91.11	10.75	65.73	83.4	91.46	99.72	110.12
V_{CDCJ}	91.28	10.51	66.59	83.66	91.82	99.86	109.72
V_{CDP}	93.32	12.09	67.67	84.11	93.72	103.38	116.85
V_{CDPJ}	92.84	11.59	67.13	84.06	93.39	102.85	113.87
V_{ED}	91.02	9.97	68.17	83.73	91.17	98.76	108.93
V_{EDJ}	88.63	10.7	64.8	81.09	88.3	97.28	108.15
V_{JPM}	94.77	5.49	81.71	90.29	96.49	99.44	103.97
V_{JPMJ}	95.22	5.41	82.23	90.73	97.01	99.81	103.95
V_{ST}	96.38	6.57	84.62	90.78	94.89	103.18	106.03
V_{STJ}	96.42	6.66	85.62	90.57	95.19	103.24	107.53

(c) *This table presents the dynamic parameters of the models to price the CS1 CoCo. The lower part of the table presents the pricing results for the different models. All monetary values are indicated in USD; the CDS spread is indicated in basis points. A_t, D_t and E_t are reported in billion. 'Std.' stands for standard deviation, 'Min.' for minimum, 'Q. 1' for the first quantile, 'Md.' for median, 'Q. 3' for the third quantile and 'Max.' for maximum. (source: based on Bürgi (2013))*

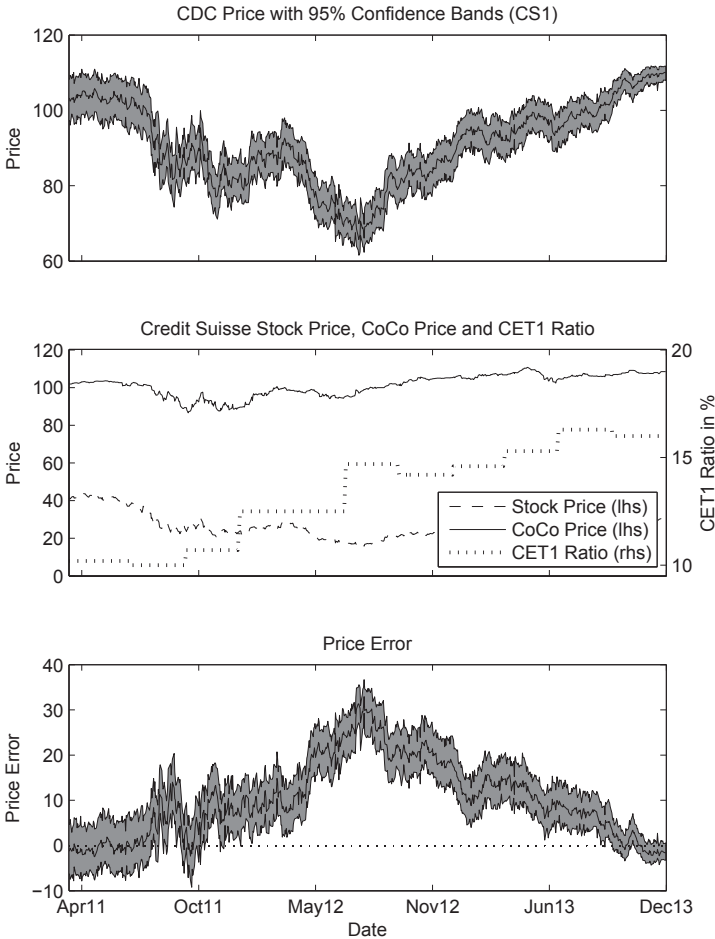**Table 5.4:** *Descriptive statistics CS1.*

Figure 5.4: *Diagram one shows the clean CoCo price as calculated with the credit derivative model with constant conversion intensity, where the trigger share price S^* has been calibrated to match the first empirical price. The 95% confidence bands result from the parameter uncertainty of the estimated five-year rolling volatility. Diagram two shows the empirical stock price of Credit Suisse and the clean empirical CS1 CoCo price in USD on the left y-axis and the core equity tier 1 ratio on the right y-axis. Diagram three shows the absolute price error $e_t = y_t - \hat{y}_t$, where $\hat{y}_t$ corresponds to the price calculated using the 50 percentile rolling standard deviation.*
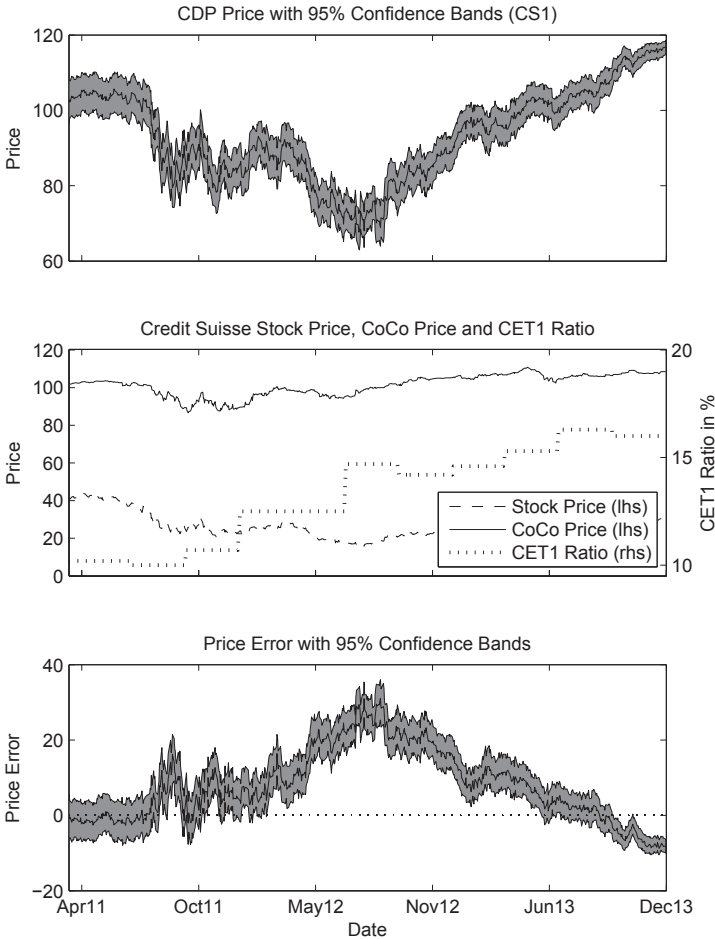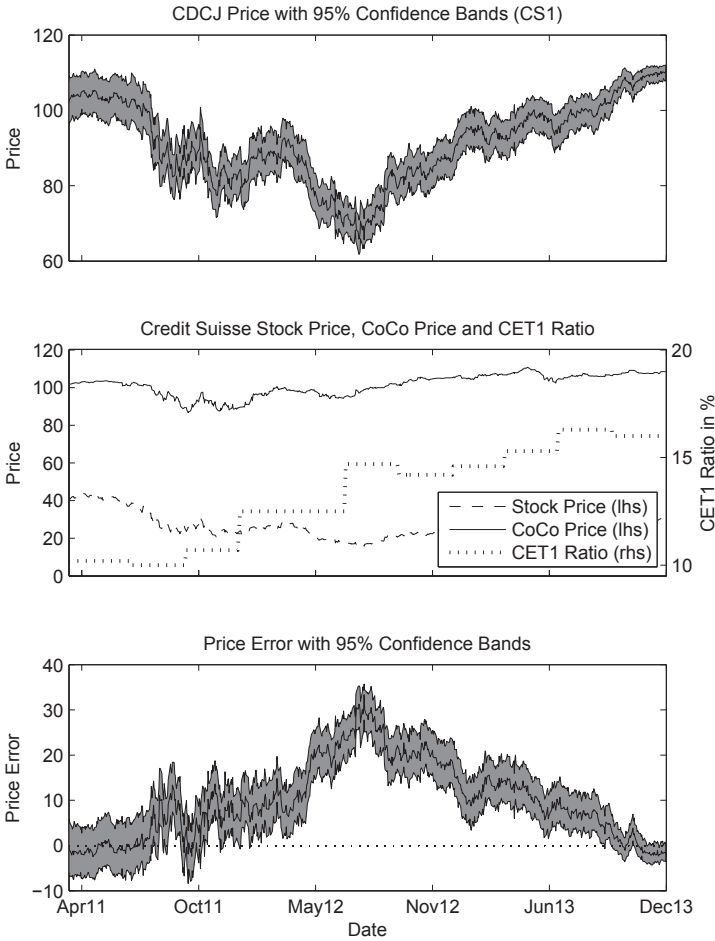
Figure 5.5: *Diagram one shows the clean CoCo price as calculated with the credit derivative model with piecewise constant conversion intensity, where the trigger share price S^* has been calibrated to match the first empirical price. The 95% confidence bands result from the parameter uncertainty of the estimated five-year rolling volatility. Diagram two shows the empirical stock price of Credit Suisse and the clean empirical CS1 CoCo price in USD on the left y-axis and the core equity tier 1 ratio on the right y-axis. Diagram three shows the absolute price error $e_t = y_t - \hat{y}_t$, where $\hat{y}_t$ corresponds to the price calculated using the 50 percentile rolling standard deviation.*

Figure 5.6: *Diagram one shows the clean CoCo price as calculated with the credit derivative model with constant conversion intensity including jumps, where the trigger share price S^* has been calibrated to match the first empirical price. The 95% confidence bands result from the parameter uncertainty of the estimated five-year rolling volatility. Diagram two shows the empirical stock price of Credit Suisse and the clean empirical CS1 CoCo price in USD on the left y-axis and the core equity tier 1 ratio on the right y-axis. Diagram three shows the absolute price error $e_t = y_t - \hat{y}_t$, where $\hat{y}_t$ corresponds to the price calculated using the 50 percentile rolling standard deviation.*
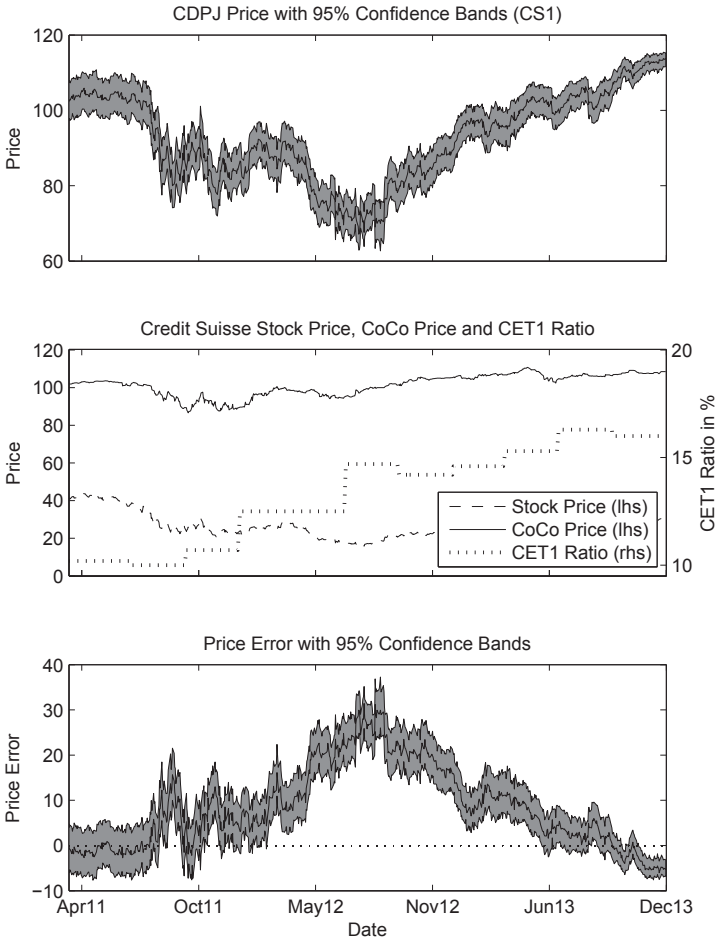
Figure 5.7: *Diagram one shows the clean CoCo price as calculated with the credit derivative model with piecewise constant conversion intensity including jumps, where the trigger share price S* has been calibrated to match the first empirical price. The 95% confidence bands result from the parameter uncertainty of the estimated five-year rolling volatility. Diagram two shows the empirical stock price of Credit Suisse and the clean empirical CS1 CoCo price in USD on the left y-axis and the core equity tier 1 ratio on the right y-axis. Diagram three shows the absolute price error $e_t = y_t - \hat{y}_t$, where $\hat{y}_t$ corresponds to the price calculated using the 50 percentile rolling standard deviation.*
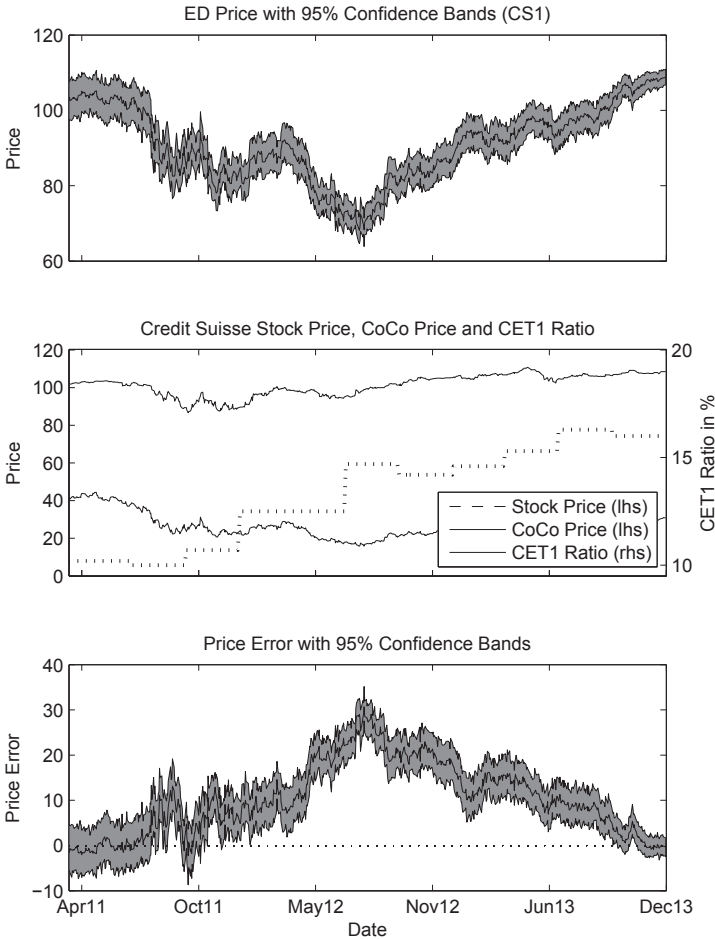
Figure 5.8: *Diagram one shows the clean CoCo price as calculated with the equity derivative model, where the trigger share price S* has been calibrated to match the first empirical price. The 95% confidence bands result from the parameter uncertainty of the estimated five-year rolling volatility. Diagram two shows the empirical stock price of Credit Suisse and the clean empirical CS1 CoCo price in USD on the left y-axis and the core equity tier 1 ratio on the right y-axis. Diagram three shows the absolute price error $e_t = y_t - \hat{y}_t$, where $\hat{y}_t$ corresponds to the price calculated using the 50 percentile rolling standard deviation.*
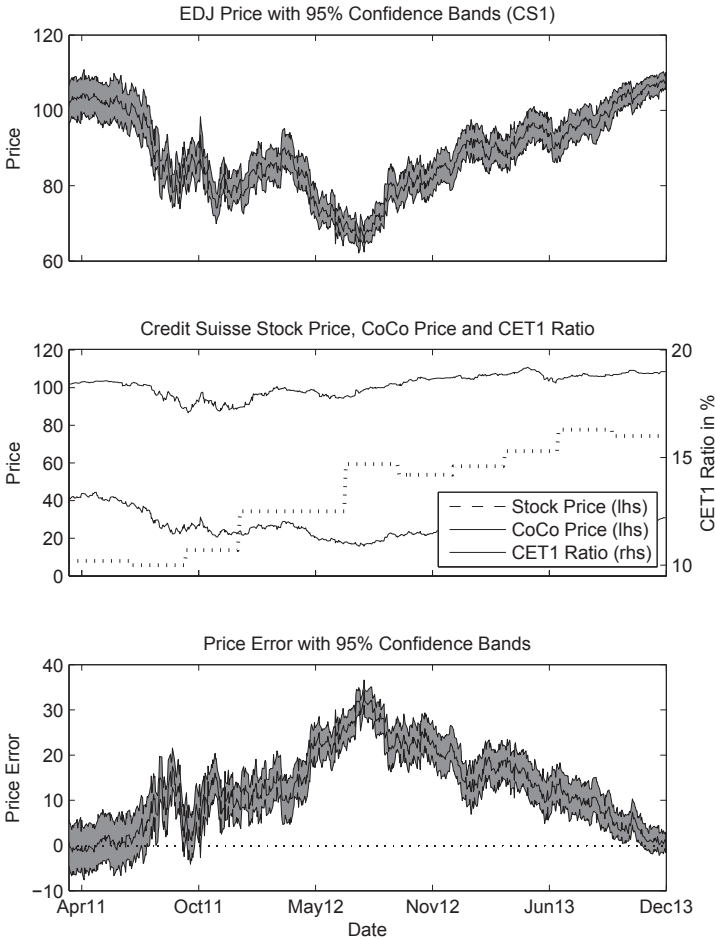
Figure 5.9: *Diagram one shows the clean CoCo price as calculated with the equity derivative model including jumps, where the trigger share price S^* has been calibrated to match the first empirical price. The 95% confidence bands result from the parameter uncertainty of the estimated five-year rolling volatility. Diagram two shows the empirical stock price of Credit Suisse and the clean empirical CS1 CoCo price in USD on the left y-axis and the core equity tier 1 ratio on the right y-axis. Diagram three shows the absolute price error $e_t = y_t - \hat{y}_t$, where $\hat{y}_t$ corresponds to the price calculated using the 50 percentile rolling standard deviation.*
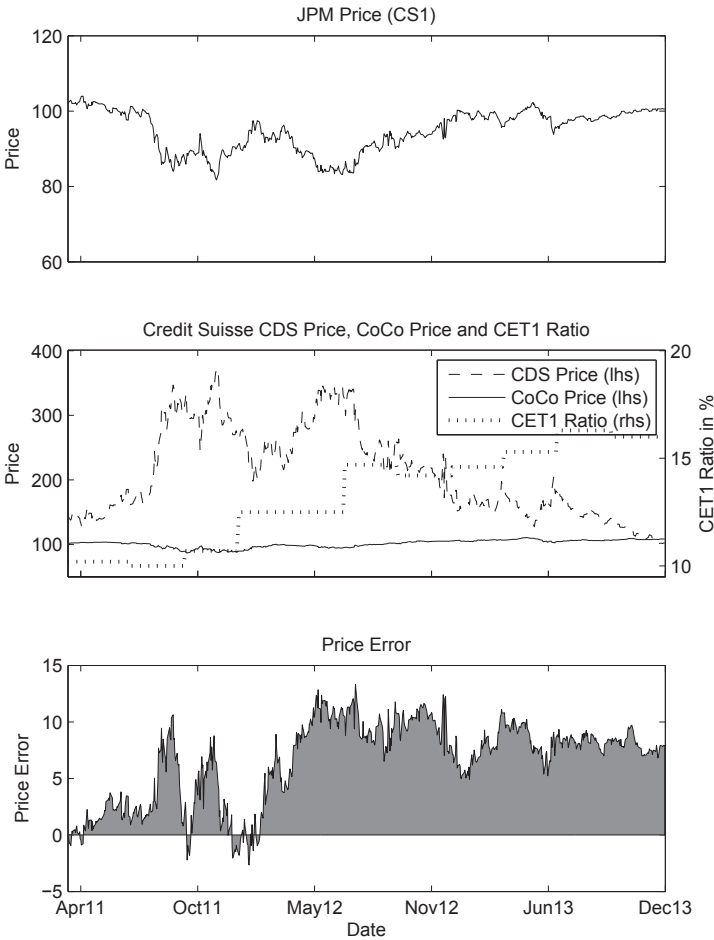
Figure 5.10: *Diagram one shows the clean CoCo price as calculated with the J.P. Morgan model, where the trigger share price S^* has been calibrated to match the first empirical price. Diagram two shows the historical CDS spread on a five year subordinated bond of Credit Suisse in basis points and the clean empirical CS1 CoCo price in USD on the left y-axis and the core equity tier 1 ratio on the right y-axis. Diagram three shows the absolute price error $e_t = y_t - \hat{y}_t$, where $\hat{y}_t$ corresponds to the price calculated using the 50 percentile rolling standard deviation.*

Figure 5.11: *Diagram one shows the clean CoCo price as calculated with the J.P. Morgan model including jumps, where the trigger share price S^* has been calibrated to match the first empirical price. Diagram two shows the historical CDS spread on a five year subordinated bond of Credit Suisse in basis points and the clean empirical CS1 CoCo price in USD on the left y-axis and the core equity tier 1 ratio on the right y-axis. Diagram three shows the absolute price error $e_t = y_t - \hat{y}_t$, where $\hat{y}_t$ corresponds to the price calculated using the 50 percentile rolling standard deviation.*
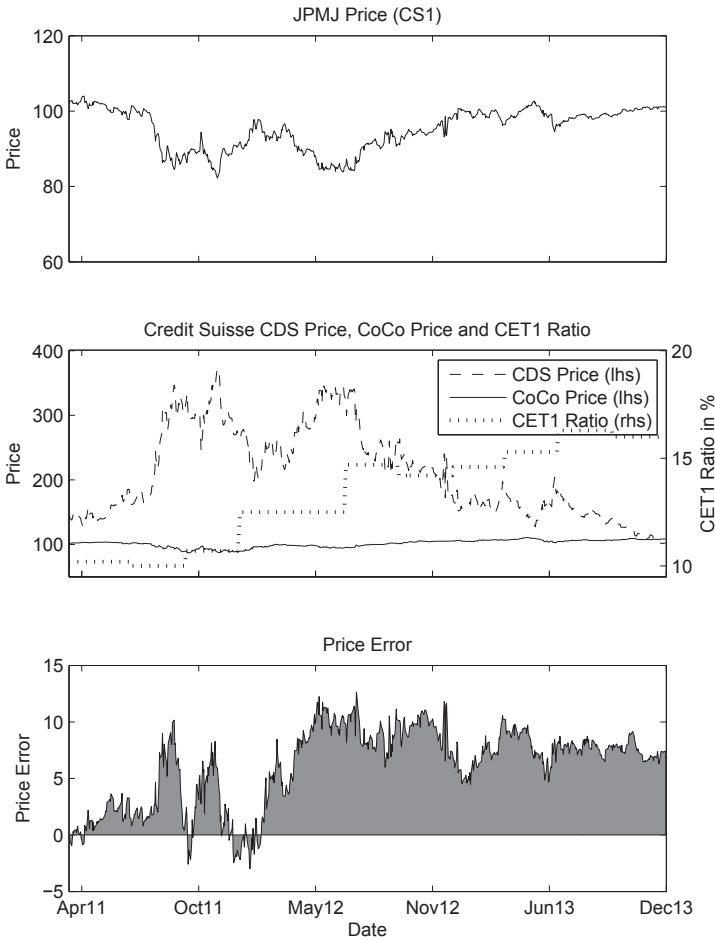
Figure 5.12: *Diagram one shows the clean CoCo price as calculated with the structural model, where the trigger asset-to-deposit ratio x^* has been calibrated to match the first empirical price. The 95% confidence bands result from the parameter uncertainty of the estimated five-year rolling volatility. Diagram two shows the empirical stock price of Credit Suisse and the clean empirical CS1 CoCo price in USD on the left y-axis and the core equity tier 1 ratio on the right y-axis. Diagram three shows the absolute price error $e_t = y_t - \hat{y}_t$, where $\hat{y}_t$ corresponds to the price calculated using the 50 percentile rolling standard deviation.*
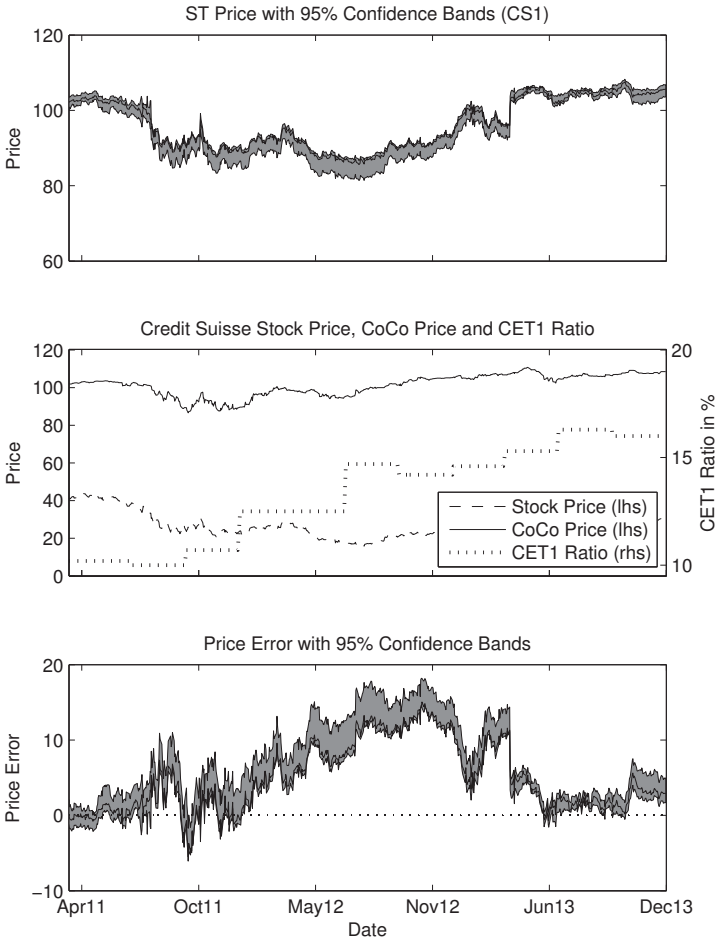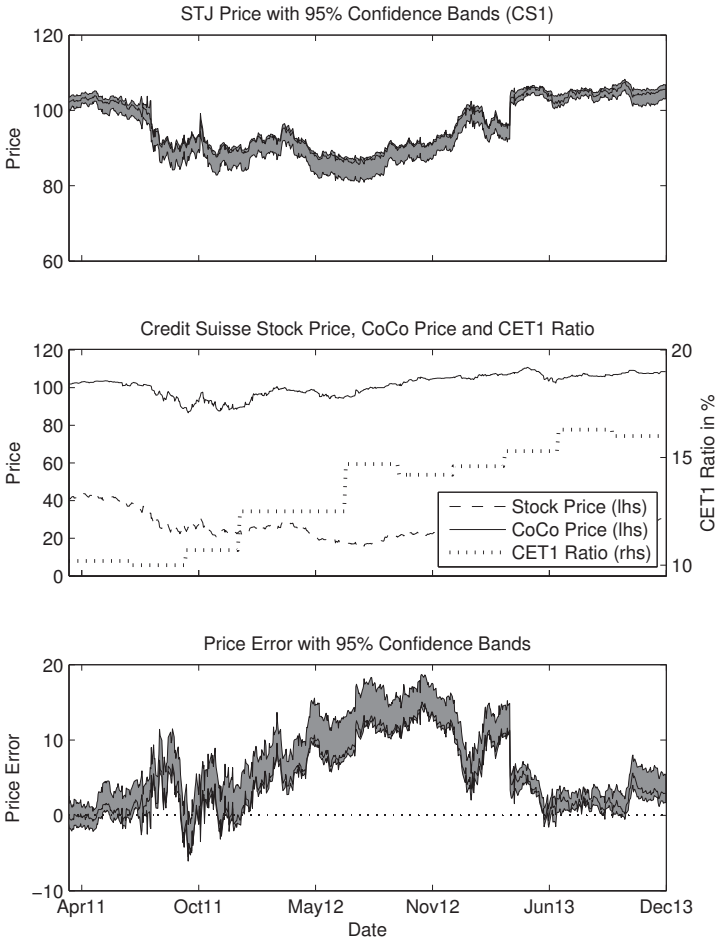
Figure 5.13: *Diagram one shows the clean CoCo price as calculated with the structural model including jumps, where the trigger asset-to-deposit ratio x^* has been calibrated to match the first empirical price. The 95% confidence bands result from the parameter uncertainty of the estimated five-year rolling volatility. Diagram two shows the empirical stock price of Credit Suisse and the clean empirical CS1 CoCo price in USD on the left y-axis and the core equity tier 1 ratio on the right y-axis. Diagram three shows the absolute price error $e_t = y_t - \hat{y}_t$, where $\hat{y}_t$ corresponds to the price calculated using the 50 percentile rolling standard deviation.*

Credit Suisse CS2

Variable	Value	Description
N	1000	Face value
c_i	7.175%	Bond coupon rate, semi-annual
α	1	Full conversion
q	2.96%	Dividend yield
λ	1	Jump intensity per year
μ_π	-0.49%	Mean jump size
	(0.0067)	
σ_π	14.03%	Jump standard deviation
	(0.0073)	
S^*_{CDC}	3.8	Implied trigger share price CDC
	(0.0003)	
S^*_{CDP}	3.94	Implied trigger share price CDP
	(0.0051)	
S^*_{CDCJ}	4.23	Implied trigger share price CDCJ
	(0.0021)	
S^*_{CDPJ}	4.31	Implied trigger share price CDPJ
	(0.0026)	
S^*_{ED}	4.01	Implied trigger share price ED
	(0.1023)	
S^*_{EDJ}	4.56	Implied trigger share price EDJ
	(0.1510)	
S^*_{JPM}	2.45	Implied trigger share price JPM
	(0.0029)	
S^*_{JPMJ}	2.27	Implied trigger share price JPMJ
	(0.0072)	

(a) *This table presents the static parameters of the credit, equity derivative and J.P. Morgan model to price the CS2 CoCo. The standard errors of the jump distribution $\phi(\mu_\pi, \sigma_\pi)$ are calculated via bootstrap sampling. The standard error of S^* is calculated via the square root of the inverse of the hessian matrix.*

Table 5.5: *Descriptive statistics CS2 (continued)*

Variable	Value	Description
N	1000	Face value
c_i	7.175%	Bond coupon rate, semi-annual
α	1	Full conversion
q	2.96%	Dividend yield
λ	1	Jump intensity per year
μ_π	-0.49%	Mean jump size
	(0.0067)	
σ_π	14.03%	Jump standard deviation
	(0.0073)	
κ	0.1751	CIR Speed of convergence
	(0.0417)	
$\bar{r}$	3.28%	Long-term interest rate
	(0.0077)	
σ_r	6.4%	Standard deviation of interest rate
	(0.0028)	
g	0.5	Deposit-growth speed of convergence
$\hat{x}$	104.78%	Target asset-to-deposit ratio
b_0	1.5%	Initial CoCo-to-deposit ratio
x^*_{ST}	101.00%	Implied trigger asset-to-deposit ratio ST
	(0.0021)	
S^*_{ST}	8.25	Implied trigger stock price ST
x^*_{STJ}	100.95%	Implied trigger asset-to-deposit ratio STJ
	(0.0018)	
S^*_{STJ}	7.87	Implied trigger stock price STJ

(b) *This table presents the static parameters of the structural model to price the CS2 CoCo. The standard errors of the jump distribution $\phi(\mu_\pi, \sigma_\pi)$ are calculated via bootstrap sampling. The standard error of $\kappa, \bar{r}, \sigma_r$ and x^* is calculated via the square root of the inverse of the hessian matrix.*

Table 5.5: *Descriptive statistics CS2 (continued)*

Variable	Mean	Std.	Min.	Q. 1	Md.	Q. 3	Max.
t_i (years)	4.11	-	3.22	3.67	4.11	4.56	5
S_t (USD)	25.48	4.52	15.81	22.07	26.72	29.2	33.84
CDS_t^{sub5}	197.72	67.13	100.8	147.05	172.39	239.93	346.09
A_t	1031.32	47.8	959.81	991.48	1020.91	1082.88	1107.64
D_t	994.48	55.4	911.81	94.13	978.53	1058.76	1074.52
E_t	36.84	8.98	21.39	29.85	35.41	45.9	53.37
σ_{A_t} (%)	2.05	0.52	1.17	1.65	2.07	2.55	2.94
x_t (%)	103.76	1.09	102.01	102.87	103.66	104.83	105.67
$CET1$ (%)	14.82	1.21	12.5	14.2	14.7	16	16.3
σ_t (%)	56.59	3.11	46.55	57.26	57.66	58.17	58.48
r_t^{f5} (%)	0.18	0.16	0.00	0.04	0.17	0.33	0.42
V_{CS2}	104.99	3.54	97.1	101.9	106.2	107.13	111.3
V_{CDC}	101.08	10.12	78.88	94.34	103.03	107.96	118.08
V_{CDCJ}	101.59	9.99	78.79	94.68	103.53	108.29	118.09
V_{CDP}	105.31	11.38	80.77	97.89	107.51	113.75	123.55
V_{CDPJ}	106.11	11.23	82.32	98.68	108.22	114.37	124.06
V_{ED}	100.87	9.65	79.38	94.25	104.41	107.33	117.6
V_{EDJ}	100.42	10.47	77.26	93.48	102.03	107.31	118.55
V_{JPM}	103.04	5.19	90.63	99.23	105.23	107.06	109.43
V_{JPMJ}	103.22	5.15	90.96	100.09	105.36	107.22	109.52
V_{ST}	103.89	4.51	97.38	99.25	103.11	108.89	111.01
V_{STJ}	102.42	4.23	96.96	99.01	102.51	108.25	110.28

(c) *This table presents the dynamic parameters of the models to price the CS2 CoCo. The lower part of the table presents the pricing results for the different models. A_t, D_t and E_t are reported in billion. 'Std.' stands for standard deviation, 'Min.' for minimum, 'Q. 1' for the first quantile, 'Md.' for median, 'Q. 3' for the third quantile and 'Max.' for maximum. (source: based on Bürgi (2013))*

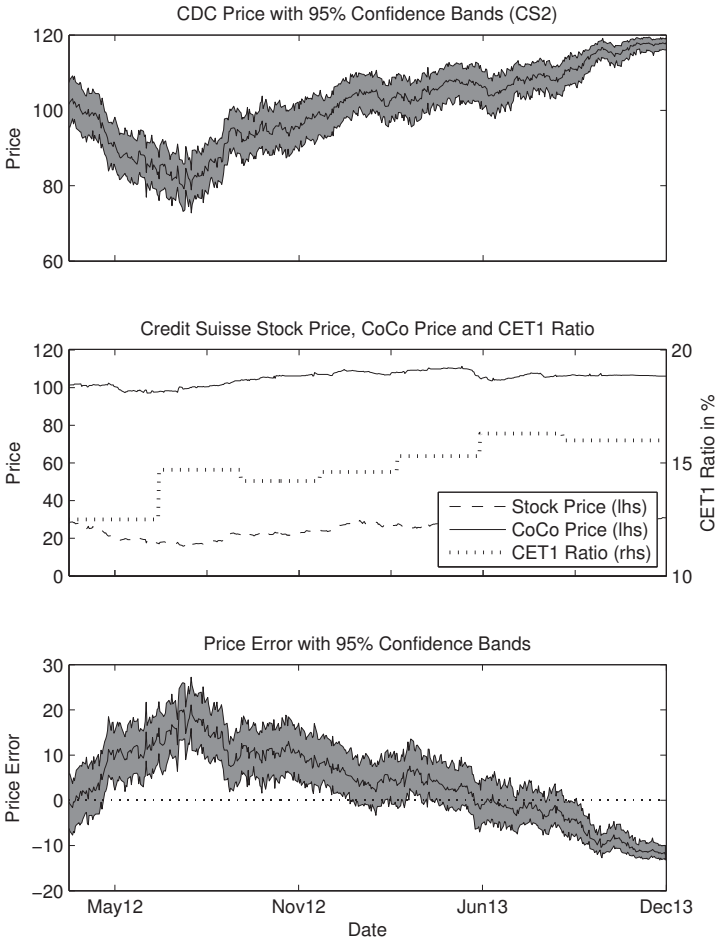**Table 5.5:** *Descriptive statistics CS2.*

Figure 5.14: *Diagram one shows the clean CoCo price as calculated with the credit derivative model with constant conversion intensity, where the trigger share price S^* has been calibrated to match the first empirical price. The 95% confidence bands result from the parameter uncertainty of the estimated five-year rolling volatility. Diagram two shows the empirical stock price of Credit Suisse in USD and the clean empirical CS2 CoCo price in CHF on the left y-axis and the core equity tier 1 ratio on the right y-axis. Diagram three shows the absolute price error $e_t = y_t - \hat{y}_t$, where $\hat{y}_t$ corresponds to the price calculated using the 50 percentile rolling standard deviation.*
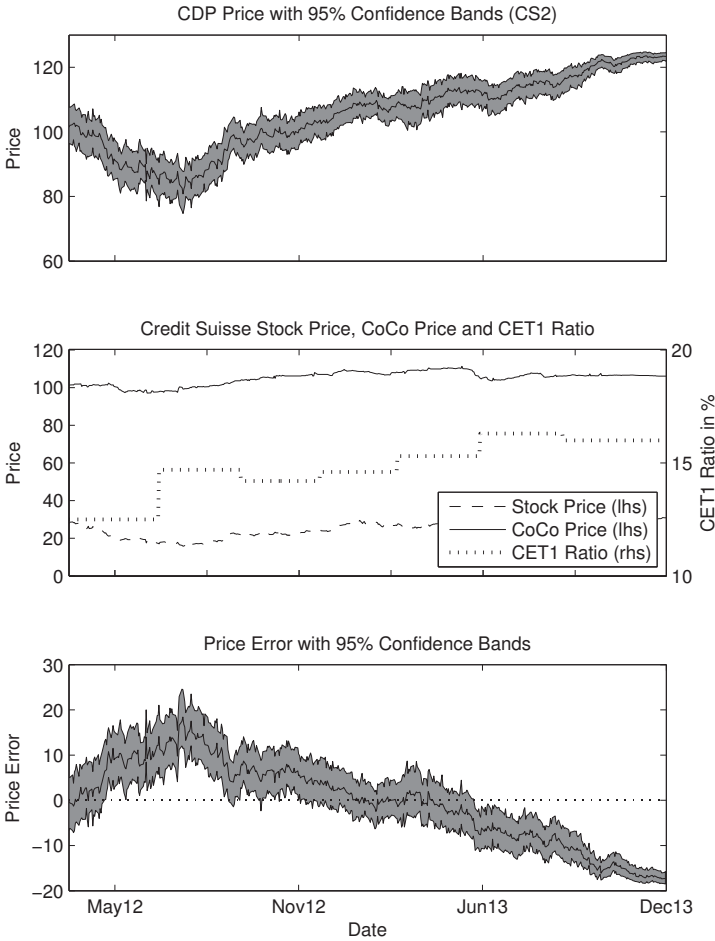
Figure 5.15: *Diagram one shows the clean CoCo price as calculated with the credit derivative model with piecewise constant conversion intensity, where the trigger share price S^* has been calibrated to match the first empirical price. The 95% confidence bands result from the parameter uncertainty of the estimated five-year rolling volatility. Diagram two shows the empirical stock price of Credit Suisse in USD and the clean empirical CS2 CoCo price in CHF on the left y-axis and the core equity tier 1 ratio on the right y-axis. Diagram three shows the absolute price error $e_t = y_t - \hat{y}_t$, where $\hat{y}_t$ corresponds to the price calculated using the 50 percentile rolling standard deviation.*
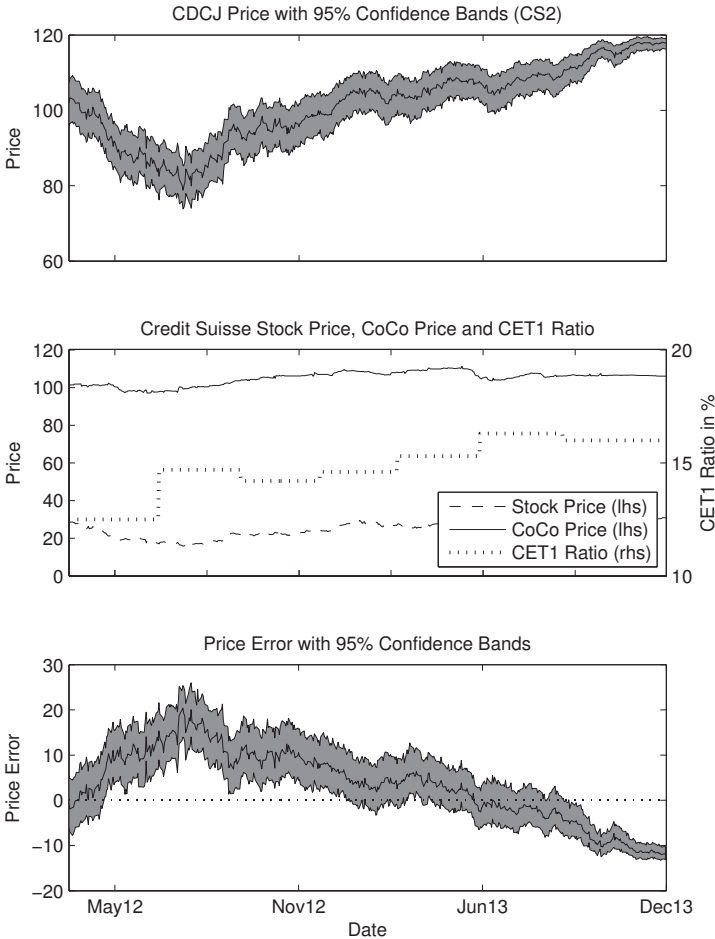
Figure 5.16: *Diagram one shows the clean CoCo price as calculated with the credit derivative model with constant conversion intensity including jumps, where the trigger share price S^* has been calibrated to match the first empirical price. The 95% confidence bands result from the parameter uncertainty of the estimated five-year rolling volatility. Diagram two shows the empirical stock price of Credit Suisse in USD and the clean empirical CS2 CoCo price in CHF on the left y-axis and the core equity tier 1 ratio on the right y-axis. Diagram three shows the absolute price error $e_t = y_t - \hat{y}_t$, where $\hat{y}_t$ corresponds to the price calculated using the 50 percentile rolling standard deviation.*
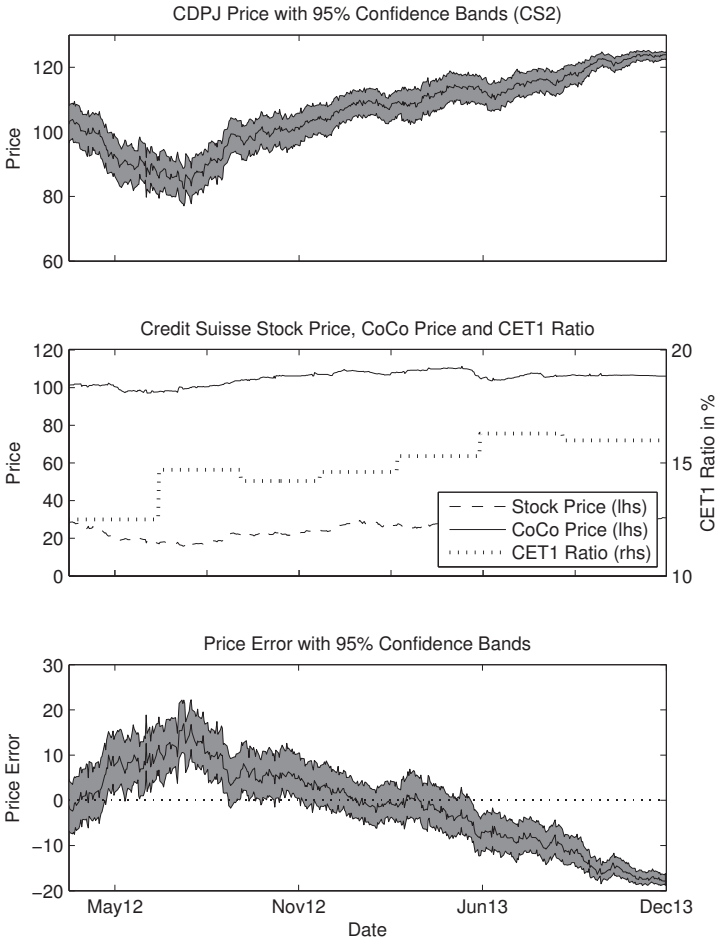
Figure 5.17: *Diagram one shows the clean CoCo price as calculated with the credit derivative model with piecewise constant conversion intensity including jumps, where the trigger share price S^* has been calibrated to match the first empirical price. The 95% confidence bands result from the parameter uncertainty of the estimated five-year rolling volatility. Diagram two shows the empirical stock price of Credit Suisse in USD and the clean empirical CS2 CoCo price in CHF on the left y-axis and the core equity tier 1 ratio on the right y-axis. Diagram three shows the absolute price error $e_t = y_t - \hat{y}_t$, where $\hat{y}_t$ corresponds to the price calculated using the 50 percentile rolling standard deviation.*
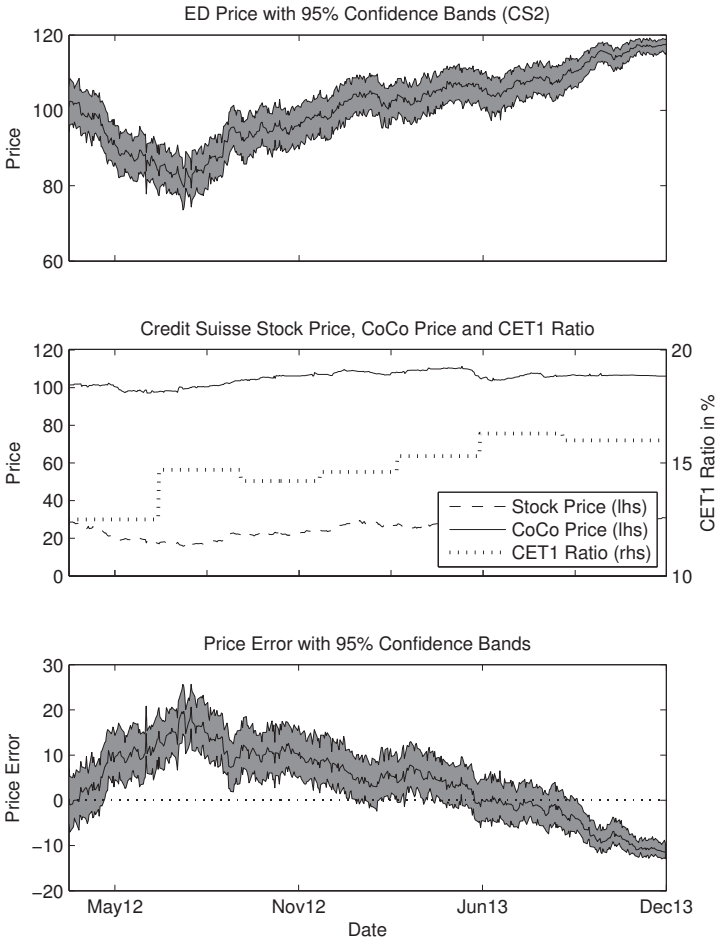
Figure 5.18: *Diagram one shows the clean CoCo price as calculated with the equity derivative model, where the trigger share price S^* has been calibrated to match the first empirical price. The 95% confidence bands result from the parameter uncertainty of the estimated five-year rolling volatility. Diagram two shows the empirical stock price of Credit Suisse in USD and the clean empirical CS2 CoCo price in CHF on the left y-axis and the core equity tier 1 ratio on the right y-axis. Diagram three shows the absolute price error $e_t = y_t - \hat{y}_t$, where $\hat{y}_t$ corresponds to the price calculated using the 50 percentile rolling standard deviation.*
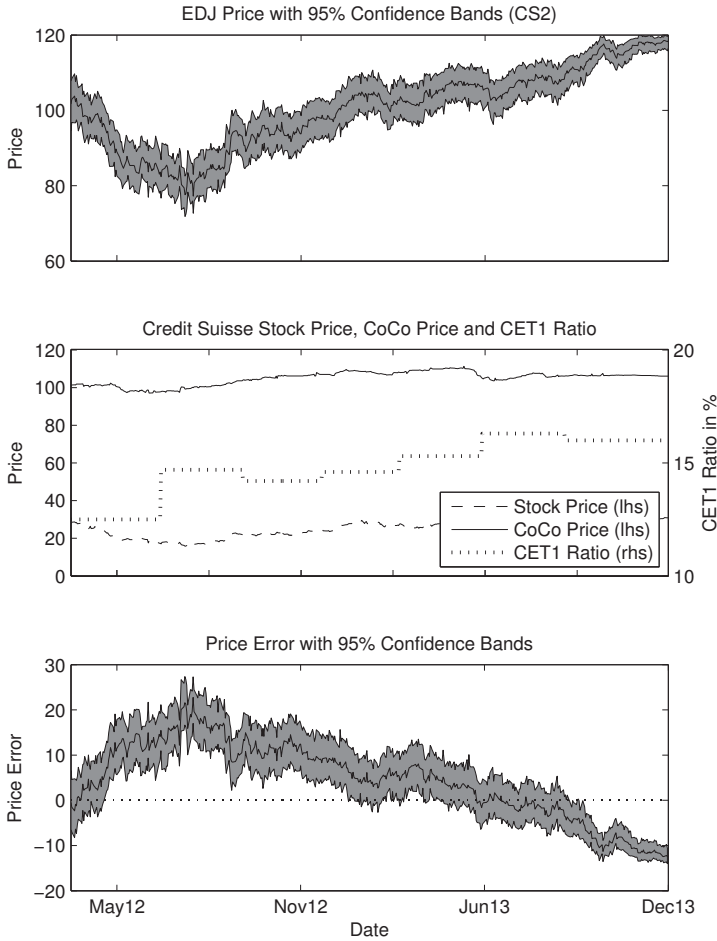
Figure 5.19: *Diagram one shows the clean CoCo price as calculated with the equity derivative model including jumps, where the trigger share price S^* has been calibrated to match the first empirical price. The 95% confidence bands result from the parameter uncertainty of the estimated five-year rolling volatility. Diagram two shows the empirical stock price of Credit Suisse in USD and the clean empirical CS2 CoCo price in CHF on the left y-axis and the core equity tier 1 ratio on the right y-axis. Diagram three shows the absolute price error $e_t = y_t - \hat{y}_t$, where $\hat{y}_t$ corresponds to the price calculated using the 50 percentile rolling standard deviation.*

Figure 5.20: *Diagram one shows the clean CoCo price as calculated with the J.P. Morgan model, where the trigger share price S^* has been calibrated to match the first empirical price. Diagram two shows the historical CDS spread on a five year subordinated bond of Credit Suisse in basis points and the clean empirical CS2 CoCo price in CHF on the left y-axis and the core equity tier 1 ratio on the right y-axis. Diagram three shows the absolute price error $e_t = y_t - \hat{y}_t$, where $\hat{y}_t$ corresponds to the price calculated using the 50 percentile rolling standard deviation.*
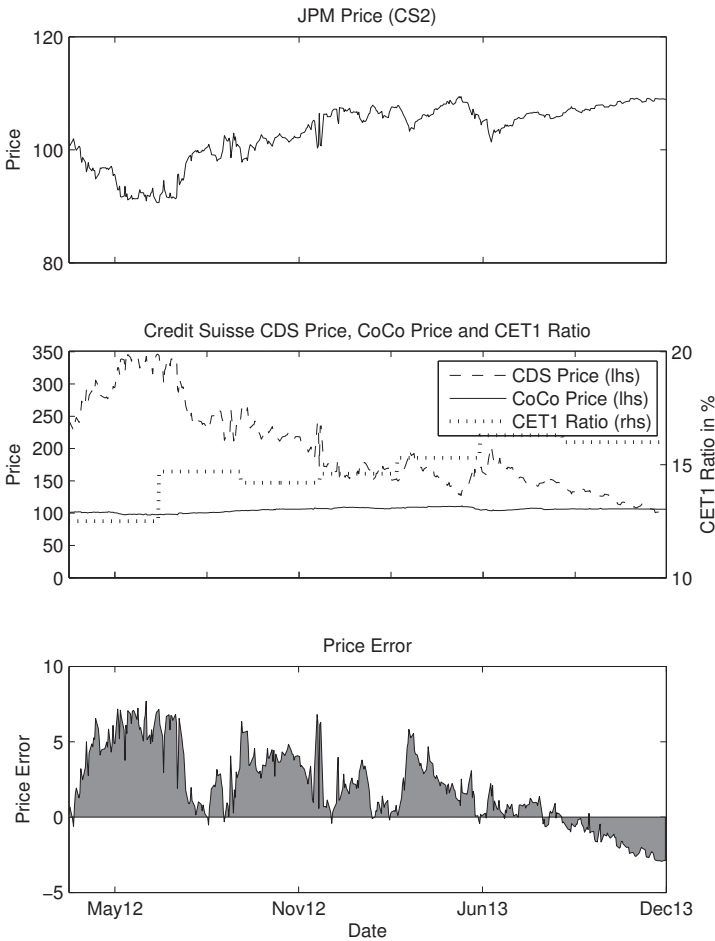
Figure 5.21: *Diagram one shows the clean CoCo price as calculated with the J.P. Morgan model including jumps, where the trigger share price S^* has been calibrated to match the first empirical price. Diagram two shows the historical CDS spread on a five year subordinated bond of Credit Suisse in basis points and the clean empirical CS2 CoCo price in CHF on the left y-axis and the core equity tier 1 ratio on the right y-axis. Diagram three shows the absolute price error $e_t = y_t - \hat{y}_t$, where $\hat{y}_t$ corresponds to the price calculated using the 50 percentile rolling standard deviation.*
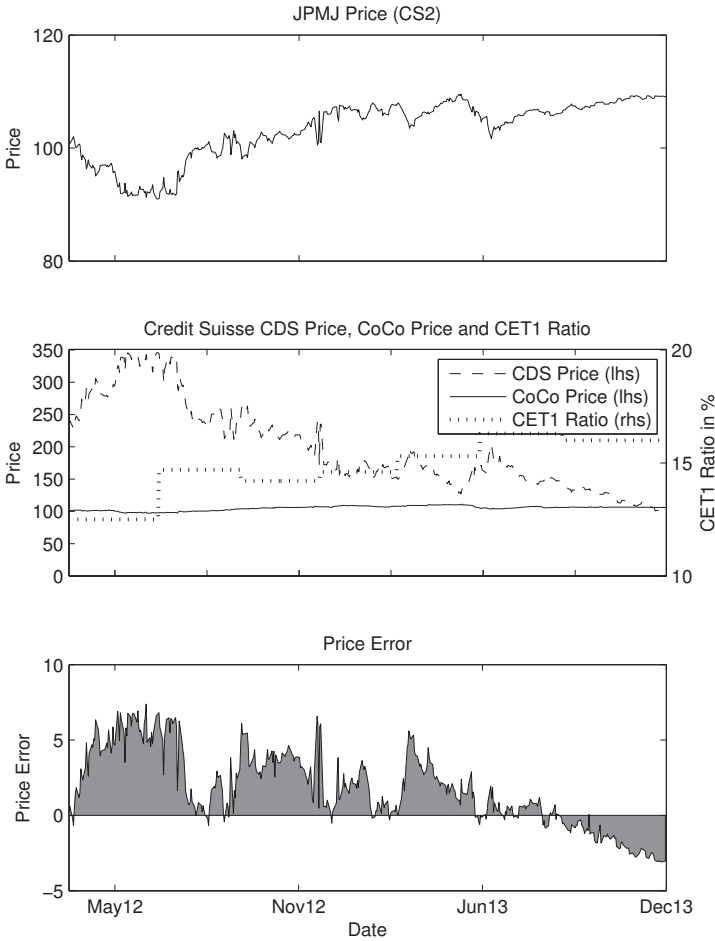
Figure 5.22: *Diagram one shows the clean CoCo price as calculated with the structural model, where the trigger asset-to-deposit ratio x^* has been calibrated to match the first empirical price. The 95% confidence bands result from the parameter uncertainty of the estimated five-year rolling volatility. Diagram two shows the empirical stock price of Credit Suisse in USD and the clean empirical CS2 CoCo price in CHF on the left y-axis and the core equity tier 1 ratio on the right y-axis. Diagram three shows the absolute price error $e_t = y_t - \hat{y}_t$, where $\hat{y}_t$ corresponds to the price calculated using the 50 percentile rolling standard deviation.*
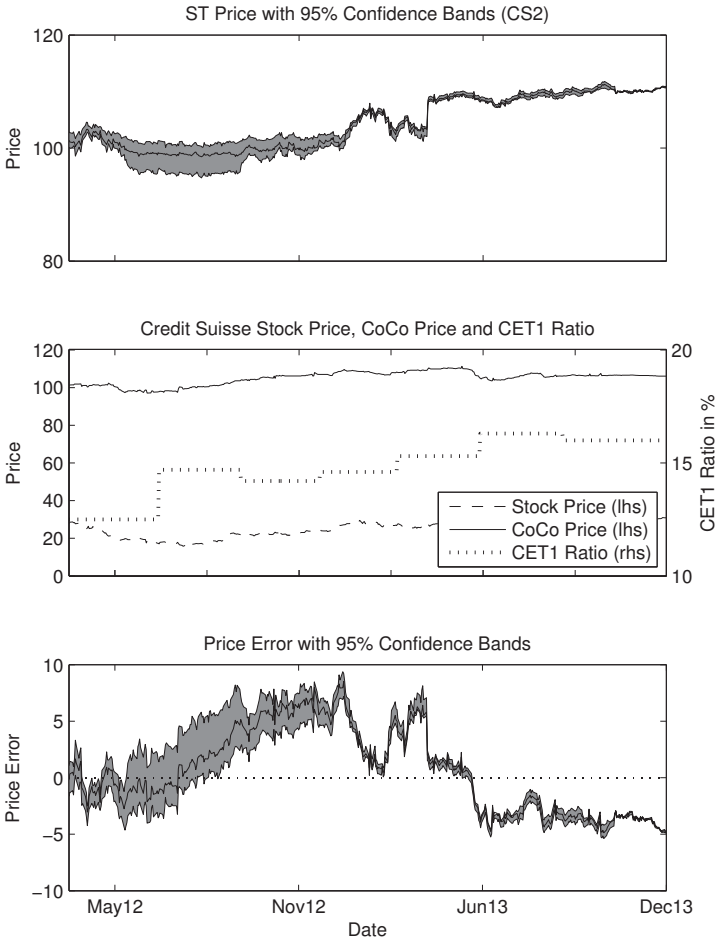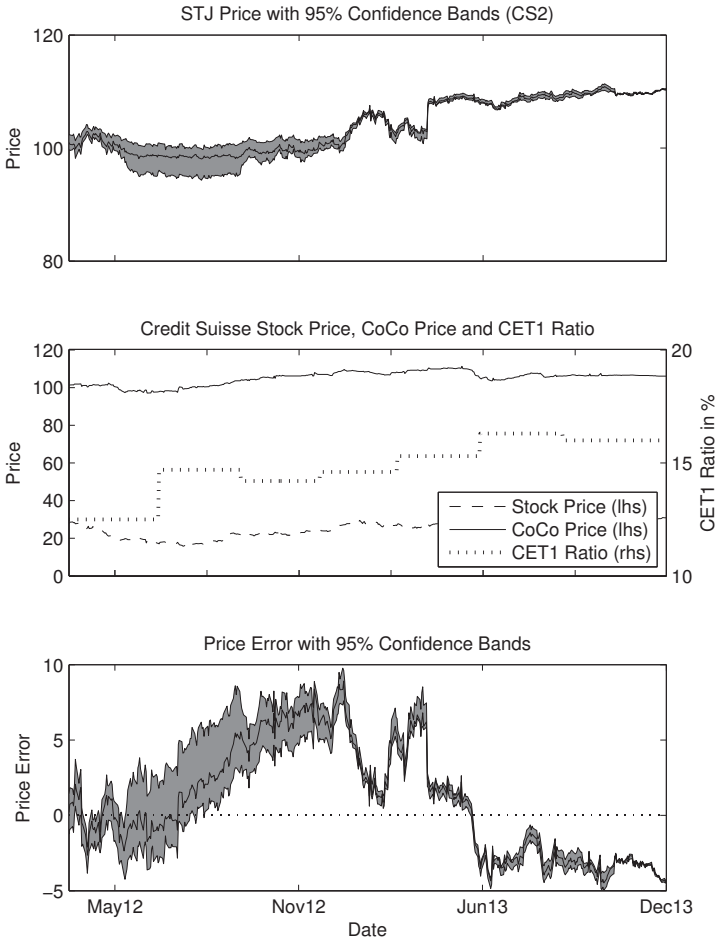
Figure 5.23: *Diagram one shows the clean CoCo price as calculated with the structural model including jumps, where the trigger asset-to-deposit ratio x^* has been calibrated to match the first empirical price. The 95% confidence bands result from the parameter uncertainty of the estimated five-year rolling volatility. Diagram two shows the empirical stock price of Credit Suisse in USD and the clean empirical CS2 CoCo price in CHF on the left y-axis and the core equity tier 1 ratio on the right y-axis. Diagram three shows the absolute price error $e_t = y_t - \hat{y}_t$, where $\hat{y}_t$ corresponds to the price calculated using the 50 percentile rolling standard deviation.*

Lloyds Banking Group LBG1

Variable	Value	Description
N	1000	Face value
c_i	7.5884%	Bond coupon rate, semi-annual
α	1	Full conversion
q	0%	Dividend yield
λ	1	Jump intensity per year
μ_π	-1.28%	Mean jump size
	(0.0152)	
σ_π	18.74%	Jump standard deviation
	(0.0186)	
S^*_{CDC}	3.92	Implied trigger share price CDC
	(0.0041)	
S^*_{CDP}	5.01	Implied trigger share price CDP
	(0.0027)	
S^*_{CDCJ}	4.32	Implied trigger share price CDCJ
	(0.0003)	
S^*_{CDPJ}	5.24	Implied trigger share price CDPJ
	(0.0013)	
S^*_{ED}	5.36	Implied trigger share price ED
	(0.32)	
S^*_{EDJ}	6.91	Implied trigger share price EDJ
	(0.2987)	
S^*_{JPM}	4.06	Implied trigger share price JPM
	(0.0016)	
S^*_{JPMJ}	3.58	Implied trigger share price JPMJ
	(0.0013)	

(a) *This table presents the static parameters of the credit, equity derivative and J.P. Morgan model to price the LBG1 CoCo. The standard errors of the jump distribution $\phi(\mu_\pi, \sigma_\pi)$ are calculated via bootstrap sampling. The standard error of S^* is calculated via the square root of the inverse of the hessian matrix.*

Table 5.6: *Descriptive statistics LBG1 (continued)*

Variable	Value	Description
N	1000	Face value
c_i	7.5884%	Bond coupon rate, semi-annual
α	1	Full conversion
q	0%	Dividend yield
λ	1	Jump intensity per year
μ_π	-1.28%	Mean jump size
	(0.0152)	
σ_π	18.74%	Jump standard deviation
	(0.0186)	
κ	0.2050	CIR Speed of convergence
	(0.0252)	
$\bar{r}$	3.87%	Long-term interest rate
	(0.0043)	
σ_r	3.81%	Standard deviation of interest rate
	(0.0017)	
g	0.5	Deposit-growth speed of convergence
$\hat{x}$	104.17%	Target asset-to-deposit ratio
b_0	2%	Initial CoCo-to-deposit ratio
x^*_{ST}	100.94%	Implied trigger asset-to-deposit ratio ST
	(0.0267)	
S^*_{ST}	14.67	Implied trigger stock price ST
x^*_{STJ}	100.85%	Implied trigger asset-to-deposit ratio STJ
	(0.0189)	
S^*_{STJ}	13.23	Implied trigger stock price STJ

(b) *This table presents the static parameters of the structural model to price the LBG1 CoCo. The standard errors of the jump distribution $\phi(\mu_\pi, \sigma_\pi)$ are calculated via bootstrap sampling. The standard error of $\kappa, \bar{r}, \sigma_r$ and x^* is calculated via the square root of the inverse of the hessian matrix.*

Table 5.6: *Descriptive statistics LBG1 (continued)*

Variable	Mean	Std.	Min.	Q. 1	Md.	Q. 3	Max.
t_i (years)	8.41	-	6.37	7.39	8.41	9.43	10.45
S_t (GBp)	52.12	15.96	21.84	35.8	53.38	65.79	80.37
CDS_t^{sub10}	395.04	150.52	168	276.23	342.19	514.1	772.25
A_t	953.87	47.58	877.4	915.01	945.85	994.42	1028.44
D_t	917.9	49.02	829.14	880.82	925.92	949.83	988.14
E_t	35.97	11.17	15.01	24.64	36.17	44.9	57.36
σ_{A_t} (%)	2.87	0.95	1.19	2	2.83	3.46	4.97
x_t (%)	103.95	1.33	101.61	102.66	103.9	104.83	106.87
$CET1$ (%)	10.68	1.69	6.3	9.5	10.4	11.5	14
σ_t (%)	71.15	2.79	63.62	69.08	70.61	74.02	74.87
r_t^{f10} (%)	2.8	0.77	1.64	2.17	2.76	3.49	4.09
V_{LBG1}	91.29	10.55	68.82	83.36	89.46	103.11	109.15
V_{CDC}	77.59	10.62	53.81	68.21	79.36	83.29	107.28
V_{CDCJ}	75.79	11.81	50.25	65.21	77.99	82.83	106.99
V_{CDP}	77.65	11.28	48.18	69.05	79.99	83.93	105.17
V_{CDPJ}	77.12	11.33	46.99	68.44	79.63	83.58	105.06
V_{ED}	76.17	10.7	51.25	66.43	78.28	82.77	104.09
V_{EDJ}	75.13	12.89	45.86	63.35	77.22	83.75	106.54
V_{JPM}	82.08	11.26	55.97	73.29	84.11	91.39	103.03
V_{JPMJ}	81.99	11.06	56.28	73.4	83.97	91.01	102.67
V_{ST}	86.87	7.85	78.12	80.09	83.23	92.21	103.92
V_{STJ}	85.73	7.56	77.67	79.71	83.01	91.71	102.99

(c) *This table presents the dynamic parameters of the models to price the LBG1 CoCo. All monetary values are reported in GBP (unless otherwise indicated); the CDS spread is indicated in basis points. A_t, D_t and E_t are reported in billion. 'Std.' stands for standard deviation, 'Min.' for minimum, 'Q. 1' for the first quantile, 'Md.' for median, 'Q. 3' for the third quantile and 'Max.' for maximum. (source: based on Bürgi (2013))*
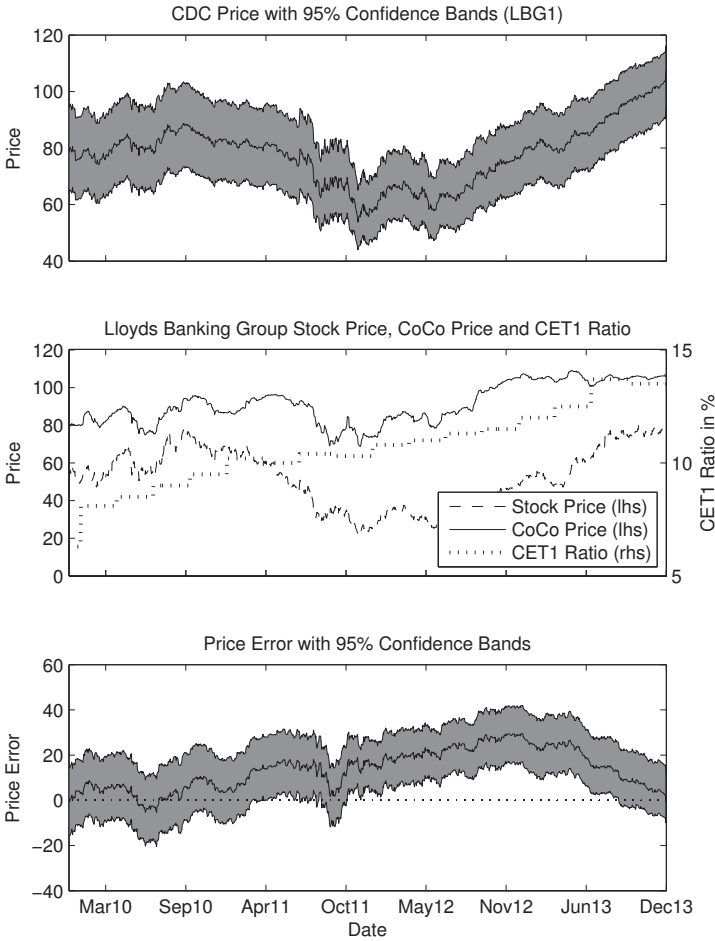
Table 5.6: *Descriptive statistics LBG1.*

Figure 5.24: *Diagram one shows the CoCo price calculated with the credit derivative model with constant conversion intensity, where the trigger share price S^* has been calibrated to match the first empirical price. The 95% confidence bands result from the parameter uncertainty of the estimated five-year rolling volatility. Diagram two shows the empirical stock price of Lloyds Banking Group in GBp and the clean empirical LBG1 CoCo price in GBP on the left y-axis and the core equity tier 1 ratio on the right y-axis. Diagram three shows the absolute price error $e_t = y_t - \hat{y}_t$, where $\hat{y}_t$ corresponds to the price calculated using the 50 percentile rolling standard deviation.*
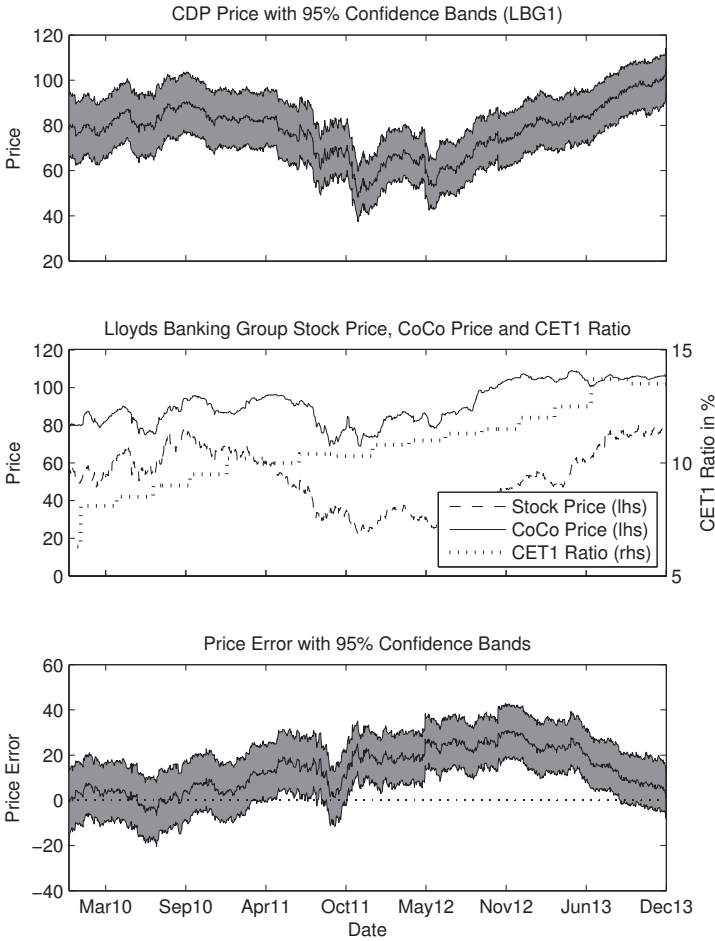
Figure 5.25: *Diagram one shows the CoCo price calculated with the credit derivative model with piecewise constant conversion intensity, where the trigger share price S^* has been calibrated to match the first empirical price. The 95% confidence bands result from the parameter uncertainty of the estimated five-year rolling volatility. Diagram two shows the empirical stock price of Lloyds Banking Group in GBp and the clean empirical LBG1 CoCo price in GBP on the left y-axis and the core equity tier 1 ratio on the right y-axis. Diagram three shows the absolute price error $e_t = y_t - \hat{y}_t$, where $\hat{y}_t$ corresponds to the price calculated using the 50 percentile rolling standard deviation.*
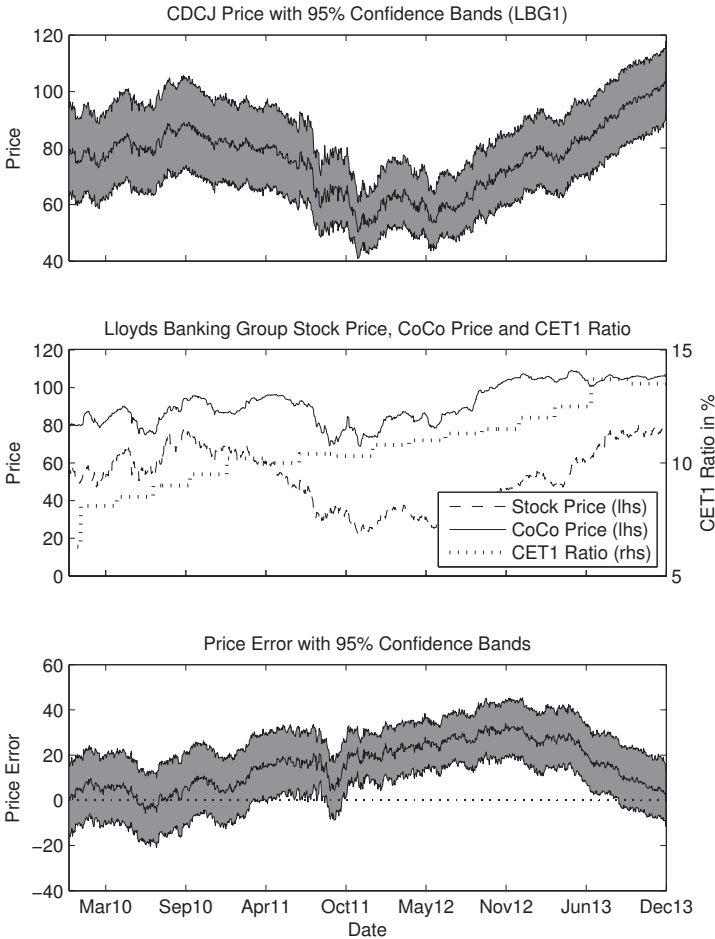
Figure 5.26: *Diagram one shows the CoCo price calculated with the credit derivative model with constant conversion intensity including jumps, where the trigger share price S^* has been calibrated to match the first empirical price. The 95% confidence bands result from the parameter uncertainty of the estimated five-year rolling volatility. Diagram two shows the empirical stock price of Lloyds Banking Group in GBp and the clean empirical LBG1 CoCo price with in GBP on the left y-axis and the core equity tier 1 ratio on the right y-axis. Diagram three shows the absolute price error $e_t = y_t - \hat{y}_t$, where $\hat{y}_t$ corresponds to the price calculated using the 50 percentile rolling standard deviation.*
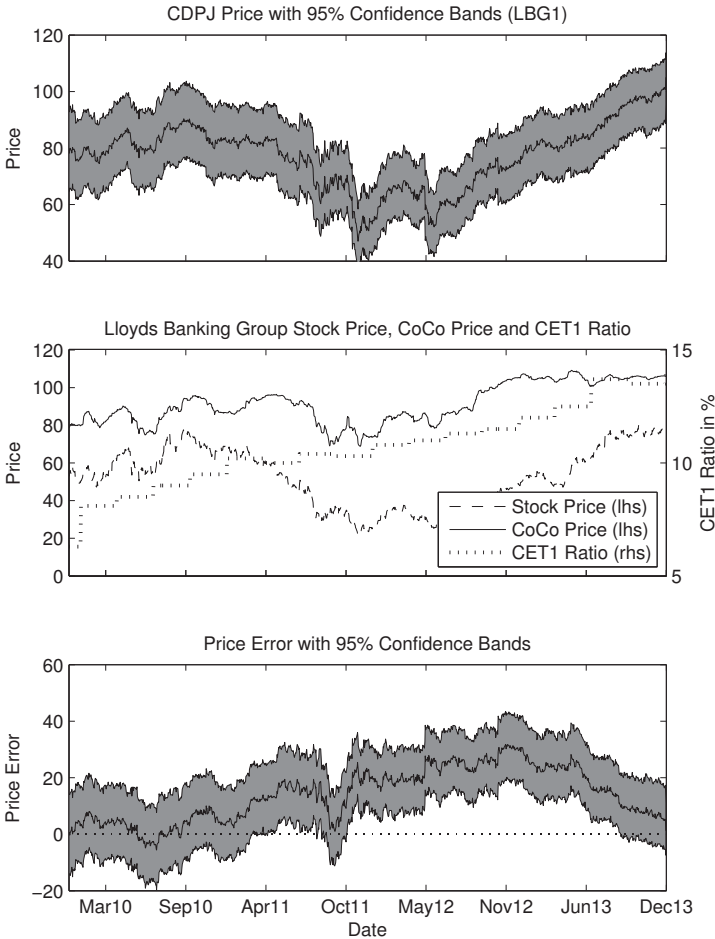
Figure 5.27: *Diagram one shows the CoCo price calculated with the credit derivative model with piecewise constant conversion intensity including jumps, where the trigger share price S^* has been calibrated to match the first empirical price. The 95% confidence bands result from the parameter uncertainty of the estimated five-year rolling volatility. Diagram two shows the empirical stock price of Lloyds Banking Group in GBp and the clean empirical LBG1 CoCo price in GBP on the left y-axis and the core equity tier 1 ratio on the right y-axis. Diagram three shows the absolute price error $e_t = y_t - \hat{y}_t$, where $\hat{y}_t$ corresponds to the price calculated using the 50 percentile rolling standard deviation.*
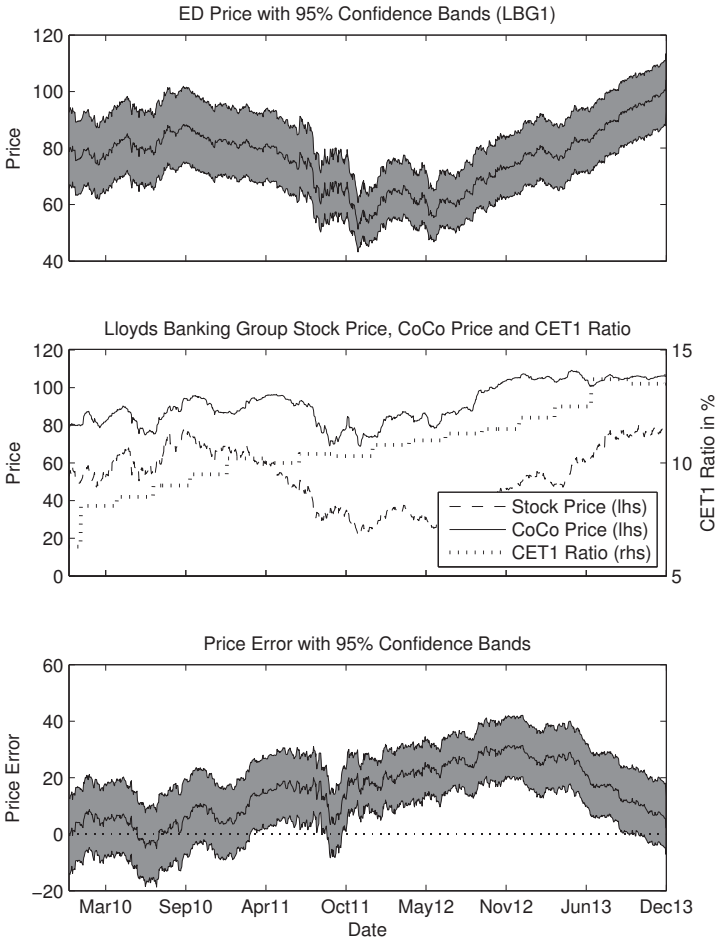
Figure 5.28: *Diagram one shows the CoCo price calculated with the equity derivative model, where the trigger share price S^* has been calibrated to match the first empirical price. The 95% confidence bands result from the parameter uncertainty of the estimated five-year rolling volatility. Diagram two shows the empirical stock price of Lloyds Banking Group in GBp and the clean empirical LBG1 CoCo price in GBP on the left y-axis and the core equity tier 1 ratio on the right y-axis. Diagram three shows the absolute price error $e_t = y_t - \hat{y}_t$, where $\hat{y}_t$ corresponds to the price calculated using the 50 percentile rolling standard deviation.*

Figure 5.29: *Diagram one shows the CoCo price calculated with the equity derivative model including jumps, where the trigger share price S^* has been calibrated to match the first empirical price. The 95% confidence bands result from the parameter uncertainty of the estimated five-year rolling volatility. Diagram two shows the empirical stock price of Lloyds Banking Group in GBp and the clean empirical LBG1 CoCo price in GBP on the left y-axis and the core equity tier 1 ratio on the right y-axis. Diagram three shows the absolute price error $e_t = y_t - \hat{y}_t$, where $\hat{y}_t$ corresponds to the price calculated using the 50 percentile rolling standard deviation.*
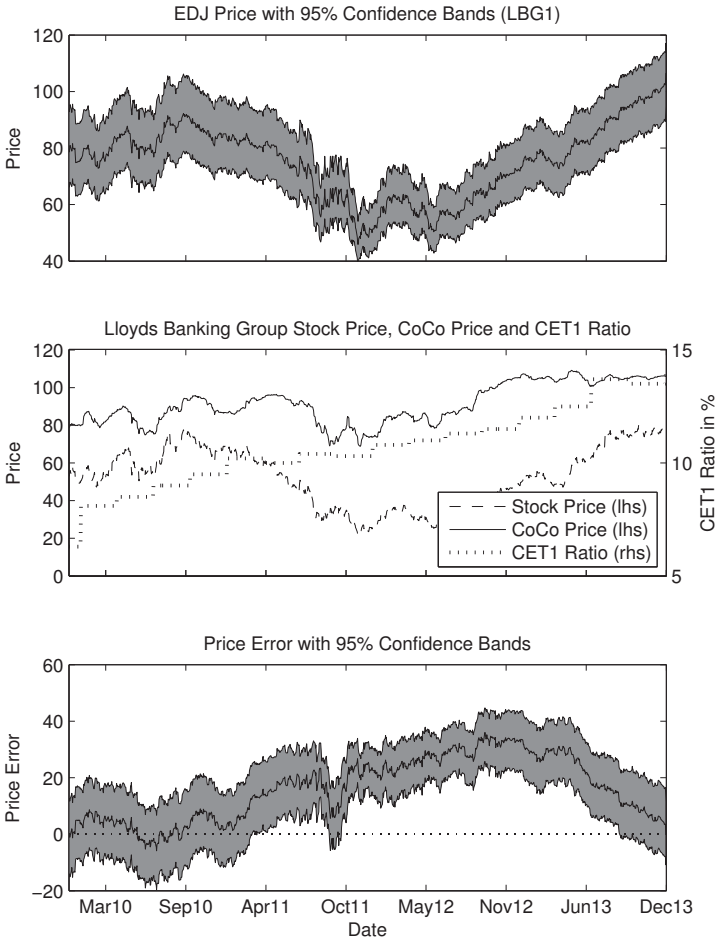
Figure 5.30: *Diagram one shows the clean CoCo price as calculated with the J.P. Morgan model, where the trigger share price S^* has been calibrated to match the first empirical price. Diagram two shows the historical CDS spread on a five year subordinated bond of Lloyds Banking Group in basis points and the clean empirical LBG1 CoCo price in GBP on the left y-axis and the core equity tier 1 ratio on the right y-axis. Diagram three shows the absolute price error $e_t = y_t - \hat{y}_t$, where $\hat{y}_t$ corresponds to the price calculated using the 50 percentile rolling standard deviation.*
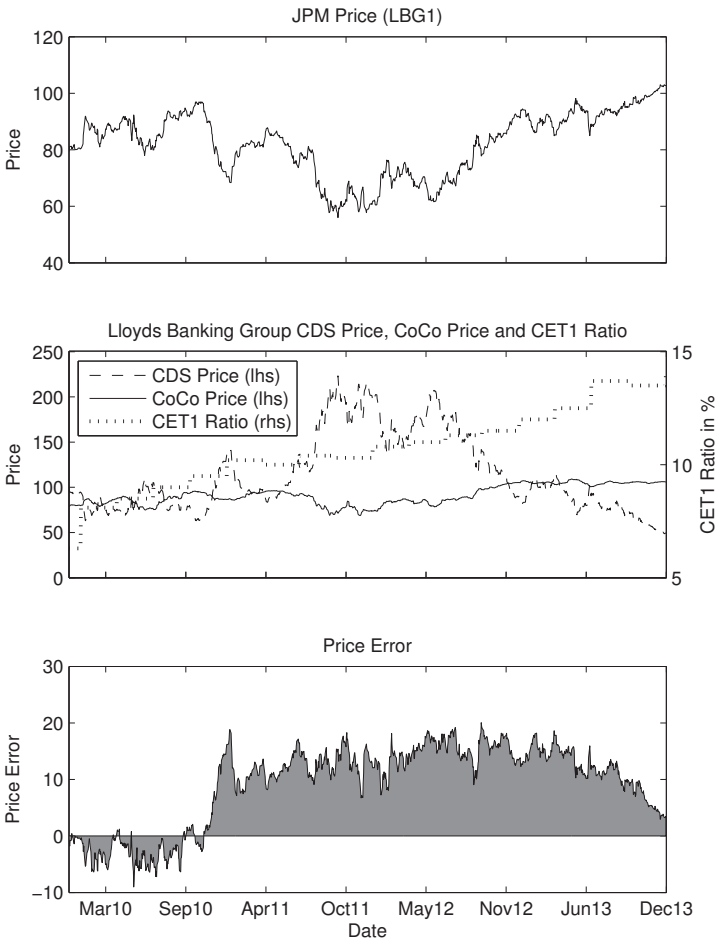
Figure 5.31: *Diagram one shows the clean CoCo price as calculated with the J.P. Morgan model including jumps, where the trigger share price S^* has been calibrated to match the first empirical price. Diagram two shows the historical CDS spread on a five year subordinated bond of Lloyds Banking Group in basis points and the clean empirical LBG1 CoCo price in GBP on the left y-axis and the core equity tier 1 ratio on the right y-axis. Diagram three shows the absolute price error $e_t = y_t - \hat{y}_t$, where $\hat{y}_t$ corresponds to the price calculated using the 50 percentile rolling standard deviation.*
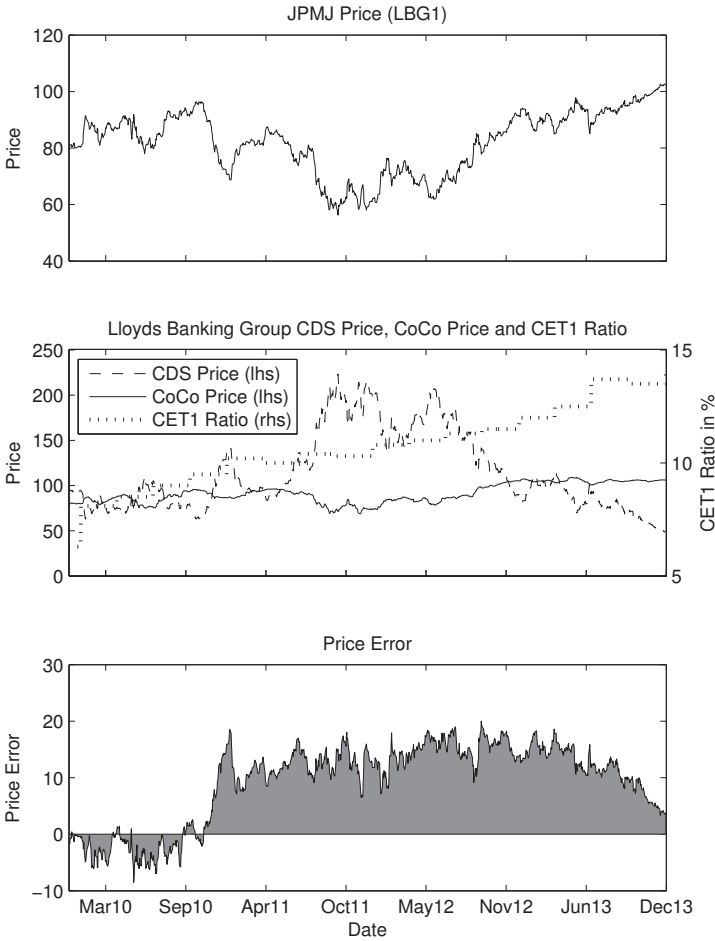
Figure 5.32: *Diagram one shows the CoCo price calculated with the structural model, where the trigger asset-to-deposit ratio x^* has been calibrated to match the first empirical price. The 95% confidence bands result from the parameter uncertainty of the estimated five-year rolling volatility. Diagram two shows the empirical stock price of Lloyds Banking Group in GBp and the clean empirical LBG1 CoCo price in GBP on the left y-axis and the core equity tier 1 ratio on the right y-axis. Diagram three shows the absolute price error $e_t = y_t - \hat{y}_t$, where $\hat{y}_t$ corresponds to the price calculated using the 50 percentile rolling standard deviation.*
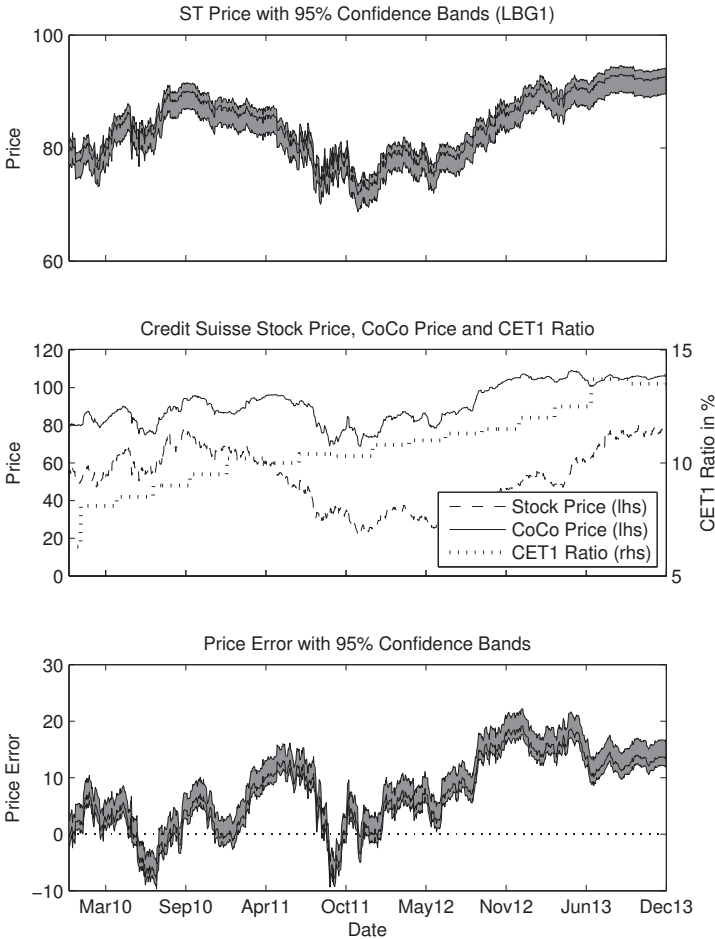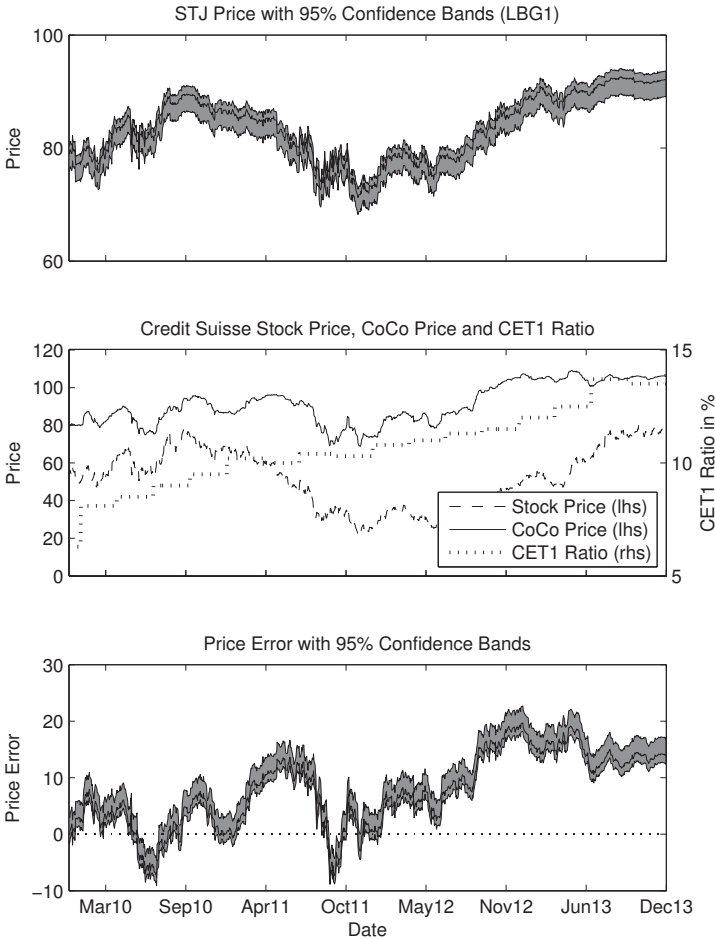
Figure 5.33: *Diagram one shows the CoCo price calculated with the structural model including jumps, where the trigger asset-to-deposit ratio x^* has been calibrated to match the first empirical price. The 95% confidence bands result from the parameter uncertainty of the estimated five-year rolling volatility. Diagram two shows the empirical stock price of Lloyds Banking Group in GBp and the clean empirical LBG1 CoCo price in GBP on the left y-axis and the core equity tier 1 ratio on the right y-axis. Diagram three shows the absolute price error $e_t = y_t - \hat{y}_t$, where $\hat{y}_t$ corresponds to the price calculated using the 50 percentile rolling standard deviation.*

Lloyds Banking Group LBG2

Variable	Value	Description
N	1000	Face value
c_i	15%	Bond coupon rate, semi-annual
α	1	Full conversion
q	0%	Dividend yield
λ	1	Jump intensity per year
μ_π	-1.28%	Mean jump size
	(0.0152)	
σ_π	18.74%	Jump standard deviation
	(0.0186)	
S^*_{CDC}	4.26	Implied trigger share price CDC
	(0.0089)	
S^*_{CDP}	5.51	Implied trigger share price CDP
	(0.0067)	
S^*_{CDCJ}	4.56	Implied trigger share price CDCJ
	(0.0012)	
S^*_{CDPJ}	5.67	Implied trigger share price CDPJ
	(0.0014)	
S^*_{ED}	5.86	Implied trigger share price ED
	(0.4124)	
S^*_{EDJ}	7.09	Implied trigger share price EDJ
	(0.3891)	
S^*_{JPM}	4.48	Implied trigger share price JPM
	(0.0018)	
S^*_{JPMJ}	3.97	Implied trigger share price JPMJ
	(0.0021)	

(a) *This table presents the static parameters of the credit, equity derivative and J.P. Morgan model to price the LBG2 CoCo. The standard errors of the jump distribution $\phi(\mu_\pi, \sigma_\pi)$ are calculated via bootstrap sampling. The standard error of S^* is calculated via the square root of the inverse of the hessian matrix.*

Table 5.7: *Descriptive statistics LBG2 (continued)*

Variable	Value	Description
N	1000	Face value
c_i	15%	Bond coupon rate, semi-annual
α	1	Full conversion
q	0%	Dividend yield
λ	1	Jump intensity per year
μ_π	-1.28%	Mean jump size
	(0.0152)	
σ_π	18.74%	Jump standard deviation
	(0.0186)	
κ	0.2050	CIR Speed of convergence
	(0.0252)	
$\bar{r}$	3.87%	Long-term interest rate
	(0.0043)	
σ_r	3.81%	Standard deviation of interest rate
	(0.0017)	
g	0.5	Deposit-growth speed of convergence
$\hat{x}$	104.17	Target asset-to-deposit ratio
b_0	2%	Initial CoCo-to-deposit ratio
x^*_{ST}	100.99%	Implied trigger asset-to-deposit ratio ST
	(0.0135)	
S^*_{ST}	15.51	Implied trigger stock price ST
x^*_{STJ}	100.94%	Implied trigger asset-to-deposit ratio STJ
	(0.0135)	
S^*_{STJ}	14.58	Implied trigger stock price STJ

(b) *This table presents the static parameters of the structural model to price the LBG2 CoCo. The standard errors of the jump distribution $\phi(\mu_\pi, \sigma_\pi)$ are calculated via bootstrap sampling. The standard error of $\kappa, \bar{r}, \sigma_r$ and x^* is calculated via the square root of the inverse of the hessian matrix.*

Table 5.7: *Descriptive statistics LBG2 (continued)*

Variable	Mean	Std.	Min.	Q. 1	Md.	Q. 3	Max.
t_i (years)	8.01	-	5.98	7	8.02	9.04	10.06
S_t (GBp)	52.14	15.96	21.84	35.81	53.42	65.86	80.37
CDS_t^{sub10}	394.85	150.14	168	275.75	342.46	513.01	772.25
A_t	953.77	47.59	877.4	915.14	945.86	994.52	1028.44
D_t	917.78	49.07	829.14	881.14	926.03	949.94	988.14
E_t	35.99	11.17	15.01	24.65	36.18	44.93	57.36
σ_{A_t} (%)	2.87	0.99	1.19	1.98	2.81	3.46	5.09
x_t (%)	103.95	1.33	101.61	102.66	103.9	104.84	106.87
$CET1$ (%)	10.69	1.69	6.3	9.5	10.4	11.5	14
σ_t (%)	71.15	2.79	63.62	69.08	70.61	74.02	74.87
r_t^{f10} (%)	2.8	0.77	1.64	2.17	2.76	3.49	4.09
V_{CoCo}	129.77	11.39	103.89	121.5	129.85	139.28	148.15
V_{CDC}	113.52	12.98	82.6	102.23	117.52	123.78	136.26
V_{CDCJ}	113.98	12.93	82.76	102.59	117.69	124.12	136.72
V_{CDP}	114.05	14.34	73.97	103.35	117.69	125.12	136.27
V_{CDPJ}	114.14	14.32	73.98	103.37	117.73	124.99	137.07
V_{ED}	111.44	14.52	75.7	98.52	115.89	123.44	133.6
V_{EDJ}	111.56	17.14	69.61	96.02	116.36	126.18	138.98
V_{JPM}	118.88	13.86	86.39	107.65	122.63	128.69	142.37
V_{JPMJ}	118.77	13.6	86.78	107.83	122.52	128.41	141.54
V_{ST}	125.81	5.51	113.74	121.09	126.11	130.54	135.09
V_{STJ}	124.50	5.24	112.64	120.79	125.81	130.24	134.79

(c) *This table presents the dynamic parameters of the models to price the LBG2 CoCo. All monetary values are reported in GBP (unless otherwise indicated); the CDS spread is indicated in basis points. A_t, D_t and E_t are reported in billion. 'Std.' stands for standard deviation, 'Min.' for minimum, 'Q. 1' for the first quantile, 'Md.' for median, 'Q. 3' for the third quantile and 'Max.' for maximum. (source: based on Bürgi (2013))*

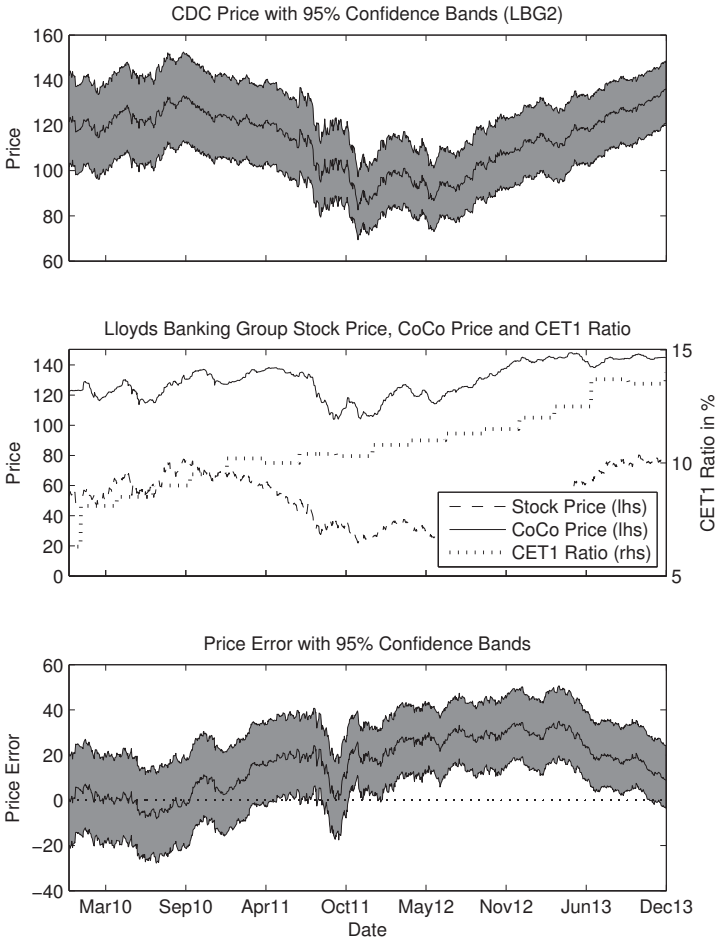**Table 5.7:** *Descriptive statistics credit derivative model LBG2*

Figure 5.34: *Diagram one shows the CoCo price calculated with the credit derivative model with constant conversion intensity, where the trigger share price S^* has been calibrated to match the first empirical price. The 95% confidence bands result from the parameter uncertainty of the estimated five-year rolling volatility. Diagram two shows the empirical stock price of Lloyds Banking Group in GBp and the clean empirical LBG2 CoCo price in GBP on the left y-axis and the core equity tier 1 ratio on the right y-axis. Diagram three shows the absolute price error $e_t = y_t - \hat{y}_t$, where $\hat{y}_t$ corresponds to the price calculated using the 50 percentile rolling standard deviation.*
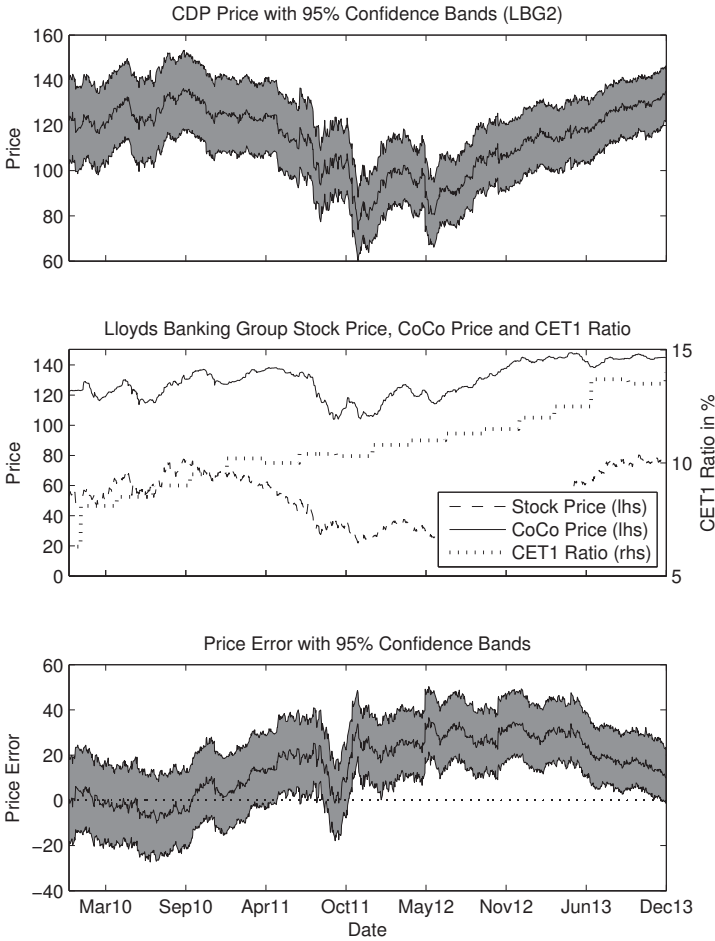
Figure 5.35: *Diagram one shows the CoCo price calculated with the credit derivative model with piecewise constant conversion intensity, where the trigger share price S^* has been calibrated to match the first empirical price. The 95% confidence bands result from the parameter uncertainty of the estimated five-year rolling volatility. Diagram two shows the empirical stock price of Lloyds Banking Group in GBp and the clean empirical LBG2 CoCo price in GBP on the left y-axis and the core equity tier 1 ratio on the right y-axis. Diagram three shows the absolute price error $e_t = y_t - \hat{y}_t$, where $\hat{y}_t$ corresponds to the price calculated using the 50 percentile rolling standard deviation.*
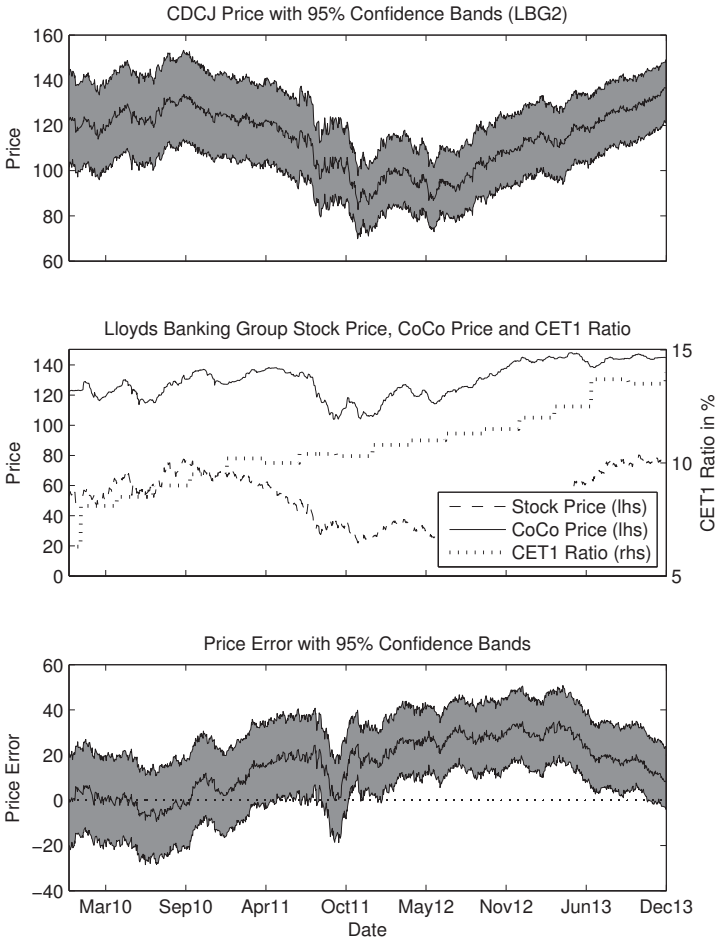
Figure 5.36: *Diagram one shows the CoCo price calculated with the credit derivative model with constant conversion intensity including jumps, where the trigger share price S^* has been calibrated to match the first empirical price. The 95% confidence bands result from the parameter uncertainty of the estimated five-year rolling volatility. Diagram two shows the empirical stock price of Lloyds Banking Group in GBp and the clean empirical LBG2 CoCo price in GBP on the left y-axis and the core equity tier 1 ratio on the right y-axis. Diagram three shows the absolute price error $e_t = y_t - \hat{y}_t$, where $\hat{y}_t$ corresponds to the price calculated using the 50 percentile rolling standard deviation.*
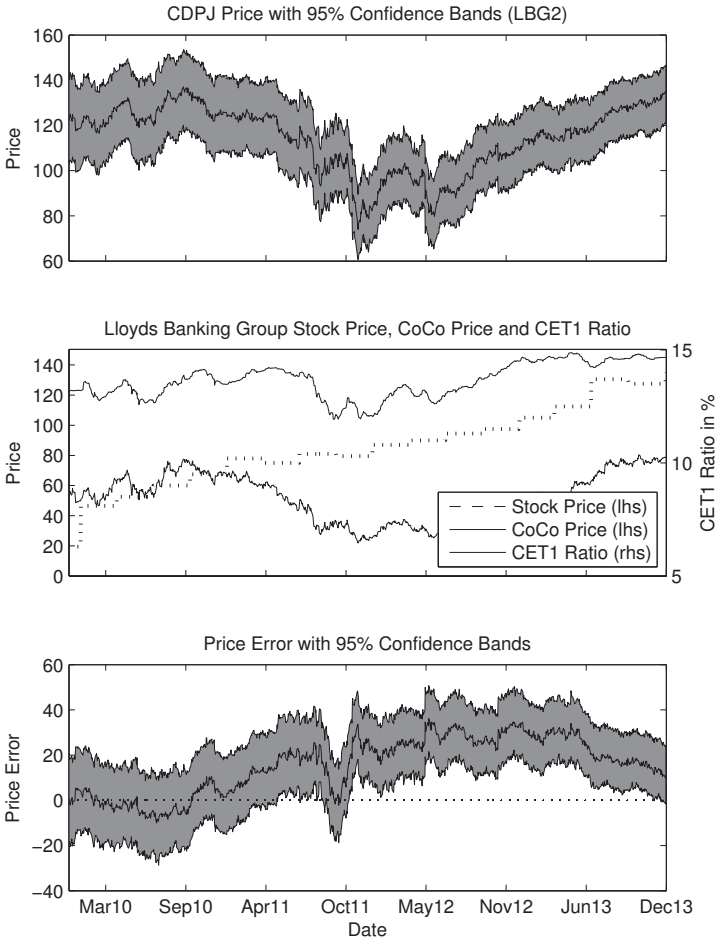
Figure 5.37: *Diagram one shows the CoCo price calculated with the credit derivative model with piecewise constant conversion intensity including jumps, where the trigger share price S^* has been calibrated to match the first empirical price. The 95% confidence bands result from the parameter uncertainty of the estimated five-year rolling volatility. Diagram two shows the empirical stock price of Lloyds Banking Group in GBp and the clean empirical LBG2 CoCo price in GBP on the left y-axis and the core equity tier 1 ratio on the right y-axis. Diagram three shows the absolute price error $e_t = y_t - \hat{y}_t$, where $\hat{y}_t$ corresponds to the price calculated using the 50 percentile rolling standard deviation.*

Figure 5.38: *Diagram one shows the CoCo price calculated with the equity derivative model, where the trigger share price S^* has been calibrated to match the first empirical price. The 95% confidence bands result from the parameter uncertainty of the estimated five-year rolling volatility. Diagram two shows the empirical stock price of Lloyds Banking Group in GBp and the clean empirical LBG2 CoCo price in GBP on the left y-axis and the core equity tier 1 ratio on the right y-axis. Diagram three shows the absolute price error $e_t = y_t - \hat{y}_t$, where $\hat{y}_t$ corresponds to the price calculated using the 50 percentile rolling standard deviation.*
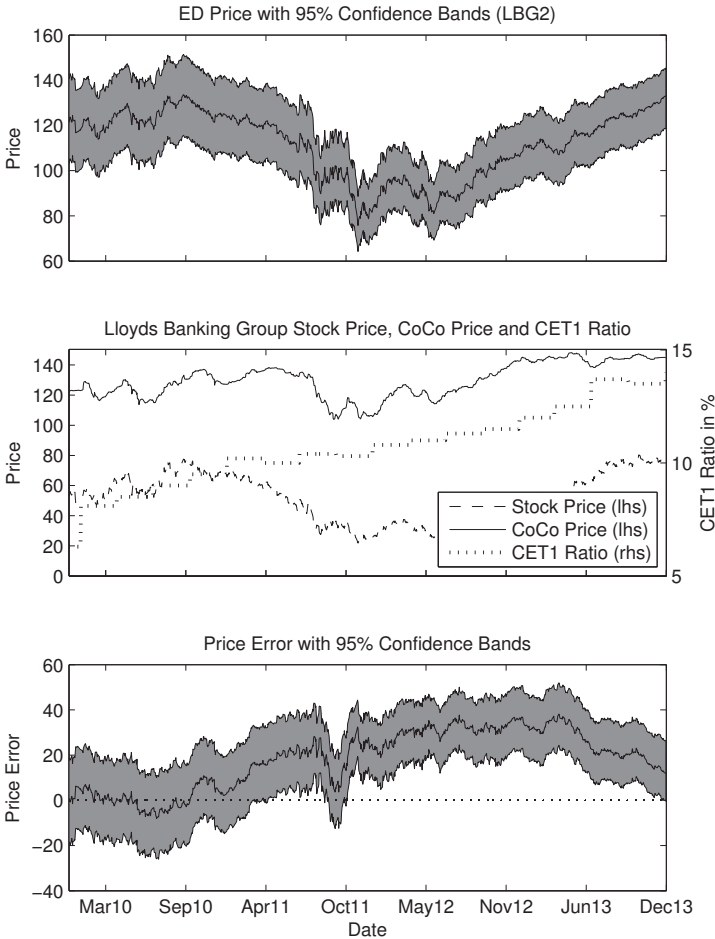
Figure 5.39: *Diagram one shows the CoCo price calculated with the equity derivative model including jumps, where the trigger share price S^* has been calibrated to match the first empirical price. The 95% confidence bands result from the parameter uncertainty of the estimated five-year rolling volatility. Diagram two shows the empirical stock price of Lloyds Banking Group in GBp and the clean empirical LBG2 CoCo price in GBP on the left y-axis and the core equity tier 1 ratio on the right y-axis. Diagram three shows the absolute price error $e_t = y_t - \hat{y}_t$, where $\hat{y}_t$ corresponds to the price calculated using the 50 percentile rolling standard deviation.*
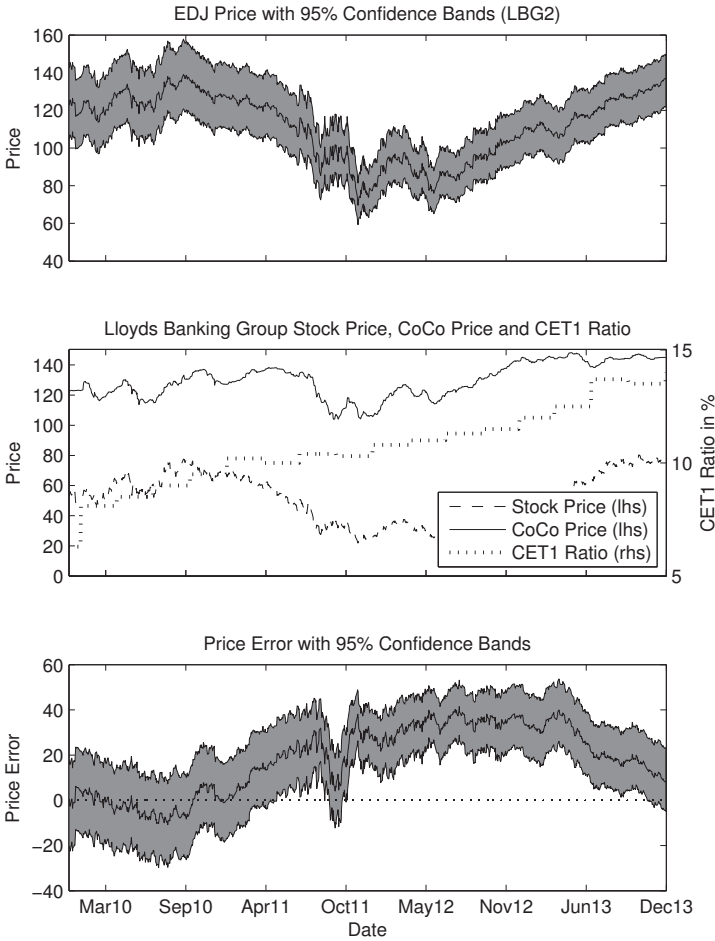
Figure 5.40: *Diagram one shows the clean CoCo price as calculated with the J.P. Morgan model, where the trigger share price S^* has been calibrated to match the first empirical price. Diagram two shows the historical CDS spread on a five year subordinated bond of Lloyds Banking Group in basis points and the clean empirical LBG2 CoCo price in GBP on the left y-axis and the core equity tier 1 ratio on the right y-axis. Diagram three shows the absolute price error $e_t = y_t - \hat{y}_t$, where $\hat{y}_t$ corresponds to the price calculated using the 50 percentile rolling standard deviation.*
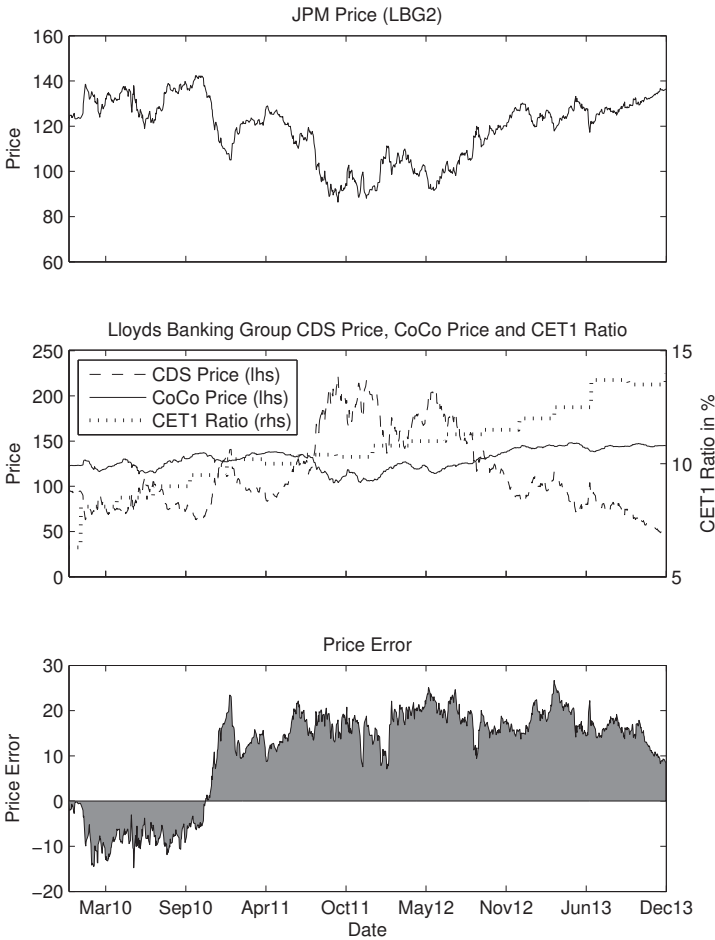
Figure 5.41: *Diagram one shows the clean CoCo price as calculated with the J.P. Morgan model including jumps, where the trigger share price S^* has been calibrated to match the first empirical price. Diagram two shows the historical CDS spread on a five year subordinated bond of Lloyds Banking Group in basis points and the clean empirical LBG2 CoCo price in GBP on the left y-axis and the core equity tier 1 ratio on the right y-axis. Diagram three shows the absolute price error $e_t = y_t - \hat{y}_t$, where $\hat{y}_t$ corresponds to the price calculated using the 50 percentile rolling standard deviation.*
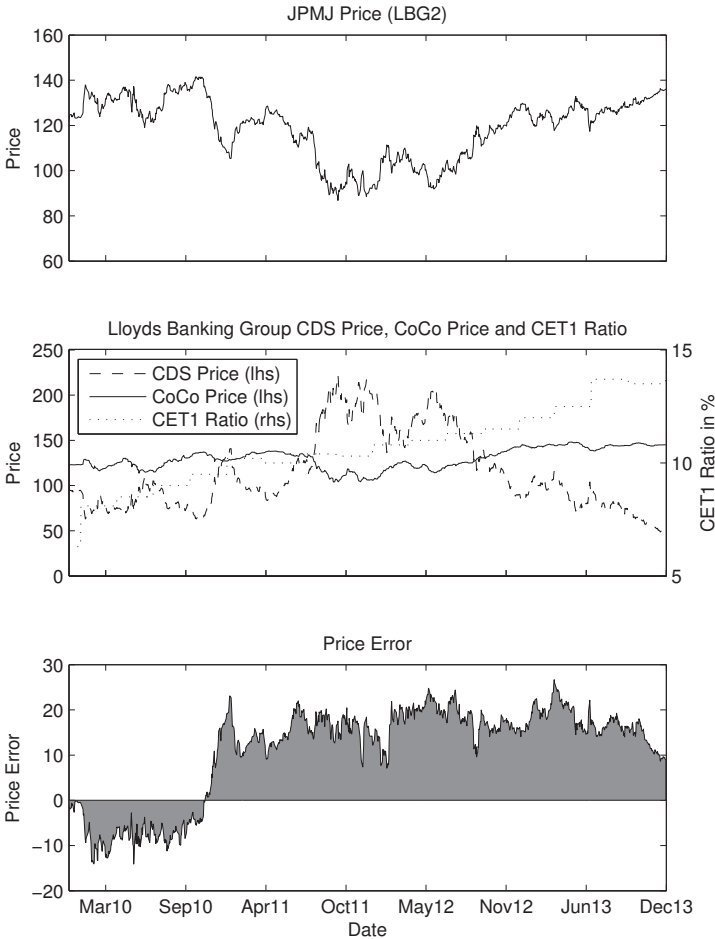
Figure 5.42: *Diagram one shows the CoCo price calculated with the structural model, where the trigger asset-to-deposit ratio x^* has been calibrated to match the first empirical price. The 95% confidence bands result from the parameter uncertainty of the estimated five-year rolling volatility. Diagram two shows the empirical stock price of Lloyds Banking Group in GBp and the clean empirical LBG2 CoCo price in GBP on the left y-axis and the core equity tier 1 ratio on the right y-axis. Diagram three shows the absolute price error $e_t = y_t - \hat{y}_t$, where $\hat{y}_t$ corresponds to the price calculated using the 50 percentile rolling standard deviation.*
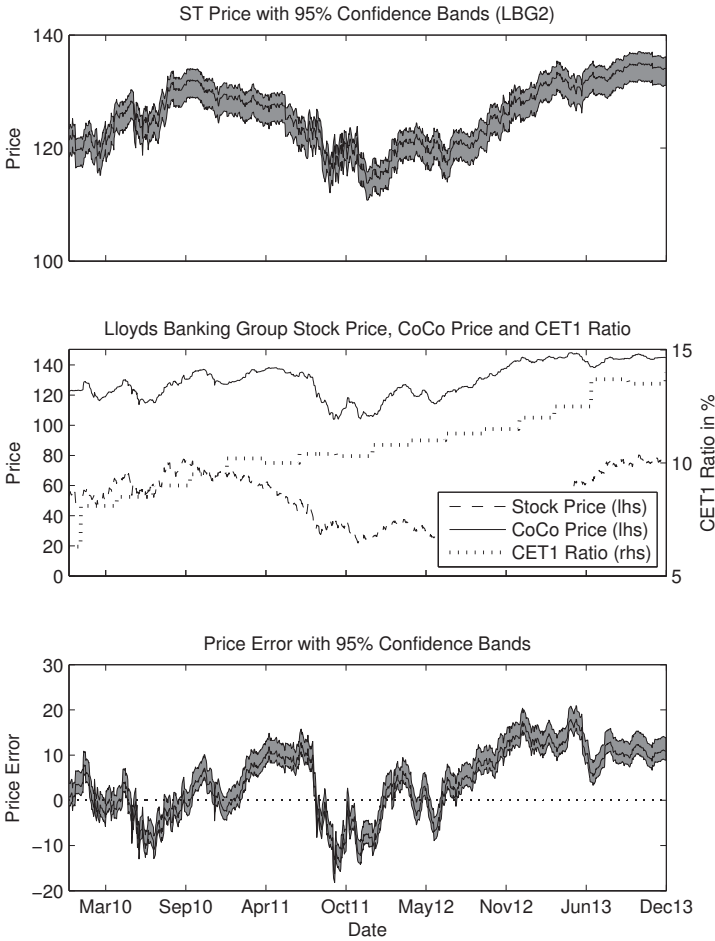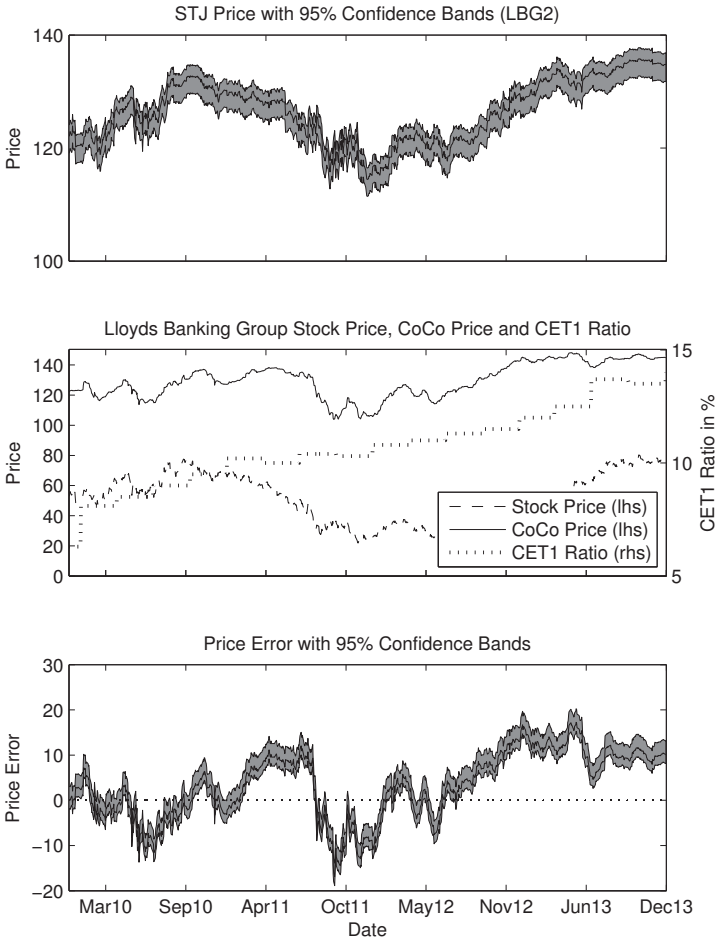
Figure 5.43: *Diagram one shows the CoCo price calculated with the structural model including jumps, where the trigger asset-to-deposit ratio x^* has been calibrated to match the first empirical price. The 95% confidence bands result from the parameter uncertainty of the estimated five-year rolling volatility. Diagram two shows the empirical stock price of Lloyds Banking Group in GBp and the clean empirical LBG2 CoCo price in GBP on the left y-axis and the core equity tier 1 ratio on the right y-axis. Diagram three shows the absolute price error $e_t = y_t - \hat{y}_t$, where $\hat{y}_t$ corresponds to the price calculated using the 50 percentile rolling standard deviation.*

This page intentionally left blank.

Chapter 6

Conclusion and Outlook

The thesis presented contingent convertible capital both in a qualitative and a quantitative framework, fostering the transparency and understanding of the new capital instrument and advancing in the field of pricing.

Whereas the first chapter provided the economic background and rationale of contingent convertible capital, the second chapter outlined its anatomy, revealing important insights with regards to the value drivers and design characteristics and the potential impact of the latter on the risk-profile both from an equity- and bondholder perspective. The introduction of the pricing models in chapter three illustrated the angle and the theory based on which the models approach the task and revealed intricate details with regards to their implementation and parametrization. Chapter three also enhanced the models' capabilities to include discontinuous returns and improve their ability to reflect fat-tail behaviour in the risky dynamics. Furthermore, the pricing examples of a generic CoCo served as a first price indication. The dynamics and sensitivity analysis in chapter four allowed to study the model behaviour with respect to single parameter movements, aiding to understand the mechanics of the models and enabling to learn about the impact of CoCo specific design characteristics and examine a jump versus non-jump environment. Chapter five finally collated the models in an extensive empirical setting, by conducting a time series analysis on Credit Suisse and Lloyds Banking Group CoCos, effectively revealing their real world performance.

Clearly the models exhibit different implementation complexities, reaching from a relatively simple 'rule-of-thumb' approach with the credit derivative model to a highly involved and complex implementation in the case of the equity derivative approach with discontinuous returns. In general, allowing for non-continuous risky dynamics clearly increases the implementation effort and takes a toll on the computational efficiency. To this end, closed form and semi-closed form approaches as e.g. the credit and equity derivative models or the J.P. Morgan approach vastly outperform simulation based models in terms of computational time.

Additionally, the parametrization poses one of the main issues. While the relevant pricing parameters are readily available in the markets for the credit derivative, equity derivative and J.P. Morgan approach, the structural model includes several non-observable variables and involves further calibration techniques. Moreover, each of the variables is attached with uncertainties, which can lead to large price spans as observed in the empirical analysis.

The models have been found to show a similar behaviour to changes in the maturity, the risk-free rate and the volatility level. More interestingly, the price reaction when the trigger price is approached is most pronounced in the credit derivative model with piecewise constant conversion intensity and least marked in the structural model. Importantly, the sensitivity analysis for varying trigger levels revealed a double equilibrium problem for the credit, equity derivative and J.P. Morgan approach, where the models exhibit the same price level at different trigger points. Furthermore, the analysis of the models for different jump configurations with a constant process variance revealed that adding the possibility of discontinuous returns has little to no effect in the credit derivative and J.P. Morgan model. However, the structural approach exhibits clear pricing differences, where adding jumps generally decreases the price levels. The option based equity derivative model has even shown increasing prices when adding jumps.

Under the given circumstances the models universally suggest too low CoCo prices as the price errors are mostly positive during the observation period.

This might indicate that the models overestimate the risk or conversely that the markets underestimate it. Clearly the model prices are strongly dependent on the parametrization of the primary input factors. Even though the structural model is one of the more complex ones to implement, it fares better than any of the purely stock price driven models, as they exhibit too high sensitivities especially in times of depressed stock price levels. As a result the model fit of the credit and equity derivative model, as measured by the root mean squared error and the mean absolute scaled error, is on average more than twice as large as with the structural model. As a close second it has been found that the J.P. Morgan model performs rather well, as it exhibits pricing errors close to those of the structural approach.

Finally, the overall low levels of the implied trigger share prices underpin the conceptual risk-profile outlined in chapter two, where a CoCo was shown to be an instrument that can result in a high loss but with a low probability.

It remains to be seen what model will persevere in the markets. Certainly more academic work will be devoted to this topic and very likely additional pricing models or derivatives of existing ones will appear. The findings of this thesis clearly suggest to focus on structural models, as they provide the natural framework for capital ratio triggered CoCos. Furthermore, the research focus should lie less on trying to enhance the underlying risky dynamics of the models, as it has been shown to have a very minor impact at best under the given circumstances. Further efforts should rather be spent on trying to evaluate and capture the essential value drivers of a CoCo, which with increasing empirical data will lead to more robust pricing models.

Bibliography

Abrahams, J. A Survey of Recent Progress on Level-Crossing Problems for Random Processes. In Blake, I. F. and Poor, H., editors, *Communications and Networks*, pages 6–25. Springer New York, 1986.

Adrian, T. and Shin, H. Liquidity and Leverage. *Journal of Financial Intermediation*, 20:418–437, 2010.

Albert, M., Fink, J., and Fink, K. Adaptive Mesh Modeling and Barrier Option Pricing Under a Jump-Diffusion Process. *James Madison University*, 2006.

Albul, B., Jaffee, D. M., and Tchistyi, A. Contingent Convertible Bonds and Capital Structure Decisions. *Working Paper, University of California at Berkeley, Haas School of Business*, 2010.

Allen & Overy LLP. Tax Treatment of Additional Tier 1 Capital under Basel III, September 2012. http://www.allenovery.com.

Alvemar, P. and Ericson, P. Modelling and Pricing Contingent Convertibles. *Master Thesis of the University of Gothenburg: School of Business, Economics and Law*, 2012.

American International Group, Inc. AIG Dividend History, December 1st 2012. http://www.aig.com.

Ammann, M., Kind, A. H., and Wilde, C. Simulation-Based Pricing of Convertible Bonds. *Journal of Empirical Finance*, 15:310–331, 2008.

Barclays Bank PLC. Prospectus: U.S.$3,000,000,000 7.625 per cent. Contingent Capital Notes due November 2022, November 19th 2012. http://www.barclays.com.

Barucci, E. and Del Viva, L. Countercyclical Contingent Capital. *Journal of Banking & Finance*, 36:1688–1709, 2012.

Basel Committee on Banking Supervision. Basel III: A Global Regulatory Framework for More Resilient Banks and Banking Systems. June 2011a. http://www.bis.org.

Basel Committee on Banking Supervision. Global Systemically Important Banks: Assessment Methodology and the Additional Loss Absorbency Requirement. November 2011b. http://www.bis.org.

Basel Committee on Banking Supervision. Basel III Monitoring Report. September 2013. http://www.bis.org.

Berg, T. and Kaserer, C. Does Contingent Capital Induce Excessive Risktaking and Prevent an Efficient Recapitalization of Banks? *Working Paper Humboldt-Universität zu Berlin*, April 2011.

Bini, M. and Penman, S. Companies with Market Value below Book Value are more common in Europe than in the US: Evidence, Explanations and Implications. *KPMG*, 2013.

Birge, J. and Linetsky, V. *Handbooks in Operations Research and Management Science: Financial Engineering.* Handbooks in Operations Research and Management Science. Elsevier Science, 2007.

Björk, T. *Arbitrage Theory in Continuous Time.* Oxford Finance Series. OUP Oxford, 2009.

Black, F. and Cox, J. C. Valuing Corporate Securities: Some Effects of Bond Indenture Provisions. *Journal of Finance*, 31:351–367, 1976.

Black, F. and Scholes, M. S. The Pricing of Options and Corporate Liabilities. *Journal of Political Economy*, 81(3):637–654, May-June 1973.

Bloomberg. Barclays Raises $3 Billion With 10-Year Contingent Capital Notes, November 30th 2012a. http://www.bloomberg.com.

Bloomberg. Barclays Contingent Notes Fall on Short Selling Speculation, November 30th 2012b. http://www.bloomberg.com.

Bodie, Z., Kane, A., and Marcus, A. *Investments*. Irwin series in finance. McGraw-Hill Education, 2009.

Borland, L. and Hassid, Y. Market panic on different time-scales. *ArXiv e-prints*, Oct. 2010.

Boyle, P. P. and Lau, S. H. Bumping Up Against the Barrier with the Binomial Method. *The Journal of Derivatives*, 1(4):6–14, 1994.

Brennan, M. J. and Schwartz, E. S. Convertible Bonds: Valuation and Optimal Strategies for Call and Conversion. *The Journal of Finance*, 32(5):1699–1715, 1977.

Brigo, D. and Mercurio, F. *Interest Rate Models - Theory and Practice*. Springer Verlag Inc., 2006.

Bürgi, M. P. H. Pricing Contingent Convertibles: A General Framework for Application in Practice. *Financial Markets and Portfolio Management*, 27: 31–63, 2013.

Burne, K. U.S. Appetite For CoCo Bonds Could Be Tested Soon, February 15th 2011. http://www.online.wsj.com.

Calomiris, C. W. and Herring, R. J. Why and How to Design a Contingent Convertible Debt Requirement. *Journal of Applied Corporate Finance*, 25 (2), Spring 2013.

Carmona, R. and Tehranchi, M. *Interest Rate Models: An Infinite Dimensional Stochastic Analysis Perspective.* Springer Verlag Inc., 2006.

Clewlow, L. and Strickland, C. *Energy Derivatives: Pricing and Risk Management.* Lacima Publications, 2000.

Cochrane, J. *Asset Pricing: (Revised Edition).* Princeton University Press, 2009.

Collin-Dufresne, P. and Goldstein, R. S. Do credit spreads reflect stationary leverage ratios? *Journal of Finance*, 56:1929–1957, 2001.

Corcuera, J. M., De Spiegeleer, J., Ferreiro-Castilla, A., Kyprianou, A. E., Madan, D. B., and Schoutens, W. Efficient Pricing of Contingent Convertibles Under Smile Conform Models. *Journal of Credit Risk*, 2013.

Cox, J. C., Ingersoll, J. E. J., and Ross, S. A. A Theory of the Term Structure of Interest Rates. *Econometrica*, 53(2), 1985.

Credit Suisse. Prospectus: U.S.\$2,000,000,000 7.875 per cent. Tier 2 Buffer Capital Notes due 2041, February 22nd 2011. http://www.credit-suisse.com.

Credit Suisse. Prospectus: CHF 750,000,000 7.125 per cent. Tier 2 Buffer Capital Notes due 2022, March 20th 2012a. http://www.credit-suisse.com.

Credit Suisse. Prospectus: U.S.\$1,725,000,000 9.5 per cent. Tier 1 Buffer Capital, August 6th 2012b. http://www.credit-suisse.com.

Credit Suisse. Annual Report 2013, 2013. http://www.credit-suisse.com.

Credit Suisse. Fixed Income Investor Presentation, 2014. http://www.credit-suisse.com.

Crosbie, P. and Bohn, J. Modeling Default Risk, 2003. http://www.moodysanalytics.com.

De Spiegeleer, J. and Schoutens, W. *Contingent Convertible (CoCo) Notes: Structure and Pricing.* Euromoney Institutional Investor PLC, 2011.

De Spiegeleer, J. and Schoutens, W. Pricing Contingent Convertibles: A Derivatives Approach. *The Journal of Derivatives*, 20(2):27–36, 2012.

De Spiegeleer, J., Schoutens, W., and Jabre, P. *The Handbook of Convertible Bonds: Pricing, Strategies and Risk Management.* The Wiley Finance Series. John Wiley & Sons, Incorporated, 2011.

Derman, E. and Iraj, K. The ins and outs of barrier options: Part 1. *Derivatives Quarterly*, 3(2):55–67, 1996.

Derman, E. and Iraj, K. The ins and outs of barrier options: Part 2. *Derivatives Quarterly*, 3(3):73–80, 1997.

Duan, J.-C. and Simonato, J.-G. Estimating and testing exponential-affine term structure models by Kalman filter. *Review of Quantitative Finance and Accounting*, 13:111–135, 1999.

Duffie, D. A Contractual Approach to Restructuring Financial Institutions. In Scott, K. E., Shultz, G. P., and Taylor, J. B., editors, *Ending Government Bailouts As We Know Them*, chapter 6. Hoover Institution, Stanford University, 2010.

Duffie, D. and Lando, D. Term structures of credit spreads with incomplete accounting information. *Econometrica*, 69:633–664, 2001.

Duffie, D. and Singleton, K. J. An Econometric Model of the Term Structure of Interest Rate Swap Yields. *Journal of Finance*, 52(4):1287–1321, 1997.

Duffie, D. and Singleton, K. J. Modeling term structures of defaultable bonds. *Review of Financial studies*, 12(4):687–720, 1999.

Duffie, D. and Singleton, K. J. *Credit Risk: Pricing, Measurement, and Management.* Princeton Series in Finance. Princeton University Press, 2003.

Embrechts, P., Klüppelberg, C., and Mikosch, T. *Modelling Extremal Events: For Insurance and Finance*. Applications of mathematics. Springer, 1997.

European Banking Authority. EBA Recommendation on the Creation and Supervisory Oversight of Temporary Capital Buffers to Restore Market Confidence. December 2011. http://www.eba.europa.eu/.

European Commission. Proposal for a Regulation of the European Parliament and of the Council on Prudential Requirements for Credit Institutions and Investments Firms Part I. July 2011. http://www.ec.europa.eu.

Financial Services Authority. Recovery and Resolution Plans. *Consultation Paper CP11/16*, August 2011.

Flannery, M. and Perotti, E. CoCo design as a risk preventive tool, 2011. http://www.voxeu.org.

Flannery, M. and Rangan, K. What caused the Bank Capital Build-up of the 1990s? *Review of Finance*, 12:391–429, 2008.

Flannery, M. J. No Pain, No Gain? Effecting Market Discipline Via 'Reverse Convertible Debentures'. *University of Florida*, 2002.

Flannery, M. J. Stabilizing Large Financial Institutions with Contingent Capital Certificates. *Federal Reserve Bank of New York Research Department*, 2009.

Glasserman, P. *Monte Carlo Methods in Financial Engineering*. Applications of Mathematics. Springer, 2004.

Glasserman, P. and Nouri, B. Contingent Capital with a Capital-Ratio Trigger. *Management Science*, pages 1816–1833, October 2012.

Haldane, A. G. Capital Discipline. *Based on a speech given at the American Economic Association*, January 2011. http://www.bis.org.

Harvey, A. C. *Forecasting, Structural Time Series Models and the Kalman Filter*. Cambridge University Press, 1990.

Haug, E. G. *The Complete Guide to Option Pricing Formulas*. McGraw-Hill, New York, second edition, 2006.

Henriques, R. and Doctor, S. Making CoCos Work. *J.P. Morgan: Europe Credit Research*, 2011.

Hilscher, J. and Raviv, A. Bank stability and market discipline: The effect of contingent capital on risk taking and default probability. *Brandeis University*, 2014.

Hull, J. and White, A. Valuing credit default swaps I: No counterparty default risk. *Journal of Derivatives*, 8(1):29–40, 2000.

Hull, J. C. *Options, Futures, & Other Derivatives*. Prentice Hall Finance Series. Pearson/Prentice Hall, 2009.

Hyndman, R. J. and Koehler, A. B. Another look at measures of forecast accuracy. *International Journal of Forecasting*, 22:679–688, 2006.

Independent Commission on Banking of U.K. Final Report. Recommendations. September 2011.

Ingersoll, J. J. A contingent-claims valuation of convertible securities. *Journal of Financial Economics*, 4(3):289–321, May 1977.

ISDA. International Swaps and Derivatives Association CDS Standard Model, December 12th 2013. http://www2.isda.org.

Jarrow, R. A. and Turnbull, S. M. Pricing Derivatives on Financial Securities Subject to Credit Risk. *Journal of Finance*, 1(1):53–85, 1995.

Joshi, M. *The Concepts and Practice of Mathematical Finance*. Cambridge University Press, 2003.

Kirchgässner, G. and Wolters, J. *Introduction to Modern Time Series Analysis*. Springer Verlag Inc., 2008.

Koziol, C. and Lawrenz, J. Contingent Convertibles. Solving or Seeding the Next Banking Crisis? *Journal of Banking & Finance*, pages 90–104, 2012.

Kuritzkes, A. and Hal, S. Markets are the best judge of bank capital. *Financial Times*, September 2009.

Lando, D. *Credit Risk Modeling: Theory and Applications*. Princeton Series in Finance. Princeton University Press, 2009.

Leland., H. E. Corporate Debt Value, Bond Covenants, and Optimal Capital Structure. Research program in finance working papers, University of California at Berkeley, Jan. 1994.

Lloyds Banking Group. Prospectus: Enhanced Capital Notes issued by LBG Capital No.1 plc or LBG Capital No.2 plc, November 3rd 2009a. http://www.lloydsbankinggroup.com.

Lloyds Banking Group. Annual Report and Accounts 2009, January 2009b. http://www.lloydsbankinggroup.com.

Lloyds Banking Group. Q1 2014 Interim Management Statement, April 3rd 2014. http://www.lloydsbankinggroup.com.

Longstaff, F. A. The valuation of options on coupon bonds. *Journal of Banking and Finance*, 17:27–42, 1993.

Madan, D. B. and Schoutens, W. Conic coconuts: the pricing of contingent capital notes using conic finance. *Mathematics and Financial Economics*, 4 (2):87–106, 2011.

Madan, D. B. and Unal, H. Pricing the Risks of Default. *Review of Derivatives Research*, 2:121–160, 1998.

Maes, S. and Schoutens, W. Contingent capital: an in-depth discussion. *European Commission (EC), DG Competition*, 2010.

McDonald, R. L. Contingent Capital with a Dual Price Trigger. *Kellogg School Northwesten University*, 2010.

McNeil, A. J., Frey, R., and Embrechts, P. *Quantitative Risk Management: Concepts, Techniques And Tools*. Princeton Series in Finance. Princeton University Press, 2005a.

McNeil, A. J., Frey, R., and Embrechts, P. *Quantitative Risk Management: Concepts, Techniques And Tools*. Princeton Series in Finance. Princeton University Press, 2005b.

Memmel, C. and Rapauch, P. How do banks adjust their capital ratios? *Journal of Financial Intermediation*, 19:509–528, 2010.

Merton, R. C. Theory of Rational Option Pricing. *Bell Journal of Economics*, 4(1):141–183, Spring 1973.

Merton, R. C. On the Pricing of Corporate Debt: The Risk Structure of Interest Rates. *Journal of Finance*, 29(2):449–70, May 1974.

Merton, R. C. Option pricing when underlying stock returns are discontinuous. *Journal of Financial Economics*, 3(1-2):125–144, 1975.

National Audit Office. The Asset Protection Scheme. *Report by the Comptroller and Auditor General*, 2010. http://www.nao.org.uk.

Neue Zürcher Zeitung. Julius-Bär-Aktie stürzt vorübergehend ab. Gerüchte über geschönte Bilanz, February 2009. http://www.nzz.ch.

Pazarbasioglu, C., Zhou, J.-P., Le Lésle, V., and Moore, M. Contingent Capital: Economic Rationale and Design Features. *International Monetary Fund*, 2011.

Pennacchi, G. G. A Structural Model of Contingent Bank Capital. *FRB of Cleveland Working Paper No. 10-04*, 2010.

Rabobank. Prospectus: Euro 1,250,000,000 6.875 per cent. Senior Contingent Notes due 2020, March 17th 2010. http://www.rabobank.com.

Rabobank. Prospectus: U.S.\$2,000,000,000 8.375 per cent. Perpetual Non-Cumulative Capital Securities, January 24th 2011. http://www.rabobank.com.

Reuters. AIG may consider dividend next year: CEO, December 1st 2012. http://www.reuters.com.

Reuters. CoCo market to go mainstream after BoAML creates index, January 2014. http://www.reuters.com.

Risk Magazine. Doubts raised over viability of Lloyds CoCo bonds trigger, April 2010. http://www.risk.net.

Ritchken, P. On Pricing Barrier Options. *The Journal of Derivatives*, 3(2): 19–28, 2005.

Rubinstein, M. and Reiner, E. Unscrambling the binary code. *Risk Magazine*, 4:75–83, October 1991.

Schönbucher, P. *Credit Derivatives Pricing Models: Models, Pricing and Implementation*. The Wiley Finance Series. Wiley, 2003.

Seydel, R. U. *Tools for Computational Finance*. Universitext (1979). Springer, 2009.

Squam Lake Working Group on Financial Regulation. An Expected Resolution Mechanism for Distressed Financial Firms: Regulatory Hybrid Securities. *Working Paper, Squam Lake Working Group on Financial Regulation*, 2009.

Su, L. and Rieger, M. O. How likely is it to hit a barrier? Theoretical and Emprical Estimates. Technical Report No. 594, Financial Valuation and Risk Management, October 2009.

Sundaresan, S. and Wang, Z. On the Design of Contingent Capital with Market Trigger. *Federal Reserve Bank of New York, Staff Report no. 448*, November 2011.

Swiss Federal Council. Verordnung über die Eigenmittel und Risikoverteilung für Banken und Effektenhändler, May 1st 2013. http://www.admin.ch.

Swiss Federal Council, Commission of Experts. Final Report of the Commission of Experts for limiting the economic risks posed by large companies. September 2010.

Swiss Financial Market Supervisory Authority. Addressing "Too Big To Fail" The Swiss SIFI Policy. June 23rd 2011. http://www.finma.ch.

Swiss Financial Market Supervisory Authority. Wegleitung zu den Modalitäten der Einreichung von SST-Berichten und von Gesuchen zur Genehmigung interner Modelle. March 2012. http://www.finma.ch.

Swiss National Bank. Decree issued by the Swiss National Bank concerning systemic importance. *Press Release*, November 2013. http://www.snb.ch.

Swiss Re. Prospectus: USD 750,000,000 Limited Recourse Secured Notes due 2024, March 8th 2013. http://www.swissre.com.

Tankov, P. *Financial Modelling with Jump Processes*. Chapman & Hall/CRC Financial Mathematics Series. Taylor & Francis, 2003.

Teneberg, H. Pricing Contingent Convertibles using an Equity Derivatives Jump Diffusion Approach. *Master Thesis KTH Royal Institute of Technology, Department of Mathematics*, 2012.

UBS. Base Prospectus, June 22nd 2012a. http://www.ubs.com.

UBS.   UBS Dividend payments history, December 1st 2012b.
http://www.ubs.com.

UBS. Prospectus: USD 2,000,000,000 Tier 2 Subordinated Notes due 2022.
August 17th 2012c.

Vasicek, O. An equilibrium characterization of the term structure. *Journal of
Financial Economics*, 5:177–188, 1977.

von Furstenberg, G. M. Contingent Capital to Strengthen the Private Safety
Net for Financial Institutions: Cocos to the Rescue? *Deutsche Bundesbank
Discussion Paper*, January 2011.

Wilkens, S. and Bethke, N. Contingent Convertible ("CoCo") Bonds: A
First Empirical Assessment of Selected Pricing Models. *Financial Analysts
Journal*, 70(2):59–77, March/April 2014.

Zhou, C. A Jump-Diffusion Approach to Modeling Credit Risk and Valuing
Defaultable Securities. *Working Paper, Federal Reserve Board*, 1997.

Zhou, C. The term structure of credit spreads with jump risk. *Journal of
Banking & Finance*, 25:2015–2040, 2001.

Zürcher Kantonalbank. Prospectus: Nachrangige Tier-1-Anleihe CHF 590
Mio., June 2013. http://www.zkb.ch.

Appendix A

Appendix

Issue Date	ISIN	Denomination	Coupon	Maturity
01.12.2009	XS0459090188	GBP 147m	9.125%	15.07.2020
01.12.2009	XS0459091582	GBP 151m	7.625%	09.12.2019
01.12.2009	XS0459091665	GBP 96m	9%	15.12.2019
01.12.2009	XS0459092473	GBP 68m	10.5%	29.09.2023
01.12.2009	XS0459092804	GBP 107m	9%	15.07.2029
01.12.2009	XS0459092986	GBP 104m	8.5%	07.06.2032
01.12.2009	XS0459090691	GBP 38m	11.125%	04.11.2020
01.12.2009	XS0459090774	EUR 94m	7.375%	12.03.2020
01.12.2009	XS0459090931	EUR 53m	3mE + 310bps	12.03.2020
01.12.2009	XS0459091079	GBP 57m	12.75%	10.08.2020
01.12.2009	XS0459091236	EUR 226m	7.625%	14.10.2020
01.12.2009	XS0459091749	GBP 4m	8.125%	15.12.2019
01.12.2009	XS0459091822	GBP 79m	14.5%	30.01.2022
01.12.2009	XS0459092127	GBP 57m	9.875%	10.02.2023
01.12.2009	XS0459092390	GBP 38m	11.25%	14.09.2023
01.12.2009	XS0459092556	GBP 35m	11.875%	01.09.2024
01.12.2009	XS0459093281	GBP 61m	16.125%	10.12.2024
01.12.2009	XS0459088281	EUR 710m	6.439%	23.05.2020
01.12.2009	XS0459088877	GBP 736m	11.04%	19.03.2020
01.12.2009	XS0459087986	EUR 125m	8.875%	07.02.2020
01.12.2009	XS0459088109	GBP 207m	9.334%	07.02.2020
01.12.2009	XS0459086582	GBP 732m	7.588%	12.05.2020
01.12.2009	XS0459093364	GBP 596m	7.869%	25.08.2020
01.12.2009	XS0459088794	EUR 661m	6.385%	12.05.2020
01.12.2009	XS0459089255	GBP 775m	15%	21.12.2019
01.12.2009	XS0459089412	EUR 486m	15%	21.12.2019
01.12.2009	XS0459086749	GBP 331m	7.867%	17.12.2019
01.12.2009	XS0459086822	GBP 102m	7.975%	15.09.2024

Table A.1: *This table shows the issued CoCos of Lloyds Banking Group, which formed part of their refinancing program in 2009.*

Curriculum Vitae

Personal Information

Name:	Marc Erismann
Date of birth:	July 22, 1983
Place of origin:	Beinwil am See (Aargau), Switzerland
Citizenship:	Swiss

Education

2011 - 2015	**University of St. Gallen (HSG)**
	Ph.D. in Management, Specialization in Finance
2009 - 2011	**University of St. Gallen (HSG)**
	Master of Arts (M.A. HSG) in Banking and Finance
2006 - 2009	**University of Applied Sciences**
	Bachelor of Science (B.Sc.) in Business Administration

Professional Experience

2008 -	**Zurich Insurance Group Ltd.**, Zürich
	Credit, Surety and Specialties (Underwriting)
2003 - 2004	**Fuchsgroup AG**, Rupperswil
	System Administration and First Level Support